REPORT DOCUMENTATION PAGE

Form Approved OMB NO. 0704-0188

1. REPORT DATE (DD-MM-YYYY)	2. REPORT TYPE	3. DATES COVERED (From - To)
15-05-2015	Ph.D. Dissertation	-

4. TITLE AND SUBTITLE
Mechanical Characterization Of Anion Exchange Membranes Under Controlled Environmental Conditions

5a. CONTRACT NUMBER
W911NF-10-1-0520

5b. GRANT NUMBER

5c. PROGRAM ELEMENT NUMBER
611103

6. AUTHORS
Benjamin R. Caire

5d. PROJECT NUMBER

5e. TASK NUMBER

5f. WORK UNIT NUMBER

7. PERFORMING ORGANIZATION NAMES AND ADDRESSES
Colorado School of Mines
1500 Illinois Street, Guggenheim Hall, Room 130
Golden, CO 80401 -1887

8. PERFORMING ORGANIZATION REPORT NUMBER

9. SPONSORING/MONITORING AGENCY NAME(S) AND ADDRESS (ES)
U.S. Army Research Office
P.O. Box 12211
Research Triangle Park, NC 27709-2211

10. SPONSOR/MONITOR'S ACRONYM(S)
ARO

11. SPONSOR/MONITOR'S REPORT NUMBER(S)
58161-CH-MUR.69

12. DISTRIBUTION AVAILIBILITY STATEMENT
Approved for public release; distribution is unlimited.

13. SUPPLEMENTARY NOTES
The views, opinions and/or findings contained in this report are those of the author(s) and should not contrued as an official Department of the Army position, policy or decision, unless so designated by other documentation.

14. ABSTRACT
While proton exchange membrane (PEM) fuel cells have been the focus of development in the past, anion exchange membranes (AEM) have the potential to dramatically lower the cost of fuel cells by utilizing non-noble catalysts and a variety of fuel sources. Although chemical degradation typically dominates membrane failure pathways in a fuel cell, mechanical breakdown due to humidity cycling is a common occurrence. This thesis aims to understand the mechanical properties of anion exchange membranes under fuel cell operating conditions. A humidity delivery system was developed for the TA Instruments ARES-G2 rheometer to allow for testing at a range of temperatures

15. SUBJECT TERMS
Anion Exchange Membrane, Mechanical Properties

16. SECURITY CLASSIFICATION OF:			17. LIMITATION OF ABSTRACT	15. NUMBER OF PAGES	19a. NAME OF RESPONSIBLE PERSON
a. REPORT	b. ABSTRACT	c. THIS PAGE			Andrew Herring
UU	UU	UU	UU		19b. TELEPHONE NUMBER: 303-384-2082

Report Title

Mechanical Characterization Of Anion Exchange Membranes Under Controlled Environmental Conditions

ABSTRACT

While proton exchange membrane (PEM) fuel cells have been the focus of development in the past, anion exchange membranes (AEM) have the potential to dramatically lower the cost of fuel cells by utilizing non-noble catalysts and a variety of fuel sources. Although chemical degradation typically dominates membrane failure pathways in a fuel cell, mechanical breakdown due to humidity cycling is a common occurrence. This thesis aims to understand the mechanical properties of anion exchange membranes under fuel cell operating conditions. A humidity delivery system was developed for the TA Instruments ARES-G2 rheometer to allow for testing at a range of temperatures (30-100°C) and relative humidity conditions (0-95% RH). A modified Sentmanat Extensional Rheometer (SER) was used to perform tensile-like testing using less than 5% of material needed for a traditional tensile tester. These tools established metrics for a robust membrane through mechanical characterization across temperatures and humidities. A pentablock AEM with a balance of stiff and elastic blocks was shown to have adequate conductivity (up to 60 mS/cm at 90°C and 95%RH), low water uptake (<25%), and good mechanical integrity under dry and hydrated conditions, showing potential for being durable under hydration and mechanical stresses.

Complementing the destructive tensile testing, a “water stress” test was explored to measure the tension and durability under hygral cycles. Membranes with a low (<5 MPa) and near constant water stress absorb and desorb water reversibly. The materials that performed poorly in the water stress tests also had elongation <50% under dry conditions and swelled with water. Membranes performing well in the water stress test also had an elongation to break 10 times that of its in-plane water swelling (in liquid water). Ion exchange membranes need to beable to mechanically stretch in the elastic region well above the in-plane swelling with water to withstand hygral stresses in an electrochemical device. By identifying a relationship between the mechanical and hygral stretching to predict durability in a working device, this thesis advanced the understanding of mechanical performance under relevant temperature and humidity conditions, which is critical to the development of durable anion exchange membranes.

MECHANICAL CHARACTERIZATION OF ANION EXCHANGE MEMBRANES UNDER CONTROLLED ENVIRONMENTAL CONDITIONS

by

Benjamin R. Caire

A thesis submitted to the Faculty and Board of Trustees of the Colorado School of Mines in partial fulfillment of the requirements for the degree of Doctor of Philosophy (Chemical Engineering).

Golden, Colorado

Date May 11, 2015

Signed: _____
Benjamin R. Caire

Signed: _____
Dr. Matthew W. Liberatore
Thesis Advisor

Golden, Colorado

Date _____

Signed: _____
Dr. Colin Wolden
Professor and Head
Department of Chemical and Biological Engineering

ABSTRACT

While proton exchange membrane (PEM) fuel cells have been the focus of development in the past, anion exchange membranes (AEM) have the potential to dramatically lower the cost of fuel cells by utilizing non-noble catalysts and a variety of fuel sources. Although chemical degradation typically dominates membrane failure pathways in a fuel cell, mechanical breakdown due to humidity cycling is a common occurrence. This thesis aims to understand the mechanical properties of anion exchange membranes under fuel cell operating conditions. A humidity delivery system was developed for the TA Instruments ARES-G2 rheometer to allow for testing at a range of temperatures (30-100°C) and relative humidity conditions (0-95% RH). A modified Sentmanat Extensional Rheometer (SER) was used to perform tensile-like testing using less than 5% of material needed for a traditional tensile tester. These tools established metrics for a robust membrane through mechanical characterization across temperatures and humidities.

A pentablock AEM with a balance of stiff and elastic blocks was shown to have adequate conductivity (up to 60 mS/cm at 90°C and 95%RH), low water uptake (<25%), and good mechanical integrity under dry and hydrated conditions, showing potential for being durable under hydration and mechanical stresses.

Complementing the destructive tensile testing, a "water stress" test was explored to measure the tension and durability under hygral cycles. Membranes with a low (<5 MPa) and near constant water stress absorb and desorb water reversibly. The materials that performed poorly in the water stress tests also had elongation <50% under dry conditions and swelled with water. Membranes performing well in the water stress test also had an elongation to break 10 times that of its in-plane water swelling (in liquid water). Ion exchange membranes need to be

able to mechanically stretch in the elastic region well above the in-plane swelling with water to withstand hygral stresses in an electrochemical device. By identifying a relationship between the mechanical and hygral stretching to predict durability in a working device, this thesis advanced the understanding of mechanical performance under relevant temperature and humidity conditions, which is critical to the development of durable anion exchange membranes.

TABLE OF CONTENTS

LIST OF FIGURES

ACKNOWLEDGEMENTS

I thank the Army Research Office for the project funding (MURI #W911NF-10-1-0520) and the instrument grant (DURIP #W911NF-11-1-030). I thank the other CSM students on this project, including Ashley Maes, Himanshu Sarode, Tara Pandey, Ye Liu, Yifan Li, Yating Yang, and Derek Strasser. I especially thank Melissa Vandiver for being a terrific collaborative partner in this work. I could always trust that her work was timely and well done, plus it was just fun to work together. Jim Horan and Mei-Chen Kuo were also always able to lend a hand and provided a lot of enthusiasm. I thank Sönke Seifert at Argonne National Lab for being so generous with his time, knowledge, and coffee while performing x-ray scattering experiments at the Advanced Photon Source. I thank Wesley Burghardt and Erica McCready of Northwestern for letting us use their custom built oven at the APS and for helping me understand the data. Several undergraduates contributed to this thesis including Sarah Lustgraaf (CSM) for the COMSOL work related to mixing in a pipe, Jessica Earl (Polymer REU EEC-1156745, University of Utah) for the COMSOL work related to environmental control in the two oven designs and for the humidity can drawing, Zach Poskin (Polymer REU EEC-1156745, University of Kansas) for the mechanical data on polymer blends, Jordan Carver (CSM) for mechanical data on the AEM benchmarking work, and Joseph Montion (Polymer REU EEC-1156745, University of Toledo) for the solution rheology work with the Brexar material. I thank TA Instruments and Aadil Elmoumni for their time and expertise. I thank Kurt Johnson and the whole team at Challenger Manufacturing Consultants for their expertise in designing and building the modified SER drums and the oven. I thank the other graduate students in the department who made my time here a real joy. I especially thank Joanna Sylman and the Neeves group for the several hundred dollars I earned 15 mL of blood at a time.

I am very thankful to have earned my Ph.D. on a large team project, and I thank all the other graduate students and post-docs that were part of the MURI. The feedback and discussion generated on the bi-weekly phone calls and annual meetings were valuable in learning things outside of my thesis topic. Bryan Coughlin and Tom Witten were especially helpful in asking thoughtful questions. I also thank Byran Pivovar at NREL for taking the time to help me better understand the mechanical stresses membranes face in fuel cells.

I thank Andy Herring for teaching me about electrochemistry and for stretching the travel budget which allowed me to attend many conferences. I am indebted to Matt for the excellent guidance and personal understanding he displayed during my time here. I truly enjoyed working for Matt and I wish him the best of luck transitioning to Toledo.

I thank my brother-in-law Christian for setting an example for me of someone who went back to graduate school after working. I thank my mom for having the patience to put up with a little boy who continued to ask "why?" past any reasonable point. Thanks to my dad for always being up for an experiment and for teaching me the scientific method when I was in 3rd grade. Thanks for nurturing my innate curiosity.

Last but not least, I thank my wife Lindsey for her love and support. She agreed to marry a guy who had no job and spend the first five years of marriage in university housing as the wife of a poor graduate student. It has not been the easiest five years, and I certainly could not have done this without her.

CHAPTER 1

INTRODUCTION

This Ph.D. thesis contributes to a larger effort to produce revolutionary, robust, durable thin anion exchange membranes with sufficiently high ionic conductivities for practical devices and to fundamentally understand the interplay of chemistry, processing, and morphology on the performance and durability of anion exchange membranes [1]. The alkaline anion-exchange membranes must have high hydroxide conductivity and low electronic conductivity, but also be chemically, dimensionally, and mechanically stable at elevated temperatures, under a range of hydration conditions, and using potentially different fuels. This thesis focused on developing the tools necessary to make mechanical measurements under fuel cell operating conditions and provided insight on interplay of mechanical properties with other functional properties of ion exchange membranes.

1.1 Alkaline Exchange Membranes and Fuel Cells

Despite the large amount of resources devoted to developing fuel cells over the past century, very little market penetration has been achieved. Proton exchange membrane fuel cells (PEMFC) have struggled primarily due to high cost, driven by the use of precious metals such as platinum for the catalyst. Proton exchange membrane (PEM) fuel cells operate in an acidic environment such that platinum is the only catalyst that leads to significant power densities [2]. Given the high cost of platinum, a significant amount of research has been devoted to reducing the amount needed in a fuel cell stack [3]. However, the aim of this research is to focus on developing a membrane that operates in an alkaline environment.

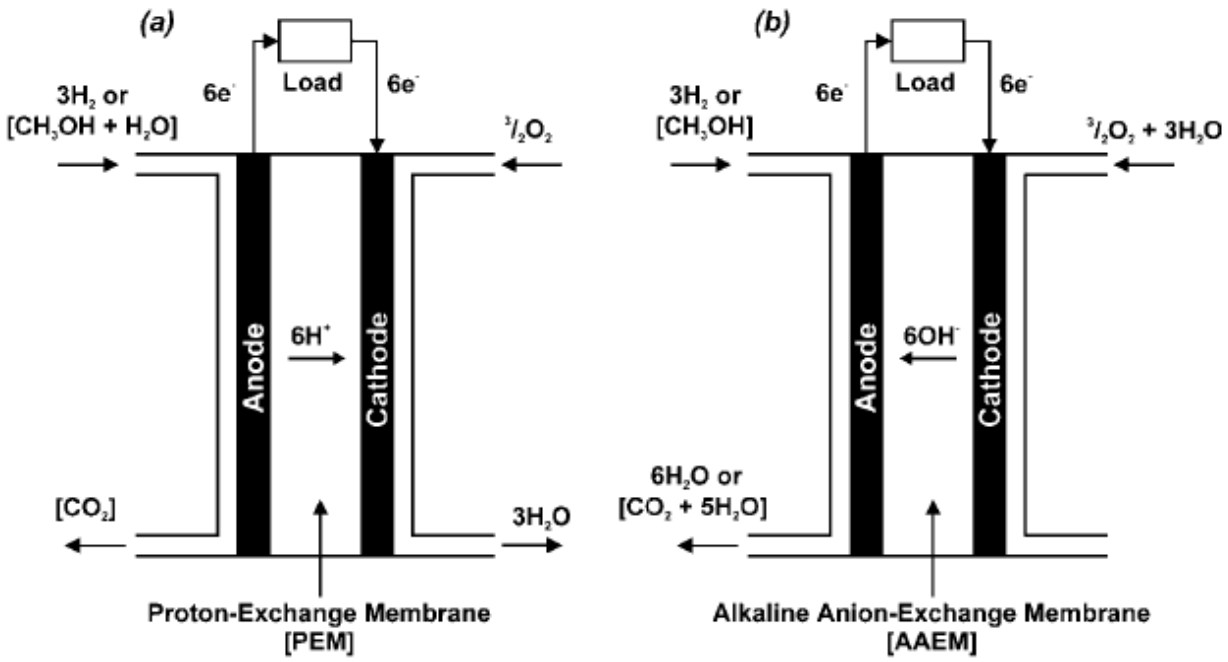

Figure 1.1 A schematic of (a) a proton-exchange membrane and (b) an alkaline-exchange membrane fuel cell both fueled either with H2 gas or directly with methanol. The stoichiometric ratio of reactants and products are shown in each case [4].

An alkaline anion-exchange membrane fuel cell has many advantages over a proton-exchange membrane fuel cell and several challenges to overcome. Proton exchange membrane fuel cells degrade because the oxygen reduction reaction in incomplete and the oxygenated radicals oxidize the system components. Since peroxides are less stable in base the use of expensive oxidatively stable components is less important. However, hydroxide is corrosive to anything polar so care has to be taken to use the correct system components. An alkali environment can support the use of non-precious metals such as silver, nickel, or copper as catalysts, thus greatly reducing the cost of the fuel cell [5–7]. An AEM fuel cell has increased electro-oxidation kinetics and easier water management [8]. However, current alkaline anion-exchange membranes have several drawbacks. Membrane stability in an alkaline environment, especially at elevated temperatures, has been poor as the cation site, typically an ammonium group, is ripe for nucleophilic attack by hydroxyl or Hoffman elimination in the presences of β-

hydrogens [9]. Additionally, the hydroxide ion is rapidly exchanged to carbonate and bicarbonate when carbon dioxide is present.

Membranes in the (bi)carbonate form yield lower conductivity than in the hydroxide form [10,11]. It is thought that a higher operating temperature produces less (bi)carbonate, however the ionic site on the polymer is more susceptible to attack at higher temperatures.

The operating temperature of a proton exchange membrane fuel cell is 90°C or less as the membrane needs to stay hydrated to effectively transport ions [12]. The alkaline exchange membranes in development are expected to operate at similar temperatures and will also need to be hydrated.

The alkaline exchange membranes on the market today are generally used in electrodialysis applications. FuMA-Tech GmbH of Germany has several anion exchange membranes and is actively developing membranes for alkaline fuel cells. The Tokuyama Corporation of Japan is the leader in AEM development for fuel cells and their membranes have been cited as the benchmark AEM or used in fuel cell performance testing in several publications [10,13–15]. The lack of commercial success of these membranes is a driving force behind this research effort.

Given the dearth of commercial membranes, recent research activity focuses on developing a stable, highly conductive, robust anion exchange membrane for a fuel cell. Several reviews have been published on the developments [4,16–18].

1.2 Extensional Rheology of Polymers

As early as the 1970s [19], the effects of stretching polymer films has been observed, but only recently have the tools been developed to quantify what happens to a polymer as it is stretched.

The Sentmanat Extensional Rheometer (SER) was introduced in 2004 [20] and has since been the standard bearer for extensional viscosity measurements. The more highly cited articles of the work with the SER has focused on characterizing polyethylene melts [21–23]. Other polymers studied include polybutene [24] (with TA Instrument's Extensional Viscosity Fixture, EVF) and a well-entangled monodisperse styrene-butadiene random-copolymer [25].

The paper that most closely resembles our experimental plan is by Sambaer, et. al. [26] The researchers electrospin polyurethane in dimethylformamide (DMF) on differing supporting textiles and test the mechanical properties. Even though their films were only 10 microns, the SER fixture was used by applying double stick tape to the drums (Figure 1.2). Successful measurements of Young's Modulus, Maximum Stress and Maximum Strain (Figure 1.3) were recorded, and it was shown that the supports made with melt blown polypropylene with and without the polyethylene foil had a higher maximum stress than the supports made with aramid and stainless steel. The authors conclude that supporting textile has a large impact on mechanical properties due to the difference in porosity of the prepared samples.

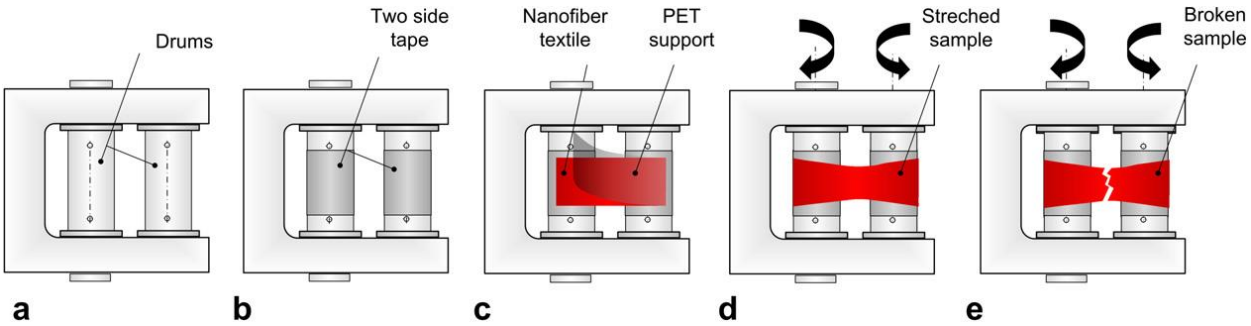

Figure 1.2 Visualized methodology for the tensile testing of the nanofiber nonwoven by using Sentmanat extensional rheometer. a) SER unit, b) SER with double-sided adhesive tape, c) Nanofiber web deposition on the SER unit, d) Sample stretching, e) Sample at break.

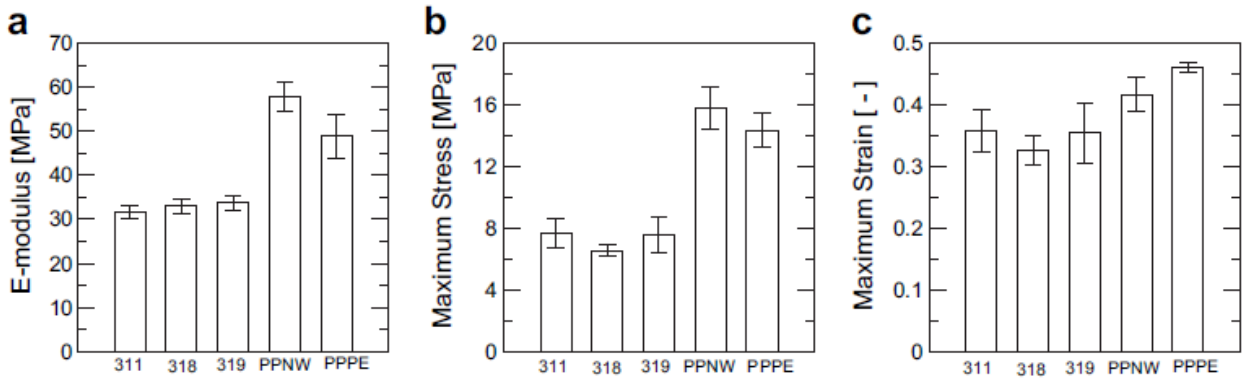

Figure 1.3 Summarized tensile strength characteristics for all investigated nonwoven samples.

The authors note: "With respect to mechanical testing by using SER, it should be mentioned that the main advantage of this 'rheology based' methodology is the possibility to measure very fine structures with low experimental error due to the utilization of very sensitive torque/normal force transducers, which are normally present on standard rotational rheometers for polymer melt rheology evaluation. Moreover, the measurements can be done at different extensional strain rates and temperatures by using the conventional rheometer oven, which is difficult or impossible to do by using standard methodologies."

1.3 Mechanical Properties of Ion Exchange Membranes

While chemical degradation remains a significant issue for membrane stability, mechanical stability is an integral factor in fuel cell lifetime [27]. The polymer needs to be processed into thin, durable membranes and withstand the stresses inside a fuel cell at operating conditions. Young's modulus and yield strength have been used to quantify membrane degradation in a fuel cell at 80°C [28]. Microcracks are a common mechanical failure in fuel cell membranes, and elongation at break correlates well with microcrack resistance [29]. In an effort to improve mechanical properties reinforcement with ePFTE has been shown to increase the fuel cell lifetime by an order of magnitude [30].

Huang, et. al., demonstrated that humidity cycles correlate well with a reduction in the strain at failure even though the yield stress and yield strain remained largely unchanged. Also demonstrated was a decreased in elastic modulus as humidity increased [31].

Most of the available literature on mechanical properties of ion conducting polymer membranes is limited to stress-strain curves in various states of hydration [32–35]. The typical trend shows a decrease in tensile strength and Young's modulus as the polymer absorbs water. The elongation at break increases due to plastic effect of the absorbed water [33]. Also noted by Marestin, et. al is that "Despite the fact that mechanical properties are now often determined for new ionomers, a complete study of the mechanical properties is still necessary including the combined effect of water content and temperature" [32].

The literature has several examples of how mechanical properties of films are related to conductivity. Pan, et. al. show how the Young's modulus decreases with increasing ion exchange capacity (IEC) in alkaline exchange quaternary ammonia polysulfone membrane, "a trend that being almost the mirror of the membrane dimension-IEC curve" [36]. Wu, et. al. created poly(vinyl alcohol) (PVA) and poly(acrylic acid) (PAA) blends and found that a 10:5 PVA:PAA ratio "offers a good balance between enhanced ionic conductivity and acceptable mechanical strength for solid polymer electrolyte applications" [37].

The hydration/dehydration cycles the membranes undergo in a fuel cell are a primary concern for membrane mechanical failure. Tang, et. al. demonstrated that the fatigue strength of the cyclic stress of Nafion NR111 is only 1/10 of the tensile strength of the membrane. They concluded that "the shrinkage stress generated by the water-uptake is responsible for the mechanical decay of the Nafion PEMs" [38].

1.4 Environmental Control in other instrumentation

There are many other scientific questions that need the ability to control the test environment. Conductivity of fuel cell membranes in air is done in a humidity oven that can hold many samples at once. Test Equity makes several models of ovens that can control a wide range of temperature and humidity conditions. TA Instruments offers a Dynamic Mechanical Analyzer that can control temperature and humidity across a wide range (Figure 1.4). The range of interest for this thesis is more similar to an environmental chamber built by Majsztrik for tensile creep experiments that has a temperature range of 20-250°C and full 0-100% relative humidity control [39]. These systems are all closed, thus enabling the highest relative humidity conditions to be achieved with back pressure.

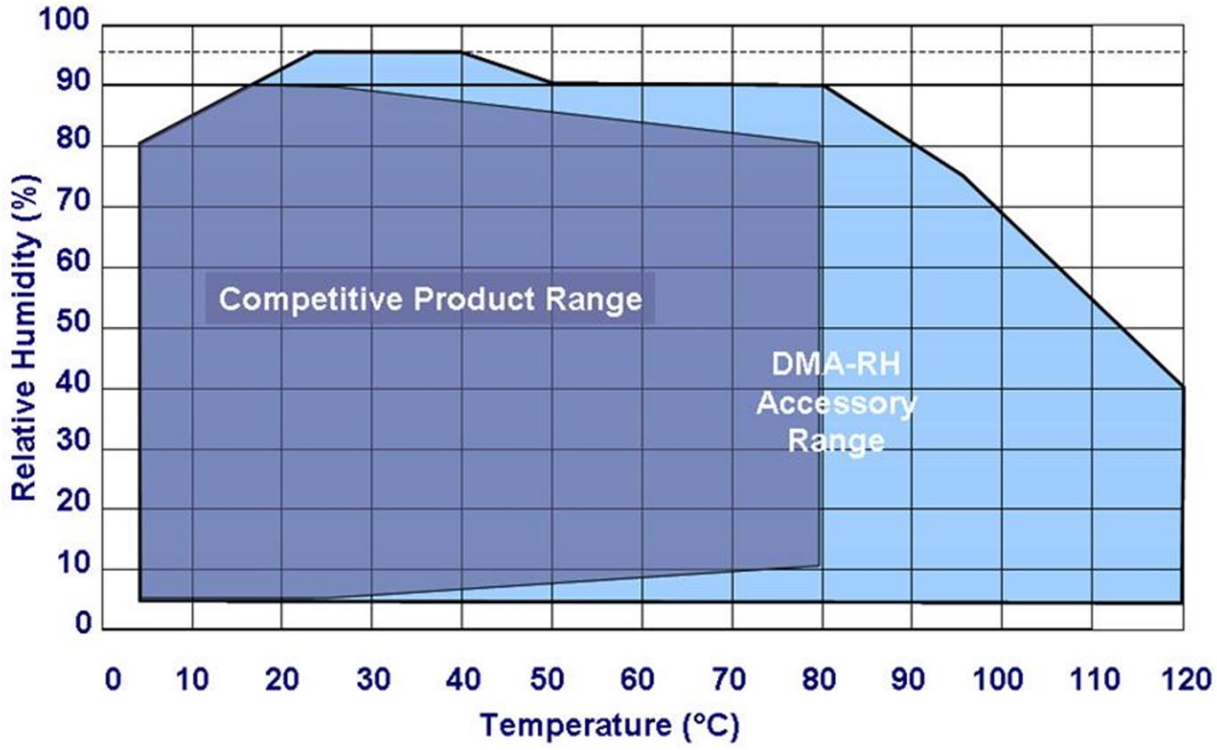

Figure 1.4 Relative humidity and temperature range of TA Instruments' DMA compared to a competitor.

The humidity is maintained with a wet gas/dry gas mixture and has a dual humidity and temperature sensor for feedback control. Systems controlled in this manner are the most effective technology for environmental control, and the system built for the ARES is similar [40].

1.5 Small Angle X-Ray Scattering (SAXS)

Small angle x-ray scattering was developed in the 1920s as a way to study natural fibers and colloidal coal [41]. The phenomenon of small angle scattering was recognized as originating from the colloidal structure of the coal dust and cellulose fibers. By the late 1960s, an ideal lamellae model had been developed by Vonk and Kortleve [42] which allowed for detailed study of solid polymer systems. Since SAXS allows for studies of structure on the order of 1.5 to 150 Å, it can lead to powerful insights into polymer structure. The x-rays interact with the electron cloud of atoms revealing structure in the resulting scattering pattern. The scattering vector, *q*, yields information on the structure and is related to the small angle of the x-ray, θ, and the x-ray's wavelength, λ (1.1).

$$q = \frac{4 \cdot \pi \cdot \sin\left(\frac{\theta}{2}\right)}{\lambda} \tag{1.1}$$

Since synchrotron sources have a high flux, the scattering from air can be neglected and environmentally controlled experiments can be undertaken. The Advanced Photon Source at Argonne National Lab in Argonne, IL has a synchrotron that was used for experiments related to this thesis.

Scattering experiments have been used to show how domains in proton exchange membranes swell with water uptake [43]. In the Herring group, SAXS experiments have been performed using a custom-built, four-sample oven that allows for temperature and humidity

control [11,43–54]. The humidity is controlled by a wet gas / dry gas mixture and a manual adjustment to achieve the desired humidity as measurement by a Vaisala HMT 337 probe. Stationary measurements of structure with humidity changes can be compared to changes in structure seen from straining the film.

Polymers can undergo a phase transition through a shear force rather than a typical thermal transition. Liu, et. al. recently demonstrated how a polybutene-1 system's percent crystallinity changed under tensile stress at isothermal conditions [55]. Using a homemade extensional rheometer, Tian, et. al. found extensional flow induced crystallization of poly(ethylene oxide) [56]. This extensional force system is similar to the experiments performed in this thesis to investigate morphology change with strain.

Mao, et. al. [57] investigated the structural evolution of a propylene-1-butylene random copolymer subjected to uniaxial tensile deformation. The majority of their quantitative work was done with the wide angle x-ray scattering. An Instron machine was used to apply the uniaxial stretching.

Kamal, et. al. [58] used a Linkam TST-350 tensile tester to uniaxially stretch a poly (e-caprolactone) sample *in situ* with SAXS and WAXS at room temperature conditions. They identified three zones of crystallinity from the stress-strain curve and verified with the scattering patterns. The x-ray data fit nicely to tell a story of how the structure evolved with increasing strain. The intensity was taken at some angle from center and was usually the max intensity point along that line. They define a parameter denoting the distance between lamellae structures and show how the length doubles with extension.

Polizzi, et. al. [59] investigated the scattering behavior of styrene-butadiene-styrene block copolymers during stretching in the early 1990s. They saw a scattering pattern that formed

elliptical patterns aligned perpendicular to the stretching direction. From this, they concluded that the polystyrene cylinders at rest were arranged in a close-packed structure and were affine up to a draw ratio of about 3. After this critical extension, the polystyrene cylinders moved such that their axes were perfectly oriented along lines parallel to the stretching direction. This transition region correlated with the inflection point in the stress-strain curve.

Stribeck, et. al. investigated blends of polyethylene and polystyrene-polybutadiene star block copolymers and observed a novel kind of deviation from Porod's law.

1.6 Thesis Statement

While others have performed basic mechanical testing of ion exchange membranes, I believe tensile testing under controlled temperature and relative humidity conditions will provide a better frame of reference for comparison between polymer chemistries. I believe a set of quantifiable set of metrics can be established based on these tensile tests and hygral cycling of the membrane. I believe a relationship between the Young's modulus, elongation, and water uptake can be used to predict membrane durability in a working electrochemical device.

CHAPTER 2

EXPERIMENTAL METHODS

2.1 Rheometry

Rheological measurements were done on an ARES-G2 rheometer (TA Instruments) using a modified Sentmanat Extensional Rheometer (SER) [40]. Details on the SER fixture are available elsewhere [20]. Samples were cut into rectangles measuring between 2-4 mm and about 20 mm long. Thicknesses ranged from 30-100 microns. Tests were run at various temperature and relative humidity conditions using the custom oven described in Chapter 3. Extensional rates were based on testing conditions modified from ASTM D882, Tensile Properties of Thin Plastic Sheeting [60]. According to the standard, the speed of the testing and the grip separation are dependent on the percent elongation at break. The speed of the testing is calculated from the initial strain rate multiplied by the initial grip separation. With the SER drums, the speed of the drum rotation can be altered, but the separation distance between the drums is fixed. Using the same formula as the ASTM standard and a fixed grip separation of 12.7 mm (distance between the center point of the two SER drums), a rate of grip separation can be calculated. This grip separation rate is then converted to an engineering strain rate using the geometry of the drums, yielding an engineering strain rate of 0.33 s^{-1} for materials whose elongation to break was greater than 100%. For elongation less than 20%, the rate used was 0.0033 s^{-1}, and for elongation between 20% and 100%, the rate of 0.0167 s^{-1} was used. At least five replicates were averaged for the final data. Error bars are one standard deviation.

Extensional tests on the SER measure stress as a function of engineering strain (Figure 2.1). To compare SER data with typical tensile measurements, an Engineering Stress was calculated using the fixed starting area of the sample. (Extensional Stress is the property that

factors in the exponential decrease in sample area.) The stress at break and Young's modulus were calculated from the Engineering Stress. Young's modulus was taken as the slope at low strains in the linear, elastic region. The stress at break was taken as the stress at the break point. Elongation is calculated by multiplying the final engineering strain by 100. A yield stress could be determined from the stress-strain curves, but it is not investigated in this work. At least five tests were run for each sample.

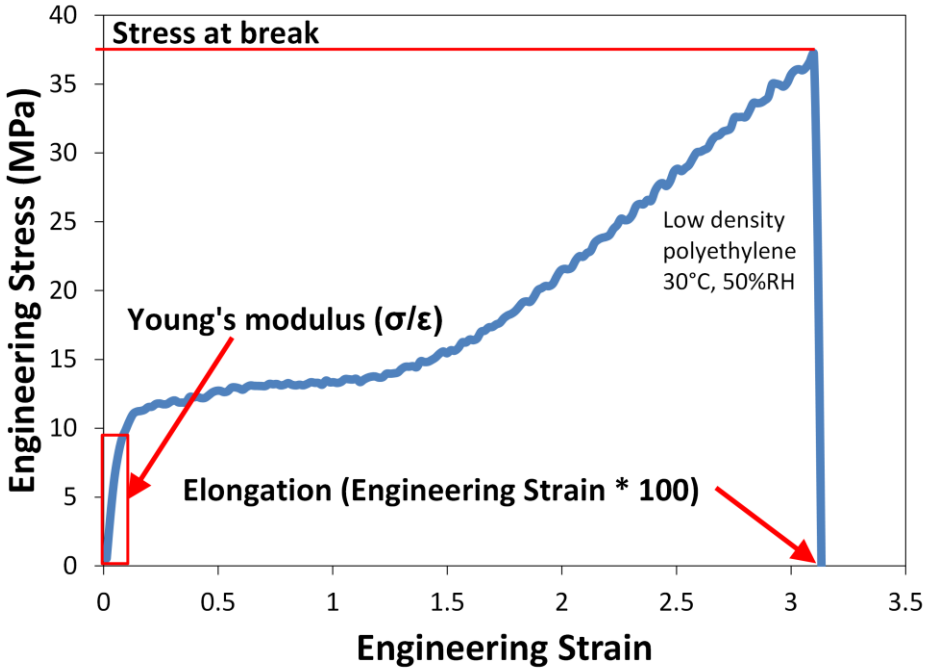

Figure 2.1 Example of a typical stress-strain curve from the modified SER tool. The three main properties (Stress at break, Young's modulus, and Elongation) are depicted.

2.2 Conductivity

Ionic conductivity was measured by electrochemical impedance spectroscopy using a four-electrode in-plane conductivity cell. Impedance spectra were obtained over a frequency range of 0.3 to 10^6 Hz using a multi-channel potentiostat (BioLogic VMP3). A TestEquity sample chamber controlled temperature and humidity during data acquisition. Membrane resistance was defined as the low frequency intercept of the Nyquist impedance plot and conductivity, σ, was calculated using the film dimensions where R is the membrane resistance, l

is the length between electrodes, and *t* and *w* are the thickness and width of the membrane sample, respectively (2.1).

$$\sigma = \frac{l}{R \cdot t \cdot w} \tag{2.1}$$

Reported conductivity data are the average of at least three separate membrane samples and multiple impedance spectra at each steady-state temperature; error bars are one standard deviation.

2.3 Water uptake

Water uptake (*WU*) was characterized using a dynamic vapor sorption apparatus (SMS DVS Advantage 1, Allentown, PA). A membrane sample, about 4 mm^2, was placed on a glass weigh plate and the change in mass was measured gravimetrically under different humidity conditions. The *WU* of the membrane was calculated based on equation (2.2).

$$WU = \frac{m_{\%RH} - m_{dry}}{m_{dry}} \times 100 \tag{2.2}$$

where $m_{\%RH}$ is the mass of the sample at the given relative humidity and m_{dry} is the mass of the dry sample. The mass of the dry membrane was taken as the measured mass at the end of the initial 4-h drying period. Given the WU at saturated conditions and the known ion exchange capacity (*IEC*) of the membrane, the hydration level, λ, which is the number of waters per cation functional group, can be calculated using equation (2.3). The molecular weight of water ($m(H_2O)$) is needed to complete the equation.

$$\lambda = \frac{WU}{m(H_2O) \cdot IEC} \tag{2.3}$$

2.4 Small angle x-ray scattering

Small angle X-ray scattering experiments were performed at the X-ray Sciences Division, beamline 12-ID-B, at the Advanced Photon Source at Argonne National Laboratory. Measurements were taken in a transmission geometry using a Pilatus 2M SAXS detector at a beam energy of about 14 keV (λ = 0.89 Å) and a sample-to-detector distance of about 2500 mm. A Sentmanat Extensional Rheometer (SER) (Xpansion Instruments) was used to apply a bidirectional strain on the films. The SER drums were modified to handle solid polymer films below their melting temperature [40]. The SER tool was powered by a stepper motor and was housed in a custom built oven with forced convection heating. The oven allowed for the x-ray beam to travel between the counter-rotating drums [61,62]. The exposure time was generally 1 s and the shots were taken either 3 or 5 seconds apart. The engineering strain rate used was 0.01 s^{-1} as this was the slowest rate the stepper motor could handle and still render a smooth rotation. The slow rate allow for the most x-ray shots while the film was undergoing extension.

In order to quantify the changes in the polymer structure with strain, the movement of peaks in defined wedges was tracked. Using the Nika macro [63] in Igor to handle the 2D SAXS image, a wedge was defined as ±2° around 90° and 180° (0° being the right horizontal line) after applying the beam mask and subtracting the background. The intensity as a function of the scattering vector q was averaged within the wedge. Using the Irena macro [64], the 1D I(q) plots were used to track the movement of peaks as strain increased.

Solutions were also run at the X-ray Sciences Division, beamline 12-ID-B, at the Advanced Photon Source at Argonne National Laboratory. Measurements were taken in a transmission geometry using a Pilatus 2M SAXS detector at a beam energy of 14 keV (λ = 0.89

Å) and a sample-to-detector distance of 2029 mm. The solutions were placed in a 2 mm diameter quartz capillary tube.

2.5 Water stress

The water stress measurement is a new method of characterizing the mechanical response of ion exchange membranes under cyclic hydration conditions. The membrane was loaded on the film/fiber tool on the TA Instruments ARES-G2 rheometer. Once the membrane was loaded, it sat for an hour at 80°C and 90%RH in order to reach a steady-state mass uptake. The membrane was then stretched to put a small tension while keeping the film in the elastic region without going to plastic deformation. This region was defined by the tensile testing data at 60°C, 90%RH. Using the environmentally controlled oven, the membrane was subjected to alternating cycles of 95%RH and 0%RH at 80°C. The cycle time varied. Short cycle times of 10 minutes were used to mimic accelerated testing protocols used by industry sources, while 60 minute cycles were done to allow the membrane to reach steady-state water absorption and desorption for each cycle. Samples were ~3 mm wide and the initial gap was set to 10 mm. At least two replicates were done for each reported measurement. The water stress was calculated by subtracting the difference in measured stress from the wet cycle to the dry cycle. As the membrane dried out, the film contracted and this contraction forced was measured by the rheometer's axial force transducer. Once the humid atmosphere was reintroduced, the film absorbed water and relaxed, thus decreasing the axial force.

CHAPTER 3

MECHANICAL TESTING OF SMALL, THIN SAMPLES IN A HUMIDITY- CONTROLLED OVEN

This chapter is modified from a paper published in

Rheologica Acta[1]

Benjamin R. Caire[2], Melissa A. Vandiver[3], and Matthew W. Liberatore[4]

3.1 Abstract

A new fixture for the mechanical characterization of thin polymer films under controlled temperature and relative humidity conditions is reported. Novel conducting polymers are often synthesized in small quantities and processed into films on the order of 10-100 microns thick. Standard tensile tests does not allow for adequate testing of these small sample sizes. Hence, a modification of the Sentmanat Extensional Rheometer (SER) to perform tensile testing on thin membranes is presented. Since the standard L-shaped pins do not secure thin polymer films at lower temperatures (i.e., below the melting point), screw down clamps were created to allow for mechanical characterization of solid polymer films. The new testing apparatus allows for mechanical characterization with as little as 2% of the material needed for testing on a traditional tensile tester. In a parallel effort, a humidity delivery system developed for the TA Instruments ARES-G2 rheometer allows for testing at a range of temperatures (30-100°C) and relative humidity conditions (0-95% RH). The novel oven was benchmarked with low density polyethylene and Nafion 115®. While the new experiment was built for characterization of ion

---

[1] Reprinted with permission of the *Rheologica Acta,* (2015), **54**, 253-261
[2] Primary author and researcher
[3] Co-author, Ph.D. Candidate
[4] Author for correspondence, advisor

exchange membranes for fuel cells, the oven is capable of characterizing any environmentally sensitive material using all standard rheometer geometries.

3.2 Introduction

The mechanical properties of numerous materials are affected by a change in either temperature or relative humidity. Consumer products, such as clothing [65–68], food packaging [69–71], elastomers/sealants [72,73], and chewing gum [74], exhibit large effects due to changes in temperature, hydration, pressure, or other environmental conditions. Ion exchange membranes, particularly polymer membranes used in fuel cells [27] are another class of environmentally sensitive materials. The performance of these membranes is greatly impacted by their hydration level and operating temperature. Specifically, understanding how temperature and humidity alter the mechanical properties of ion exchange membranes is critical to optimal fuel cell performance.

The three most commonly reported mechanical properties are Young's modulus, tensile strength, and elongation to break [75]. These properties are determined from a stress-strain curve obtained by pulling the sample at a known rate and measuring the resulting resistance force until the specimen breaks. The testing rate and specimen size are determined based on the material and the testing station; the ASTM has published guidelines for appropriate testing procedures. The Young's modulus, a measure of the stiffness or elasticity of a material, is the slope at low strain. The break point defines the elongation and tensile strength. Changes in the mechanical properties of polymers will be explored here and can range from elastic and rubbery (e.g., polybutadiene) to stiff and brittle (e.g., polystryrene, polycarbonate).

Mechanical testing of thin polymer films is covered by ASTM spec D882, Standard Test Method for Tensile Properties of Thin Plastic Sheeting [60]. The specimens are cut into rectangular shapes instead of the dog-bone shape traditionally used in tensile testing. The

guidelines for strain rate account for the elongation of the material being tested, with faster rates given for materials with a large elongation to break. Since the D882 standard is used for plastic sheeting and films less than 1 mm thick, it is used a basis for the test protocol developed in this work.

Since the introduction of Xpansion Instruments' Sentmanat Extensional Rheometer (SER) [20] in 2004, it has been the standard method for extensional viscosity measurements. Highly cited articles using the SER have focused on characterizing polyethylene melts [21–23]. Other polymers studied include polybutene [24] (with TA Instrument's Extensional Viscosity Fixture) and a well-entangled monodisperse styrene-butadiene random-copolymer [25]. While the SER tool is excellent at characterizing polymers in their melt state, few examples study solid polymer films [20]. The mechanical properties of electrospun polyurethane from a dimethylformamide (DMF) solution onto differing supporting textiles were investigated using the SER [26]. Even though their films were only 10 microns thick and in the solid state, the SER fixture was used by applying double stick tape to the drums. Successful measurements of Young's Modulus, Maximum Stress and Maximum Strain were recorded. The authors note: "With respect to mechanical testing by using SER, it should be mentioned that the main advantage of this 'rheology based' methodology is the possibility to measure very fine structures with low experimental error due to the utilization of very sensitive torque/normal force transducers, which are normally present on standard rotational rheometers for polymer melt rheology evaluation. Moreover, the measurements can be done at different extensional strain rates and temperatures by using the conventional rheometer oven, which is difficult or impossible to do by using standard methodologies."

Environmentally controlled ovens are used in many other mechanical characterization techniques. A commercial DMA with relative humidity control is sold by TA Instruments. Majsztrik, et. al., built an oven to perform tensile creep experiments [39], and White, et. al., built an oven to perform accelerated stress testing on building sealants, which included UV exposure in conjunction with temperature and relative humidity control [73]. The most common way to control relative humidity is with a wet gas/dry gas mixture.

This work showcases a new way to test thin polymer films below their melting temperature on the SER tool as well as a custom-built oven to control the environment. The oven is capable of a range of temperatures and can control steady-state humidity conditions from dry up to 95% as well as transient temperature and relative humidity ramps. The system is verified using a non-water absorbent material, polyethylene, and a water absorbent material, Nafion® 115. While a few measurements from this device were featured in a previous publication on anion exchange membranes [76], the complete description and validation of the system is reported here.

3.3 Experimental

3.3.1 Modification of SER fixture

The SER fixture was designed primarily to test the extensional viscosity of thick polymer samples at or near their melting temperature; however, our goals are to test thin polymer films at temperatures below the melting point. The standard L-shaped pins did not hold our thinner samples to perform the desired tensile test at temperatures well below the polymer melting temperature. Several attachment mechanisms were attempted to enable testing of polymer films less than 100 microns thick. Double stick tape, glue, and magnets were not able to hold the films in place consistently (or provide statistically reproducible data). Since most tensile testers use

screw down clamps to hold the samples in place, new drums were machined with screw down clamps (Figure 3.1). A silicone rubber pad was added to the underside of the clamps to soften the grip on the sample. One of the main advantages of using the SER tool as a tensile-like tester is the reduced amount of material needed for characterization. According to ASTM D882, a specimen with greater than 100% elongation will need to be at least 100 mm long and could be as wide as 25.4 mm for a sample area of 2540 mm^2. The SER tool can handle a sample as small as 20 mm long and 3 mm wide for a sample area of only 60 mm^2 (i.e., <2.5% of the material of a traditional tensile test).

The SER tool is a bidirectional tester with a fixed length between the grips and requires the sample be elastic enough to wrap around the drums, which differs from a typical tensile tester that operates unidirectionally and has a fixed volume for testing. Using the SER tool on a rheometer has the advantages of faster testing speeds and a more sensitive transducer for the characterization of a wide range of materials.

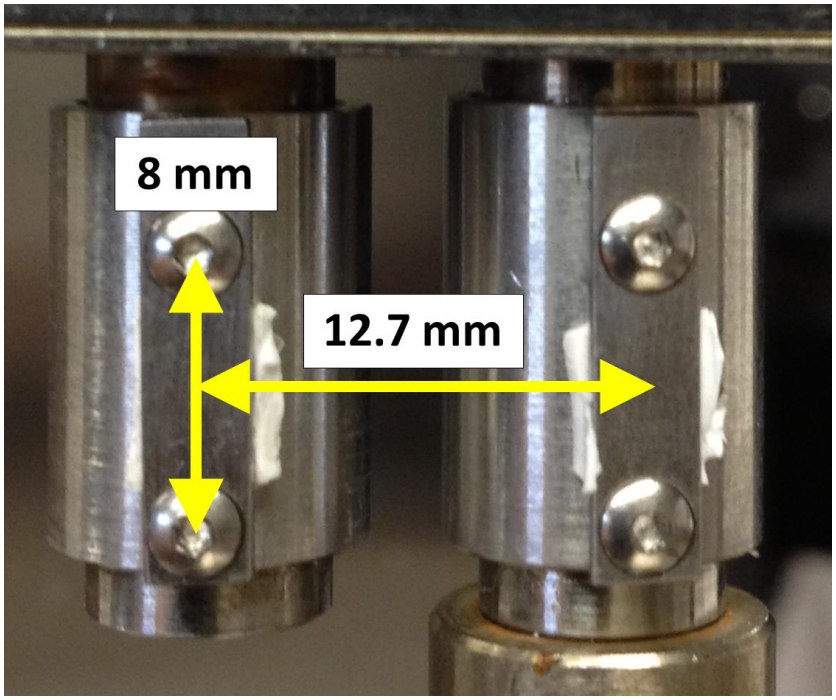

Figure 3.1 Modified SER fixture with screw down clamps and rubber pads

3.3.2 Humidity delivery system

In order to control humidity, dry and wet air streams were mixed and delivered to the oven. Building air was supplied at 80-100 psig, dry (<5%RH), and unfiltered. A filter/regulator combination cleaned and controlled the base air supply to 50 psig. The clean air was subsequently split into two separate mass flow controllers (MKS 1179A, 10,000 SCCM max flow rate), for a wet and dry gas supply. A bypass line on the dry gas side with a manual ball valve allows for purging. The wet gas exits the mass flow controller and enters a high flow humidity bottle (Fuel Cell Technologies, Inc.) containing 10 m of Nafion® tubing. The humidity bottle is designed to produce an exiting gas stream that is completely saturated. The bottle can be heated such that higher dew points can be achieved. The bottle is the same as ones in use on similar setups [43,44], but is bigger due to the larger oven volume needed for rheology testing. The larger bottle with more Nafion® tubing allows for the longer residence time needed for high relative humidity conditions at elevated temperatures. Tubing between the humidity bottle and oven was heated and insulated to prevent condensation in the lines. The wet and dry gas lines merge at a tee junction and enter a static mixer (Koflow, 12 elements). Finally, a flexible heated line connected the mixer to the custom built oven. The flexible heated line allows for the oven to be moved out of the way for sample loading. The oven is mounted on a swinging arm attached to the existing support bar on the rheometer (Figure 3.2).

The custom built oven was designed for temperature control via electrical heaters independent from the humidity control via a wet gas/dry gas mixture. The clam-shell design features four cartridge heaters (Omega 500W, 128 W/in^2) wired in parallel to act as a single heater placed in the outer shell of the oven. Ports were placed on the oven to allow for a camera,

gas inlet, dew point sensor, thermocouple and light (Figure 3.3). Insulation was wrapped around the oven to minimize heat loss and for safer operation.

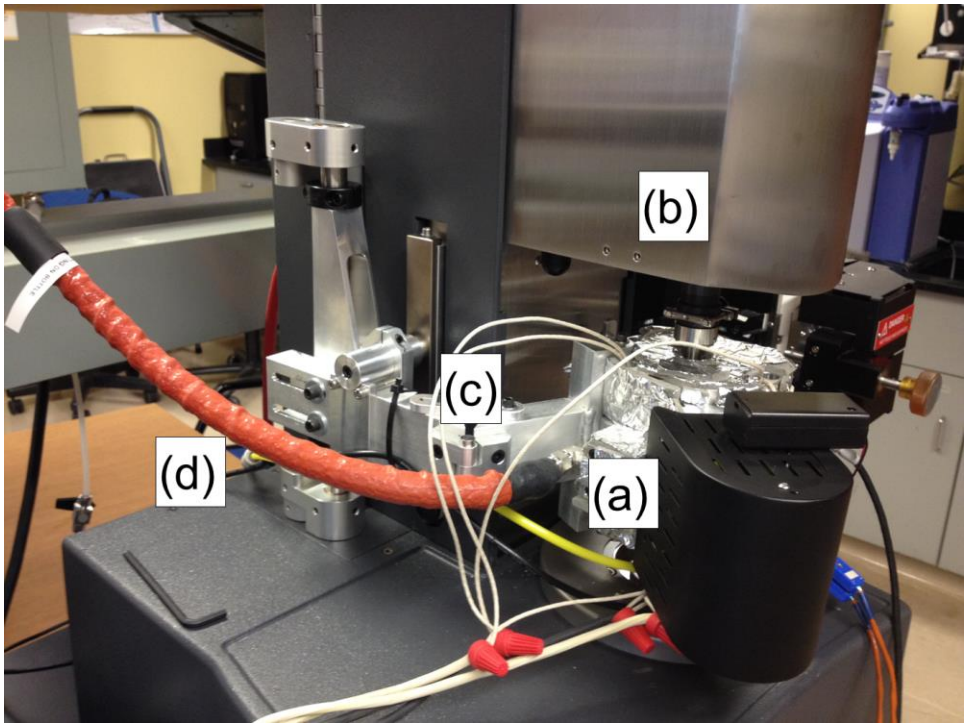

Figure 3.2 Custom oven (a) attached to rheometer (b) with a swinging arm (c) and gas delivered through heated flex tubing (d)

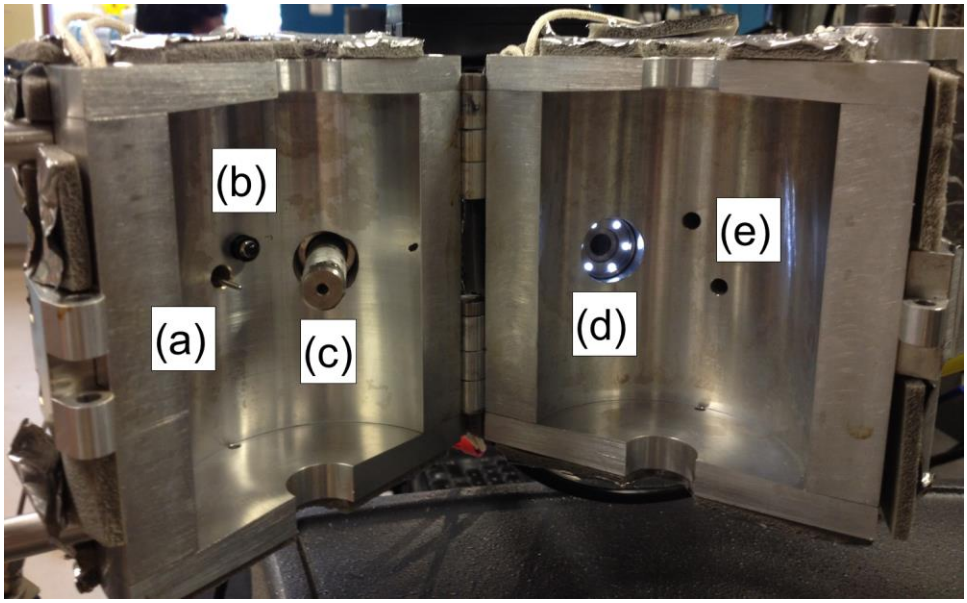

Figure 3.3 Picture of the inside of the oven: a) thermocouple, b) light, c) dewpoint sensor, d) camera, e) gas inlets

The temperature of the lines and oven are controlled via a thermocouple feedback loop (Watlow EZ-ZONE PM6). A Vaisala HMT337 dew point sensor was installed in the oven for relative humidity measurement. All the system inputs were brought into LabView for control of the entire system via two PID feedback loops; relative humidity is controlled by adjusting the wet gas flow and the temperature is controlled by electrical heaters.

A previous attempt to control temperature and humidity in the rheometer's Forced Convection Oven provided a limited range of conditions. This system attempted to control both temperature and humidity with the incoming gas stream. Hot, humid air delivery was able to generate some humidity conditions up to 60 °C, although simultaneous temperature and humidity control was difficult.

3.3.3 Materials

A low density/linear low density polyethylene (LDPE/LLDPE) film was obtained from a local custom blown film manufacturing plant (ExxonMobil Exceed 1018). The thickness of the film was 36 microns and all tests were completed in the machine direction. Nafion® 115 (DuPont) was obtained from Ion Power, Inc. The film was prepared via the standard method [77] of boiling in 0.5M sulfuric acid for an hour, deionized water for an hour, 3 wt% hydrogen peroxide for an hour, and finally deionized water again for an hour. The membrane was then placed in an oven at 80°C for over 12 hours.

3.3.4 Testing procedure

To benchmark the new testing apparatus, the LDPE/LLDPE and Nafion® N115 were tested. The polyethylene was tested in the dry and wet environments to find any effects the humidification system has on mechanical testing. Humidity induced changes in the mechanical properties of Nafion are well studied and will be compared to in this work.

The mechanical testing was performed using the SER attached to an ARES-G2 Rheometer (TA Instruments) using testing conditions modified from ASTM D882, Tensile Properties of Thin Plastic Sheeting [60]. According to the standard, the speed of the testing and the grip separation are dependent on the percent elongation at break. The speed of the testing is calculated from the initial strain rate multiplied by the initial grip separation. With the SER drums, the speed of the drum rotation can be altered, but the separation distance between the drums is fixed. Using the same formula as the ASTM standard and a fixed grip separation of 12.7 mm (distance between the center point of the two SER drums), a rate of grip separation can be calculated. This grip separation rate is then converted to an engineering strain rate using the geometry of the drums, yielding an engineering strain rate of 0.33 s^{-1} for materials whose elongation to break was greater than 100%.

Extensional tests on the SER measure stress as a function of engineering strain (Figure 3.4). To compare SER data with typical tensile measurements, an Engineering Stress was calculated using the fixed starting area of the sample. (Extensional Stress is the property that factors in the exponential decrease in sample area.) The stress at break and Young's modulus were calculated from the Engineering Stress. Young's modulus was taken as the slope at low strains in the linear, elastic region. The stress at break was taken as the stress at the break point. Elongation is calculated by multiplying the final engineering strain by 100. A yield stress could be determined from the stress-strain curves, but it is not investigated in this work. At least five tests were run for each sample. The samples were about 20 mm in length and between 2-4 mm in width. The thickness varied from 20-140 microns. The mass of one sample was on the order of 5 mg.

The humidified tests with Nafion® were allowed a soak time of 15 minutes before testing began, which is similar to soak times found elsewhere [78–80].

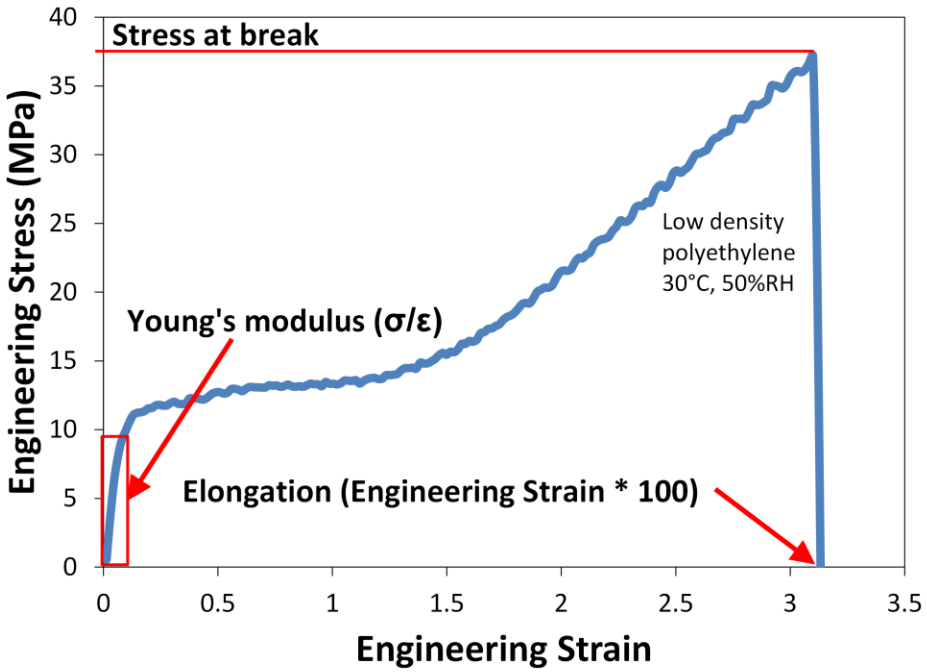

Figure 3.4 Typical stress-strain curve with the Stress at break, Elongation, and Young's modulus shown.

3.4 Results and Discussion

3.4.1 Environmentally controlled oven

The new oven is capable of generating a wide range of temperature and relative humidity conditions needed for mechanical characterization of anion exchange membranes (Figure 3.5). Although not shown, temperatures up to 150°C are possible in the new oven. Conditions available include steady-state relative humidity and temperature (Figure 3.6), ramps of relative humidity at constant temperature (Figure 3.7), and ramps of temperature at constant relative humidity (Figure 3.8). Ramps of temperature or relative humidity can be combined with dynamic mechanical analysis testing to probe other properties, such as the glass transition temperature (T_g) of polymers.

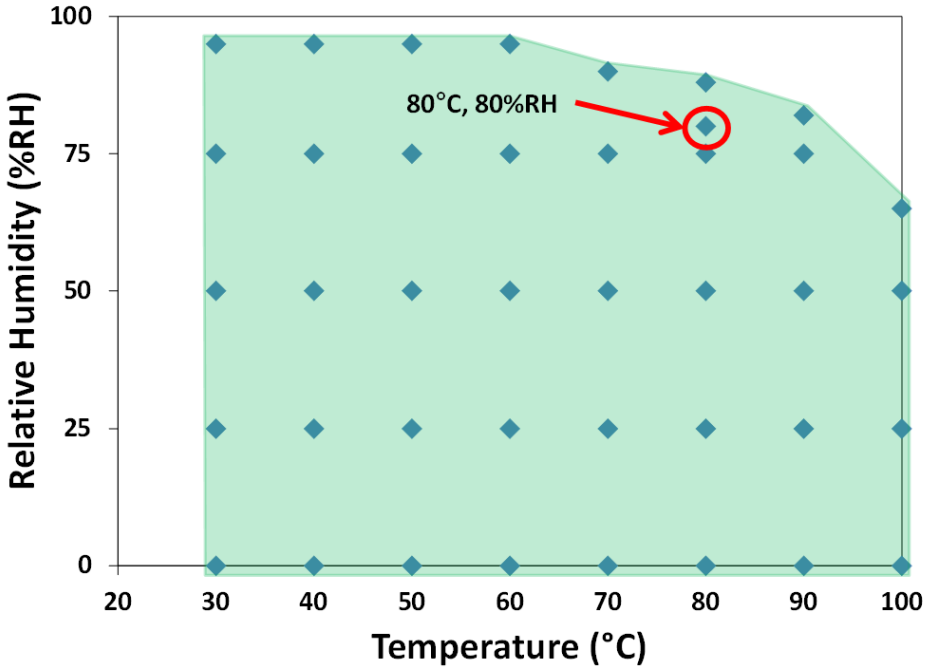

Figure 3.5 Range of temperature and relative humidity conditions available

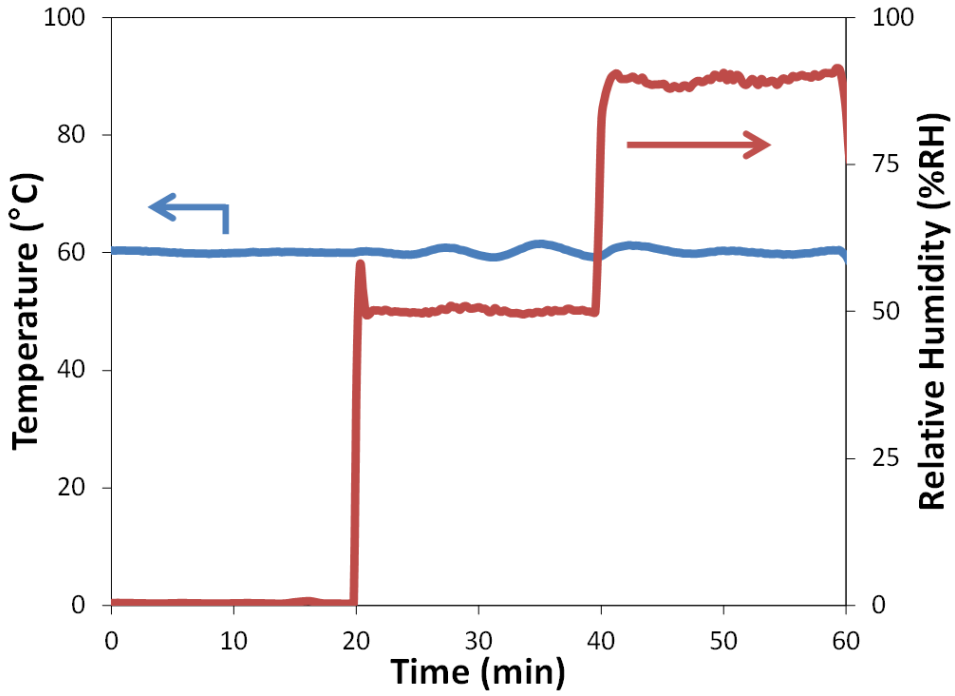

Figure 3.6 Step changes in relative humidity at 60°C

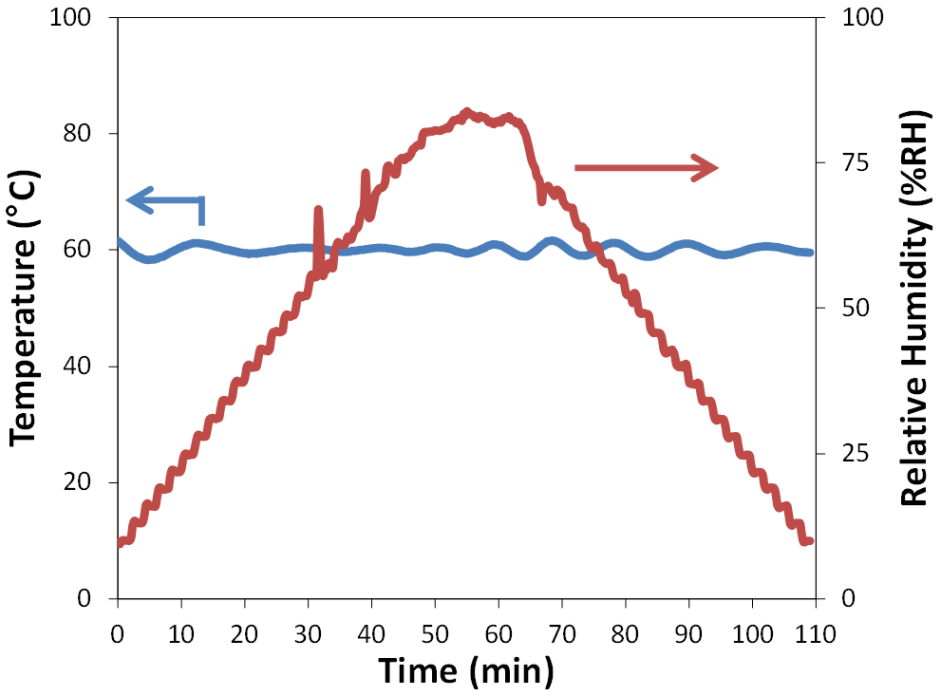

Figure 3.7 The relative humidity can be ramped at constant temperature, in this case, 60°C

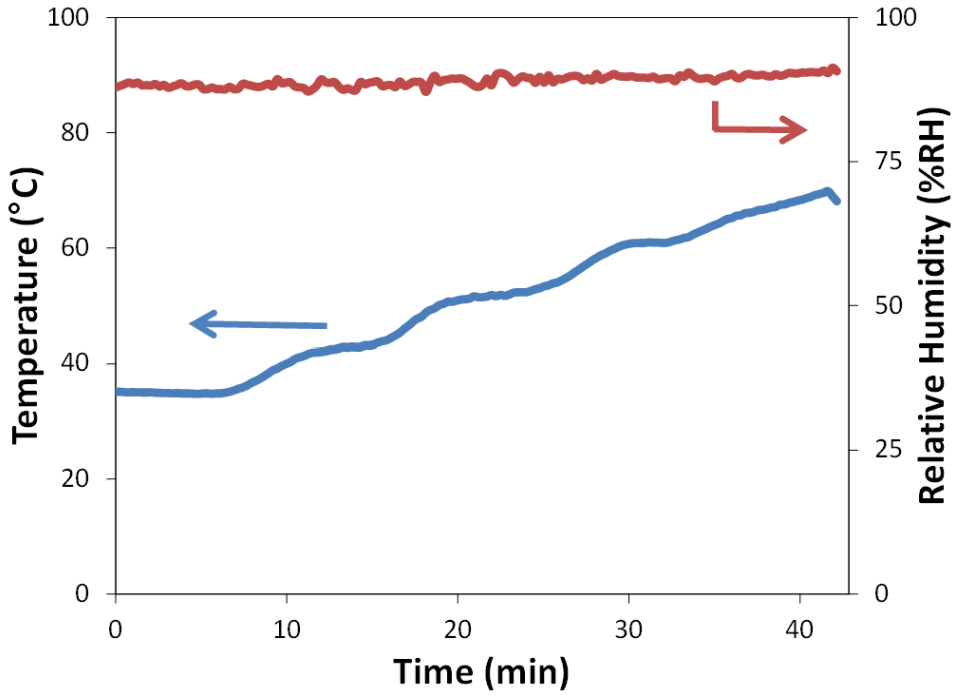

Figure 3.8 The temperature can be ramped while maintain constant humidity, in this case, 90%RH

3.4.2 Tensile-like testing on the SER

To quantify the effects of the relative humidity on SER extensional measurements, LDPE/LLDPE was tested at dry, 50%RH, and 90%RH conditions. The samples were ~3 mm wide and 36 microns thick. Polyethylene should have negligible response to water as it is a hydrophobic polymer. This hypothesis was confirmed as relative humidity did not have significant effects on the mechanical properties at 30°C or 60°C (Figure 3.9). For example, the stress at break at 30°C (~35 MPa) and the Young's modulus at 60°C (~73 MPa) are statistically the same across all humidity conditions.

As an example of a polymer that has a mechanical response to water content, Nafion ® 115 was also tested. The specimens were ~3 mm wide and 125 microns thick. Mechanical properties measured at three different conditions were similar to information on the DuPont™ data sheet [81] (Figure 3.10). We were able to match the room temperature condition, but the 23°C, water soaked and 100°C, water soaked conditions reported by DuPont were compared with data taken at 30°C, 90%RH and 90°C, 80%RH, respectively. The tensile strength reported here was 12-15% less than what DuPont reports for the 23°C condition and 36% less for the 100°C condition. Water soaked properties are generally taken by removing the sample from water, blotting the sample dry, and then testing immediately, although DuPont does not state this explicitly in their data sheet. A water soaked membrane will have a higher water content than one in a saturated gas environment at the same temperature. The hydration difference most likely explains the difference as excess water lowers strength. The differences in morphology and other properties in membranes were explored in water soaked versus saturated vapor. [82,83]

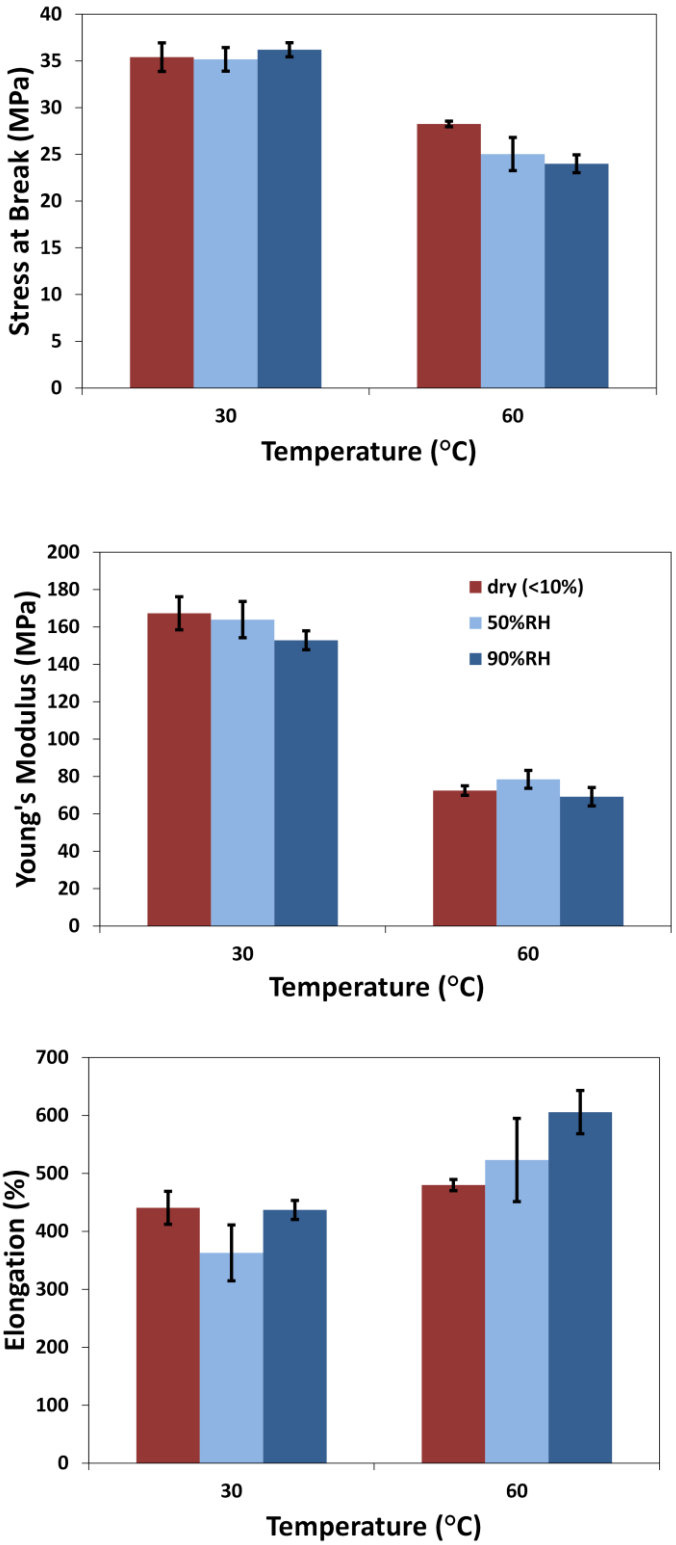

Figure 3.9 LDPE/LLDPE mechanical properties at elevated humidity compared to dry

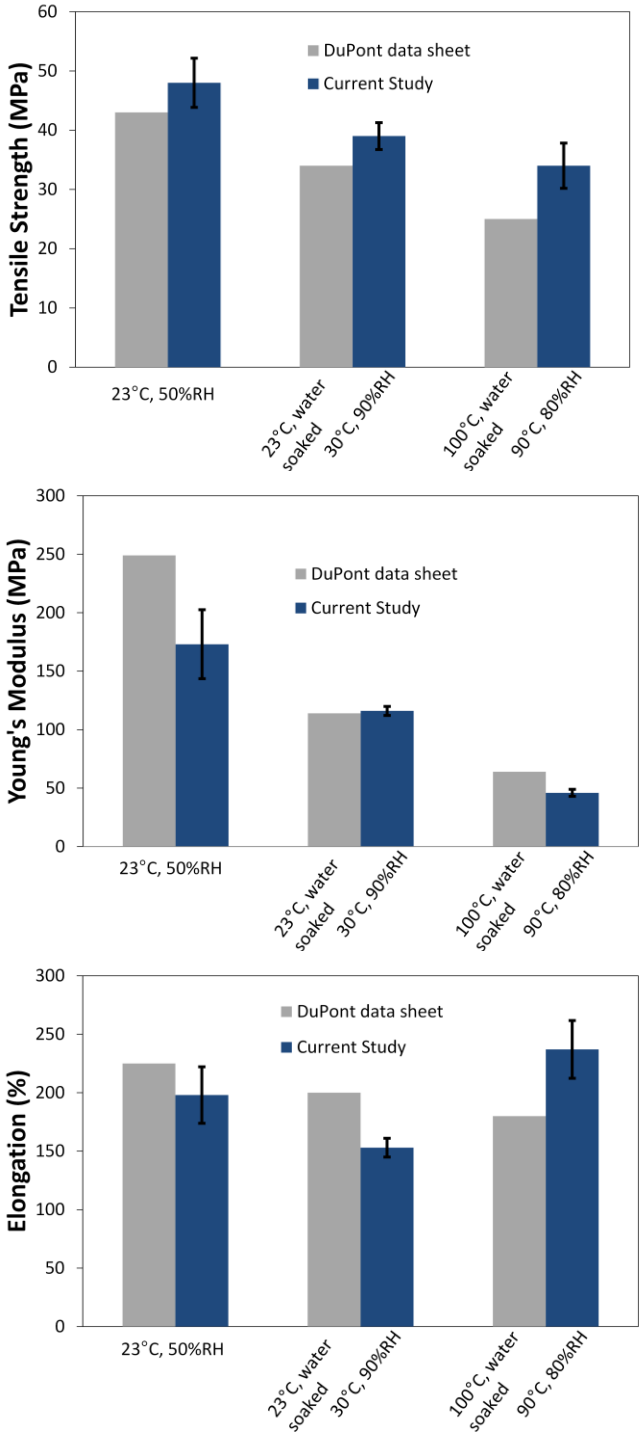

Figure 3.10 Comparison of data from DuPont™ (Data sheet) and data gathered from this work on Nafion® 115

Nafion® 115 samples were also tested at a low (30°C), medium (60°C), and high (90°C) temperature in dry (10%RH) and wet (90%RH) conditions (Figure 3.12). Intermediate relative humidity conditions of 25%RH, 50%RH, and 75%RH were also tested at 60°C (Figure 3.13). It is well known that water plasticizes Nafion® and our work confirms this effect. Young's modulus and tensile strength decrease with increased humidity (Figure 3.11). Temperature has a greater effect on Young's modulus than stress at break and elongation.

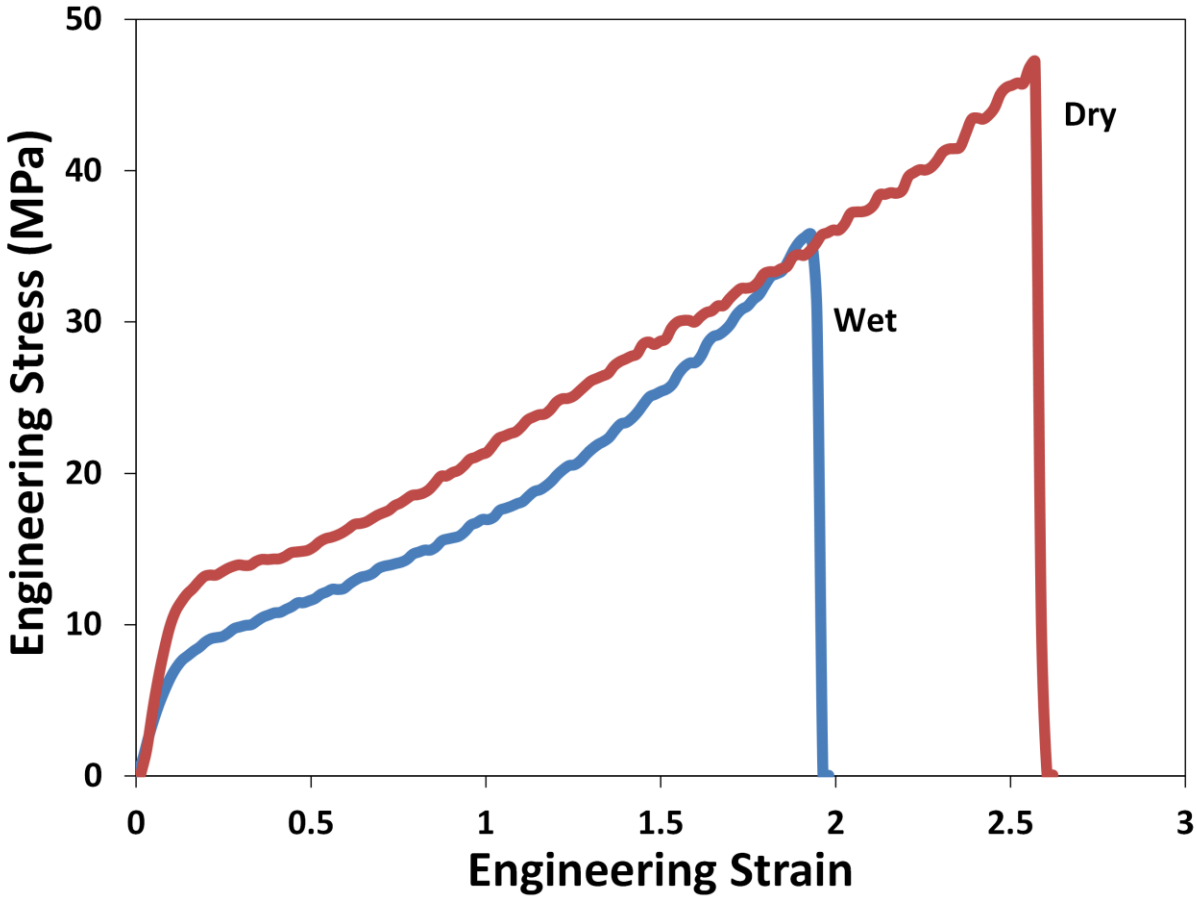

Figure 3.11 Stress-strain curve at 60°C of Nafion® 115 in both dry and wet conditions

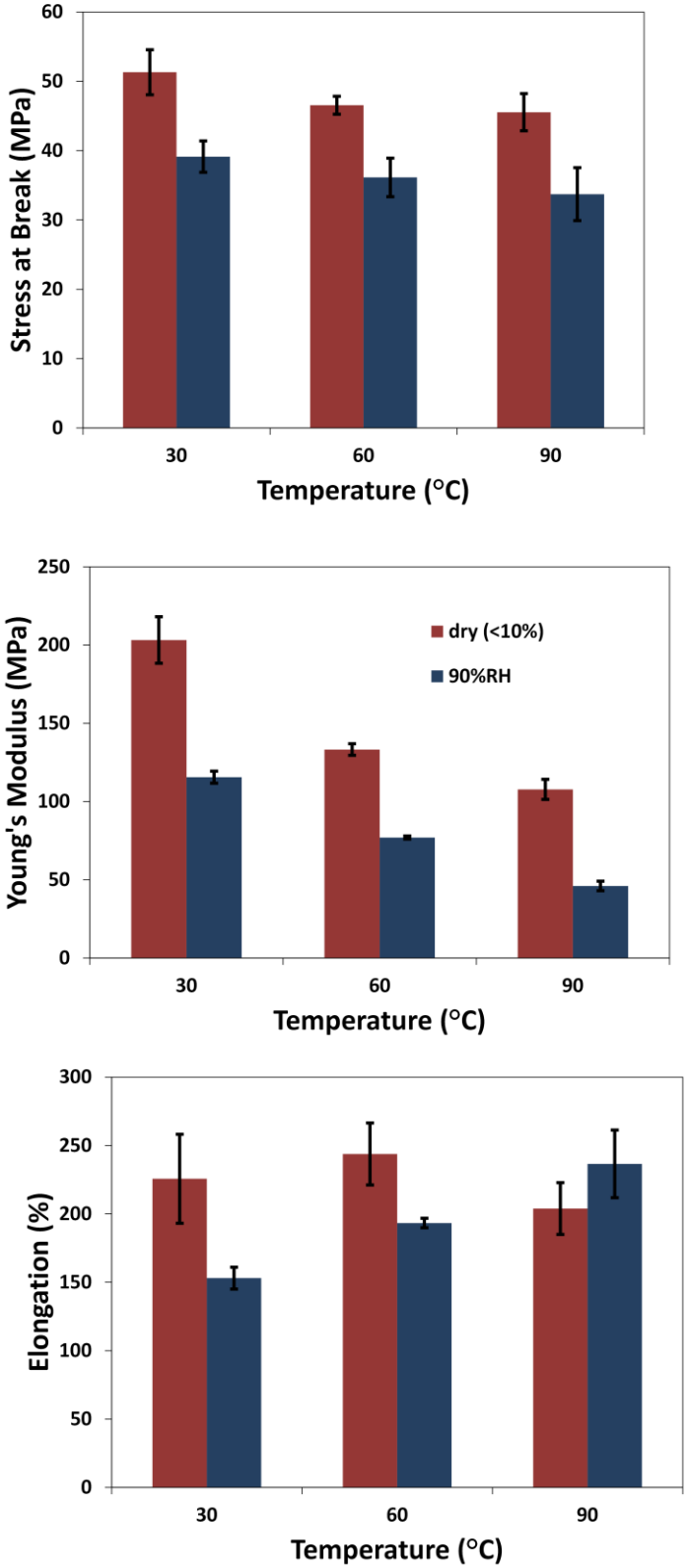

Figure 3.12 Mechanical properties of Nafion® 115 at 10% and 90%RH across multiple temperatures

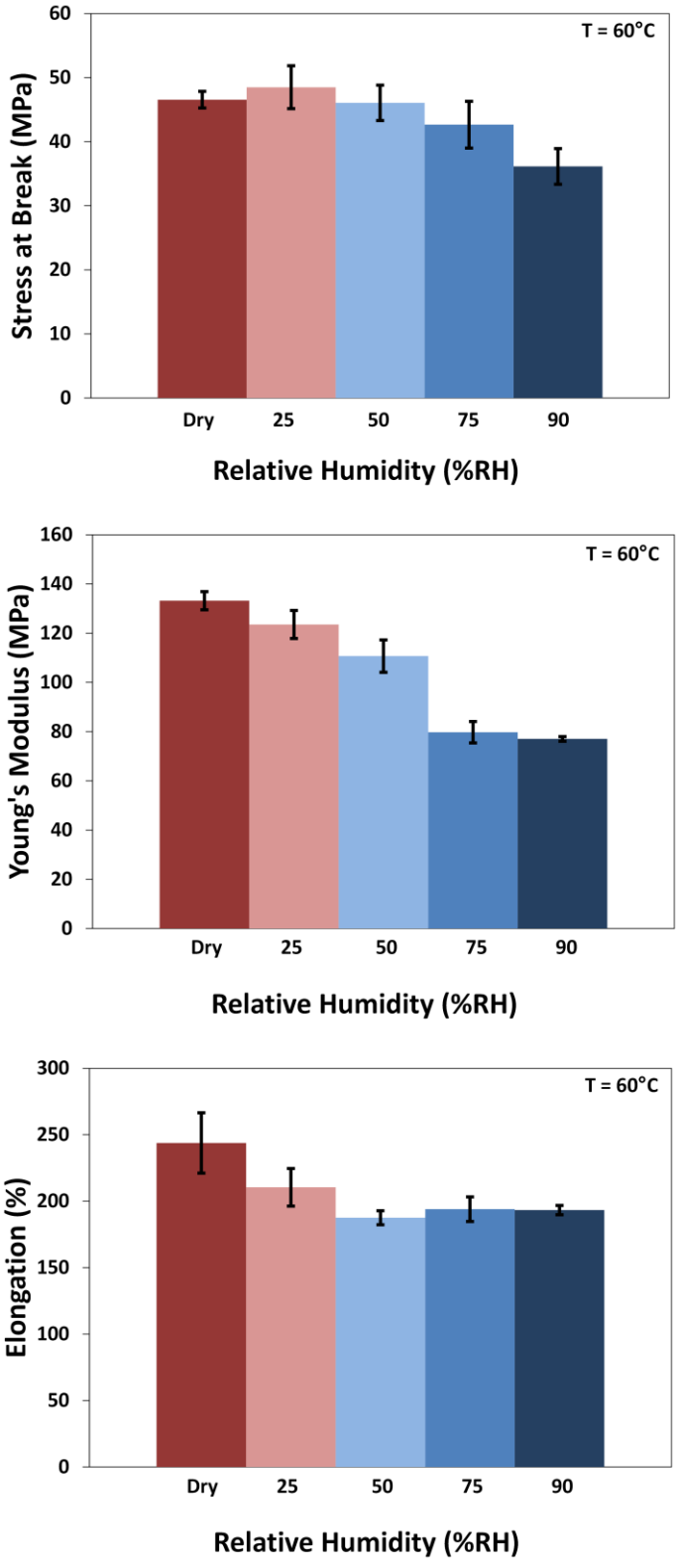

Figure 3.13 Mechanical properties of Nafion ® 115 at 60°C and multiple relative humidity conditions

The intermediate humidity data at 60°C shows the gradual transition of all the properties as the water content increases. The strength and elasticity was maintained until the relative humidity was 75% or greater while the elongation drops off at only 50%RH (Figure 3.13).

These results compare favorably with other work done on the mechanical properties of Nafion®. The modulus data reported here at all conditions is within the error of data reported by Tang, et. al., [84] on a thinner version of Nafion® (112), and qualitatively matches the trends in tensile strength and elongation. The 90°C elastic modulus data at dry conditions reported here (~110 MPa) match work done by Jalani, et. al. [85] The Young's modulus at 60°C and 90%RH reported here (~75 MPa) is similar to work done by Satterfield et. al., [86,87] who used an Instron tensile tester and controlled humidity by equilibrating over saturated salt solutions. We report the elongation at room temperature conditions to be about 200%, which matches several literature sources [88–90]. Overall, an increase in elasticity with increasing temperature and relative humidity is reported consistently in the literature as well [84,86,91,92]. The effect of water and temperature on the mechanical properties of Nafion® is still a widely studied topic [93–95].

3.5 Conclusion

We have developed tools to perform tensile-like testing of small, thin (10-100 micron) polymer films at controlled temperature and relative humidity conditions. The modified SER fixture is shown to be an adequate replacement for tradition tensile testers to evaluate small quantities of thin polymer films. The environmental chamber is robust and can handle steady-state as we well as transient conditions. In a steady-state test at 60°C and 50%RH, the temperature control is ±1.5°C of set point and the humidity is ±0.6% of set point. The humid environment does not affect the SER tool's measurement as evidenced by insignificant variation

in data obtained at dry and wet conditions on the hydrophobic polymer polyethylene. Tensile strength of Nafion® 115 at room conditions was measured within about 10% of specification values. Properties obtained at elevated temperature and relative humidity conditions were consistent with several literature sources. While our future work will focus on anion exchange membranes, other materials, such as clothing, food packaging, elastomers, chewing gum, and electronics, will exhibit differences in mechanical properties with humidity, and these tools can facilitate the engineering of improved products.

3.6 Acknowledgements

The authors thank the U.S. Army Research Office (MURI Grant #W911NF-10-1-0520 and DURIP Grant #W911NF-11-1-0306) for its support of this work. The authors thank Aadil Elmoumni of TA Instruments for useful discussions. The authors thank Mountain States Plastics for the samples of LDPE/LLDPE blown films they provided. The authors thank Kurt Johnson and the whole team at Challenger Manufacturing Consultants for their expertise in designing and building the modified SER drums and the oven. The authors thank Jessica Earl (NSF sponsored REU student) for early modeling work on the transport dynamics in the oven.

CHAPTER 4

TRANSPORT AND MECHANICAL PROPERTIES OF A PENTABLOCK ANION EXCHANGE MEMBRANE

4.1 Abstract

Anion exchange membranes (AEMs) are a promising class of materials for use in fuel cells, barrier layers, and water splitting devices. In this study a pentablock commercial copolymer system is modified to form an anion exchange membrane via bromination chemistry. Three levels of bromination with resulting ion exchange capacities (IEC) ranging from 0.4 to 0.9 are investigated. Despite the low IEC, the polymer is highly conductive (up to 60 mS/cm at 90°C and 95%RH) with low water absorption (<25%) while maintaining adequate mechanical properties in both dry and hydrated conditions at 60°C. In solution, the brominated polymer forms a structure modeled as polydisperse hard spheres ~ 20 nm in diameter, and a film drop cast from the solutions forms lamellae about double the sphere size. The ionic polymer also forms a lamellar structure with a d-spacing of ~35 nm and the structure is maintained under hydration and extensional strain. The Brexar polymer delivers good conductivity with low water uptake and maintains mechanical integrity at high hydration conditions. The highest IEC level is a promising material for a separating membrane in an AEM fuel cell, while the lower IEC values are appropriate for applications where mechanical integrity is valued more than conductivity.

4.2 Introduction

Anion exchange membranes (AEMs) are a promising class of materials with applications such as electrochemical separation membranes and protective barrier layers [4,17,18,96]. Balancing conductivity with mechanical stability is one of the main challenges. Higher IEC materials have better conductivity, but absorb more water causing them to become mechanically

unstable. Mechanical reinforcement [30] or chemical cross-linking [47] can improve the mechanical integrity of the film, but it comes at the cost of lower conductivity. Optimizing both conductivity and mechanical properties is a significant challenge.

Structured polymers, which self-assemble into phase-separated morphologies, have shown great promise as ion conducting membranes for their potential to form ion conducting pathways [97,98]. Structured morphologies in diblock copolymers have higher conductivity than blends of the same materials [48]. Other diblock chemistries of poly(vinyl benzyl trimethylammonium) with a high T_g material (polystyrene [45]) and a low T_g material (polyethylene [99]) have been studied, but have fallen short of the properties needed for a successful AEM. A multi-block copolymer that balances the strength of a high T_g material with the flexibility of a low T_g material is presented here. Kraton Performance Polymers Inc. (Houston, TX) produces a pentablock copolymer under the tradename Nexar comprising of poly[t-butyl styrene-b-hydrogenated isoprene-b-sulfonated styrene-b-hydrogenated isoprene-b-t-butyl styrene] (tBS-HI-SS-HI-tBS), which they market for water transport, filtration, and separation applications.

Nexar in a mixed solvent of cyclohexane and heptane solution forms spherical micelles containing dense cores of SS and coronas of HI-tBS swollen by the solvent [100] (Figure 4.1). The degree of sulfonation affected the size of micelles formed. Both the radius of the micelle core and the closest approach distance between cores increased with sulfonation level, while the number density of micelles decreased. The micelle volume fraction plateaus as the degree of sulfonation increases. The solution study was followed up by casting membranes from the solutions and relating the structure-property relationship [101]. In membranes, the SS domains

were discrete when 2R < d and interconnected when 2R > d, where R indicates the core radius in solution and d represents the center-to-center distance of the SS microdomains in the membrane (Figure 4.2). Water uptake increased once the domains were interconnected. The polymer solution was neutralized with triethylaluminum (Et_3Al) and the micelle structure was maintained with the Al (3+) ions joining the SS in the core [102]. The neutralized structure exhibited lower water uptake, but improved the mechanical integrity and dimensional stability.

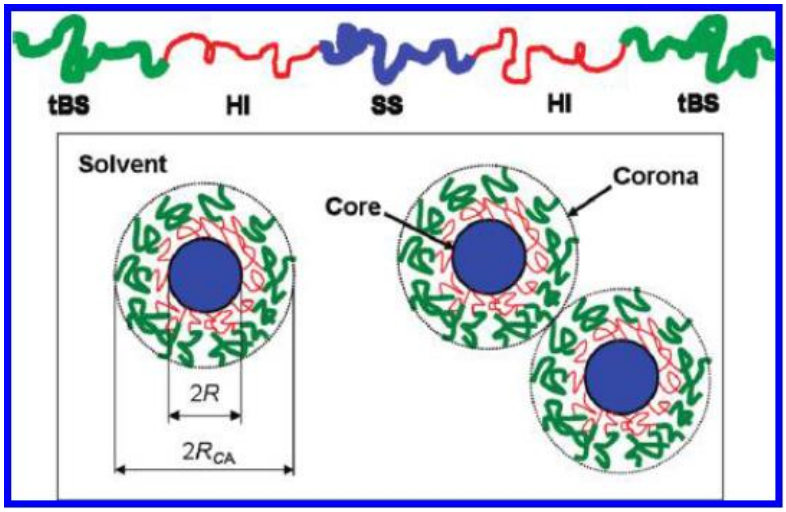

Figure 4.1 Spherical micelles containing dense cores of SS and coronas of HI-tBS swollen by solvent [100]

Laprade, et. al. [103] investigated the mechanical and microstructural characteristics of the Nexar pentablock. Grazing-incident SAXS (GISAXS) provided real-time measurements during solvent casting. The micelle size shrunk as the solvent evaporated, leaving the final domain spacing of 30 nm, which was confirmed by atomic force microscopy (AFM). A comparison between structureless and interconnected domain morphologies suggests that sulfonation level rather than morphology plays the dominant role in the hydrated deformation behavior of these membranes.

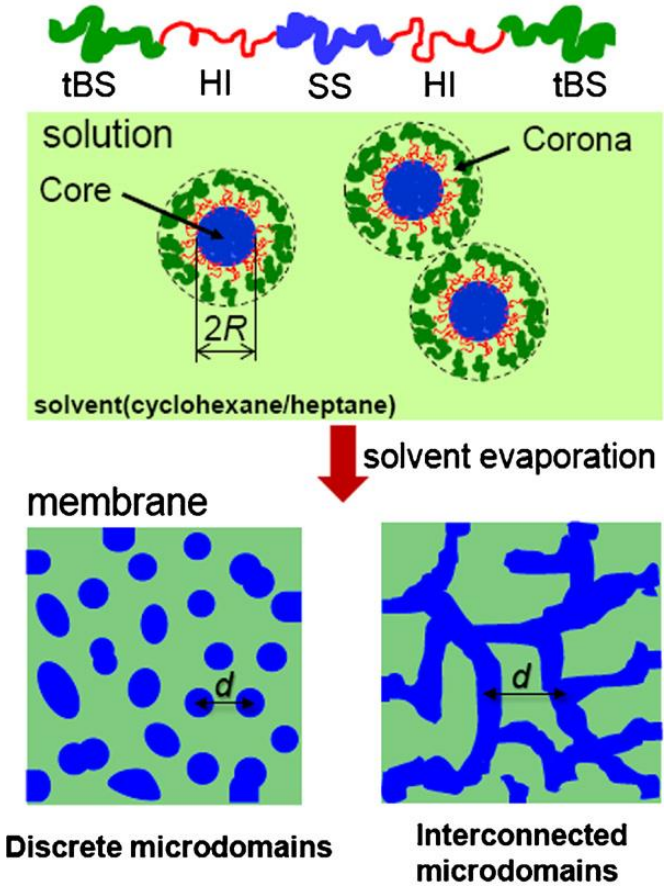

Figure 4.2 In Nexar membranes the SS domains are discrete when 2R < d and interconnected when 2R > d, where R indicates the core radius in solution and d represents the center-to-center distance of the SS microdomains in the membrane [101]

The effect of solvent polarity on final membrane morphology was also investigated [104]. Casting from cyclohexane displayed ion-rich spherical microdomains, which suggests the solvent evaporated early during nanostructure development and the ionomer was effectively templated by the nonpolar species. Alternatively, the use of THF results in coexisting nonpolar cylinders and lamellae.

Based on the characterization efforts of proton exchange membrane Nexar, the base pentablock forms a structured morphology and has good water transport. It is desired to investigate a cationic form of Nexar that will maintain a phase separated structure for anion

transport while the hydrophobic blocks provide mechanical stability. Characterizing the anion-exchange version of Nexar is reported here.

Scattering experiments can investigate how domains in proton exchange membranes swell with water uptake [43]. In the Herring group, SAXS experiments have been performed using a custom-built, four-sample oven that allows for temperature and humidity control [11,43–54]. The humidity is controlled by a wet gas / dry gas mixture with manual adjustment to achieve the desired humidity. Stationary measurements of structure with humidity changes can be compared to changes in structure seen from straining the film.

Polymers can undergo a phase transition through a force rather than a typical thermal transition. Strain induced crystallization at isothermal conditions has been demonstrated in polybutene-1 [55], poly(ethylene oxide) [56], and a propylene-1-butylene random copolymer [57]. The multi-step crystallization of a poly (e-caprolactone) sample was observed using a tensile tester to uniaxially stretch sample *in situ* with SAXS and WAXS at room temperature conditions [58]. Three zones of crystallinity were identified from the stress-strain curve and verified with the scattering patterns. The x-ray data measured the evolving structure with increasing strain. The distance between lamellae structures doubled with extension. The scattering behavior of styrene-butadiene-styrene block copolymers during stretching was investigated as far back as the early 1990s [59]. A scattering pattern formed elliptical patterns aligned perpendicular to the stretching direction. From this, it was concluded the polystyrene cylinders were placed with their axes perfectly oriented along lines parallel to the stretching direction. These extensional force systems are similar to the experiments performed here to investigate morphology change with strain.

There are few anion exchange membranes that have high ionic conductivity at low ion exchange capacity with low water uptake while still maintaining mechanical integrity at elevated temperature and relative humidity conditions. Identifying polymer architectures that achieve minimum performance metrics in a wide range of properties is critical to the advancement of anion exchange membrane science. In this study, an anion exchange membrane synthesized from a commercial pentablock copolymer platform was explored. Viscosity and the structure of polymer solutions were investigated. Polymer films were prepared in solution, functionalized, and characterized. Conductivity, water uptake, mechanical properties, and morphology were investigated at a range of humidity conditions. Fundamental insights into the polymer arrangement in solutions and films as well as performance in conductivity, water uptake, and mechanical testing are reported here.

4.3 Experimental

The pentablock anion exchange membrane was synthesized by others and characterization efforts are presented here.

4.3.1 Materials

The starting material poly[t-butyl styrene-b-hydrogenated isoprene-b-methyl styrene-b-hydrogenated isoprene-b-t-butyl styrene] polymer was gifted by Kraton Performance Polymers Inc. (Houston, TX). The molecular weight of the base pentablock is approximately 15-10-28-10-15 kg/mol [105]. The middle block was then brominated (Figure 4.3) and further quaternized with trimethyl ammonium, yielding the final pentablock polymer poly[t-butyl styrene-b-hydrogenated isoprene-b-vinyl benzyl trimethylammonium-b-hydrogenated isoprene-b-t-butyl styrene] (Figure 4.4). The synthesis and confirmation analysis was done by S. Piril Ertem in E. Bryan Coughlin's group at the University of Massachusetts Amherst and will not be discussed in

this thesis. The brominated polymer in powder form was mixed with tetrahydrofuran (THF) at a concentration of 20 wt% in a round bottom flask at room temperature for at least two hours. The solution was pipetted onto a Teflon substrate and drawn across the substrate with a micrometer adjusted film applicator set at 200 μm. The film applicator was drawn at a constant speed of 50 mm/s using a film coater (MTI Corporation's MSK-AFA-III, Richmond, CA). The solution was allowed to evaporate in the fume hood overnight before using a razor to remove the film form the Teflon substrate. The brominated film was then placed in a 25wt% trimethylamine solution for at least 48 hrs to achieve quaternization of the brominated end group. The final film had a thickness of about 60 microns. This polymer will be referred to as "BrexarXX", where XX is the % bromination as it is the brominated version of the commercial polymer named Nexar.

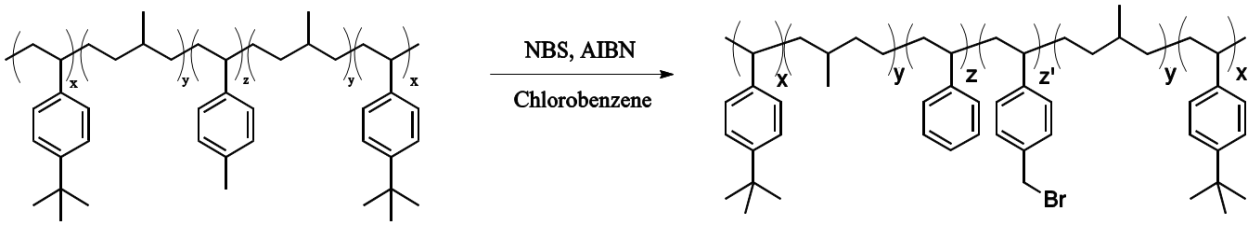

Figure 4.3 Synthesis step for unfuntionalized pentablock to the brominated material named "Brexar"

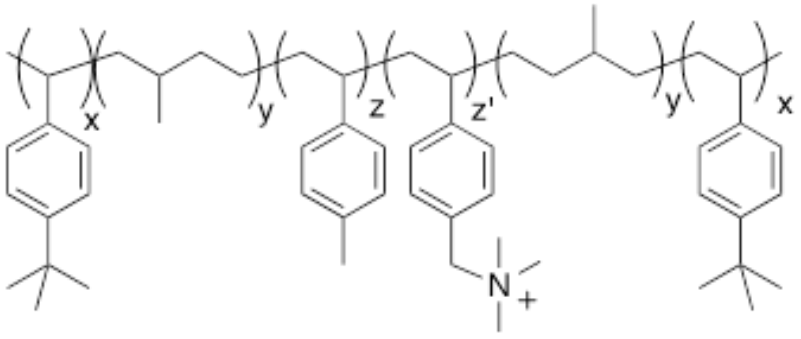

Figure 4.4 Chemical structure of Brexar. The z' group is noted by BrexarXX moving forward.

Table 4-1 Table of theoretical and titrated ion exchange capacity values for the Brexar series

	Theoretical IEC (mmol/g)	Titrated IEC (mmol/g)
Brexar20	0.6	0.4
Brexar43	1.1	0.8
Brexar70	1.7	0.9

4.3.2 Rheometry

Rheological measurements were done on an ARES-G2 rheometer (TA Instruments) using a modified Sentmanat Extensional Rheometer (SER) [40]. Details on the SER fixture are available elsewhere [20]. Samples were cut into rectangles measuring between 2-4 mm and about 20 mm long. Thicknesses ranged from 30-100 microns. Tests were run at 30°C with a 0.01 s^{-1} engineering strain rate to match the SAXS conditions. Tests were also run at 60°C under dry (<1%RH) conditions with a Engineering rate of 0.0033 s^{-1} due to elongation less than 20% and 0.33 s^{-1} for saturated conditions due to elongation greater than 100% At least five replicates were averaged for the final data.

4.3.3 Conductivity

Ionic conductivity was measured by electrochemical impedance spectroscopy using a four-electrode in-plane conductivity cell. Impedance spectra were obtained over a frequency range of 0.3 to 10^6 Hz using a multi-channel potentiostat (BioLogic VMP3). A TestEquity sample chamber controlled temperature and humidity during data acquisition. Membrane resistance was defined as the low frequency intercept of the Nyquist impedance plot and conductivity was calculated based on Equation (4.1).

$$\sigma = \frac{l}{R \cdot t \cdot w} \tag{4.1}$$

Where R is the membrane resistance, l is the length between electrodes, and t and w are the thickness and width of the membrane sample, respectively. Reported conductivity data are the average of at least three separate membrane samples and multiple impedance spectra at each steady-state temperature; error bars are one standard deviation. Conductivity measurements were performed with a bromide counterion.

4.3.4 Water uptake

Water uptake (*WU*) was characterized using a dynamic vapor sorption apparatus (SMS DVS Advantage 1, Allentown, PA). A membrane sample, about 4 mm^2, was placed on a glass weigh plate and the change in mass was measured gravimetrically under different humidity conditions. The *WU* of the membrane was calculated based on equation (2.2).

$$WU = \frac{m_{\%RH} - m_{dry}}{m_{dry}} \times 100 \tag{4.2}$$

where $m_{\%RH}$ is the mass of the sample at the given relative humidity and m_{dry} is the mass of the dry sample. The mass of the dry membrane was taken as the measured mass at the end of the initial 4-h drying period. Given the WU at saturated conditions and the known ion exchange capacity (*IEC*) of the membrane, the hydration level (λ) is the number of waters per cation functional group and can be calculated using equation (2.3). The molecular weight of water ($m(H_2O)$) is needed to complete the equation.

$$\lambda = \frac{WU}{m(H_2O) \cdot IEC} \tag{4.3}$$

4.3.5 Small angle x-ray scattering

Small angle X-ray scattering experiments were performed at the X-ray Sciences Division, beamline 12-ID-B, at the Advanced Photon Source at Argonne National Laboratory. Measurements were taken in a transmission geometry using a Pilatus 2M SAXS detector at a beam energy of about 14 keV (λ = 0.89 Å) and a sample-to-detector distance of about 2500 mm. A Sentmanat Extensional Rheometer (SER) (Xpansion Instruments) was used to apply a bidirectional strain on the films. The SER drums were modified to handle solid polymer films below their melting temperature [40]. The SER tool was powered by a stepper motor and was

housed in a custom built oven with forced convection heating. The oven allowed for the x-ray beam to travel between the counter-rotating drums [61,62]. The exposure time was generally 1 s and the images were taken either 3 or 5 seconds apart. The engineering strain rate used was 0.01 s^{-1} as this was the slowest rate the stepper motor could handle and still render a smooth rotation. The slow rate allow for the most x-ray images while the film was undergoing extension.

In order to quantify the changes in the polymer structure with strain, the movement of peaks in defined wedges was tracked. Using the Nika macro [63] in Igor Pro 6.36 (Wavemetrics) to handle the 2D SAXS image, a wedge was defined as ±2° around 90° and 180° (0° being the right horizontal line) after applying the beam mask and subtracting the background. The intensity as a function of the scattering vector q was averaged within the wedge. Using the Irena macro [64], the 1D I(q) plots were used to track the movement of peaks as strain increased.

Solutions were also completed at the X-ray Sciences Division, beamline 12-ID-B, at the Advanced Photon Source at Argonne National Laboratory. Measurements were taken in a transmission geometry using a Pilatus 2M SAXS detector at a beam energy of 14 keV (λ = 0.89 Å) and a sample-to-detector distance of 2029 mm. The solutions were placed in a 2 mm diameter quartz capillary tube. A blank tube of THF was used for background subtraction. The solutions were drop cast onto Teflon sheets, dried overnight, and then placed in a vacuum oven at 50°C for 10 hours. The resulting films were imaged at rest in a dry oven at 60°C. Since the 2D SAXS patterns for both the solutions and small films were isotropic, the intensity was radially averaged and the I(q) data was plotted directly in Igor with the Irena macro [64].

4.4 Results and Discussion

The solution rheology of the base pentablock and properties of brominated and quaternized films are discussed.

4.4.1 Structure of polymer solutions and films

Using the base material, Brexar0, viscosity measurements were taken with increasing concentrations of polymer in a THF solution. The solutions were tested with a 40 mm 2° cone and plate geometry on a TA Instruments AR-G2 rheometer with the use of a solvent trap to prevent evaporation effects. The polymer solutions fell into three distinct regions corresponding to dilute, semi-dilute, and entangled regimes [106]. The viscosity (η) versus concentration (C) data was fit to a power law model, Equation (4.4), and the power law exponent (x) defines the entanglement regions (Table 4-2).

$$\eta = C^{x} \tag{4.4}$$

Table 4-2 Power law exponents for neutral polymer solutions in theta and good solvents

	Neutral Polymer			
Solvent	θ	Reference	Good	Reference
Entangled	$\eta \sim c^{14/3}$	[107]	$\eta \sim c^{3.9}$	[107]
Semidilute	$\eta \sim c^{2}$	[107]	$\eta \sim c^{1.3}$	[107]
Dilute	$\eta \sim c^{1.0}$	[108]	$\eta \sim c^{1.0}$	[109]

Based on the viscosity measurements, the dilute regime ranged from 1-9 wt%, the semi-dilute regime ranged from 10-15 wt%, and the entangled regime was above 16 wt% (Figure 4.5). 20 wt% was the maximum concentration examined as a 22 wt% solution failed to dissolve in the solvent.

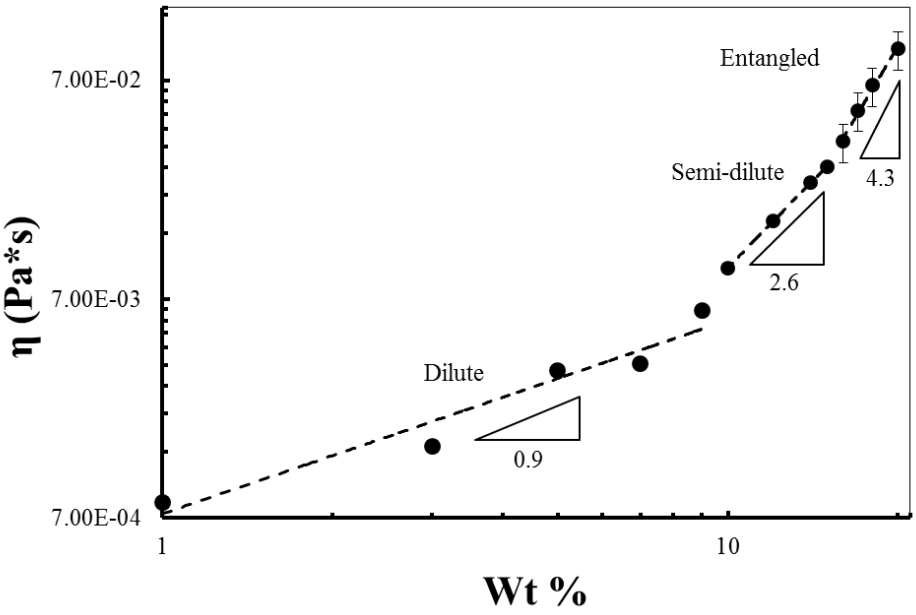

Figure 4.5 Viscosity as a function of concentration for the base pentablock in THF solution. The viscosity regimes are defined by the power law slope.

The solution regimes were also investigated with SAXS. Solutions of 5 wt% (dilute), 10 wt% (semi-dilute), and 15 wt% (entangled) solution were placed in quartz capillary tubes and shot at the Advanced Photon Source at room temperature. The intensity increases with increasing concentration and there is a shoulder around 0.03 – 0.04 $Å^{-1}$ corresponding to a d-spacing of about 18 nm.

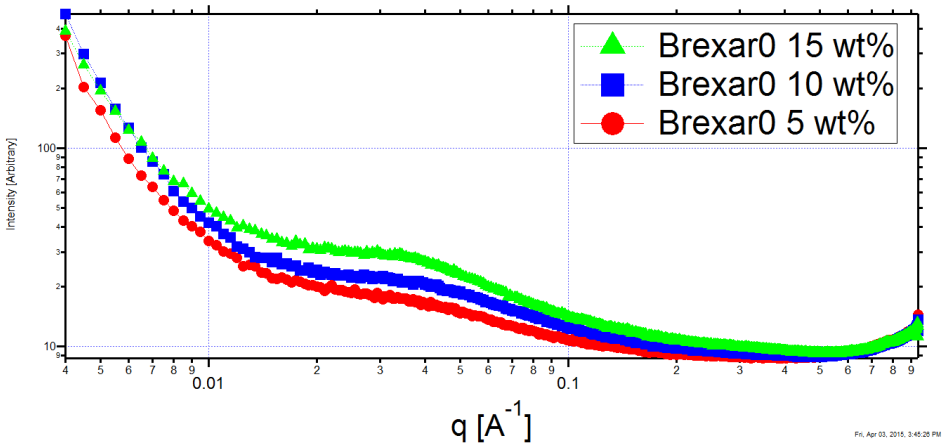

Figure 4.6 SAXS of Brexar0 at 0 (red), 10 (blue), and 15 (green) wt% solution in THF

The morphology of the brominated polymer was investigated in a THF solution. The work was done in the brominated form due to the insolubility of the quaternized, ionic polymer. An analogous sulfonated polymer formed micelles in solution and a higher degree of sulfonation led to a larger micelle [100]. Several models (Kinning-Thomas, hard sphere, polydisperse hard sphere) were unsuccessfully used in an attempt to model the solutions. The solutions have a single peak which corresponds to a d-spacing of ~20 nm (Figure 4.7).

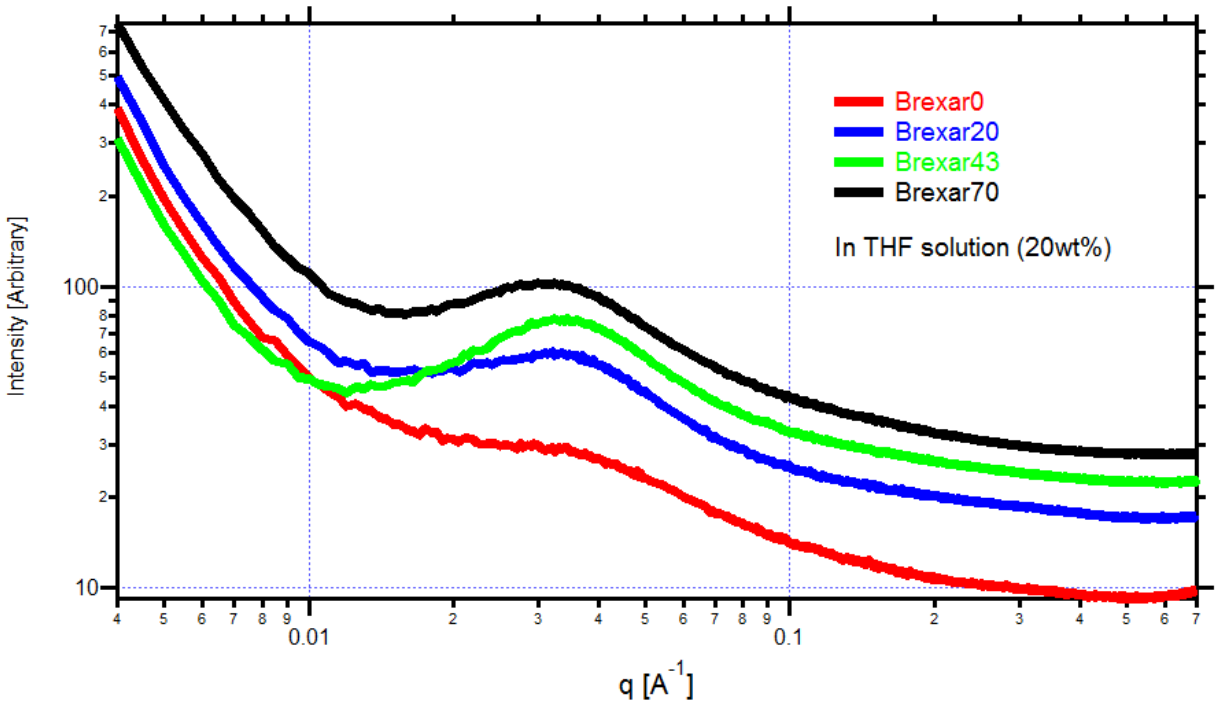

Figure 4.7 Small angle x-ray scattering of BrexarXX in a THF solution

The small films cast from the solutions showed sharp peaks for all functionalities of Brexar, with the higher degrees of bromination showing more defined peaks (Figure 4.8). The Brexar0 film has a peak corresponding to a d-spacing of 19 nm. Since the polymer lacks large atoms, such as bromine, the scattering is most likely due to the π-bond stacking of the aromatic rings.

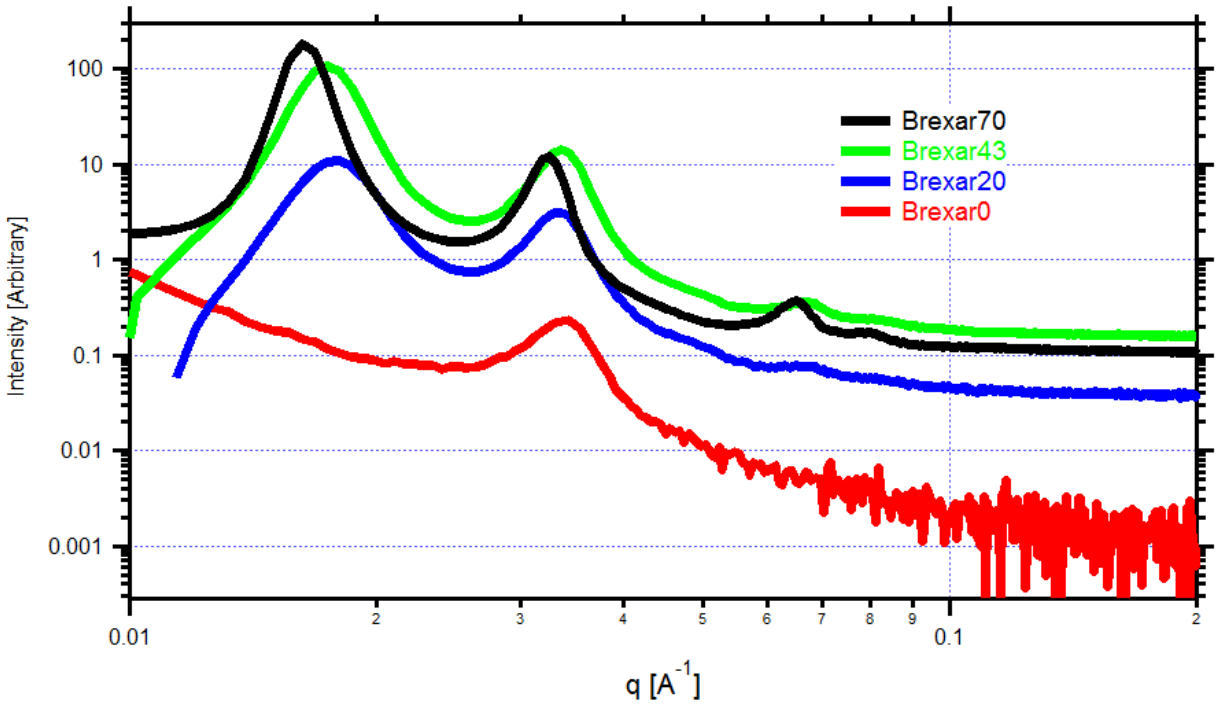

Figure 4.8 Intensity versus the scattering vector q for small films made from drop casting 20 wt% solutions of various Brexar functionalities in THF

The peak ratios of the films and the characteristic lengths indicated the polymer formed a lamellar structure and the distance between the mid-blocks with bromide increased with increasing bromination levels (Table 4-3).

Table 4-3 Peak ratios and d-spacing of lowest q feature for the varying levels of bromination in the Brexar material

Bromination level	**Peak ratio**	**d-spacing of lowest q peak (nm)**	**Reference**
0% (base pentablock)	---	19	
20%	3.7 : 2 : 1	35	
43%	3.8 : 2 : 1	36	
70%	4 : 2 : 1	39	
Nexar 52% sulfonation		30	[101]

4.4.2 Water Uptake

The Brexar material did not show appreciable water uptake compared to other AEMs. The maximum mass uptake was only 22% for the Brexar70 material at 95%RH. While water is needed for ion conduction, if the polymer absorbs an excess of water then swelling can lead to mechanical instability. The trend in hydration values was the opposite of the trend in overall water uptake, meaning the higher IEC material is more efficient in absorbing water. The maximum hydration level was between 11 and 18 which is similar to PEMs (14 to 22) [77,110,111] and other AEMs (12 to 25) [112–114]. The modest water uptake of Brexar, which maintains conductivity and mechanical stability, is desirable.

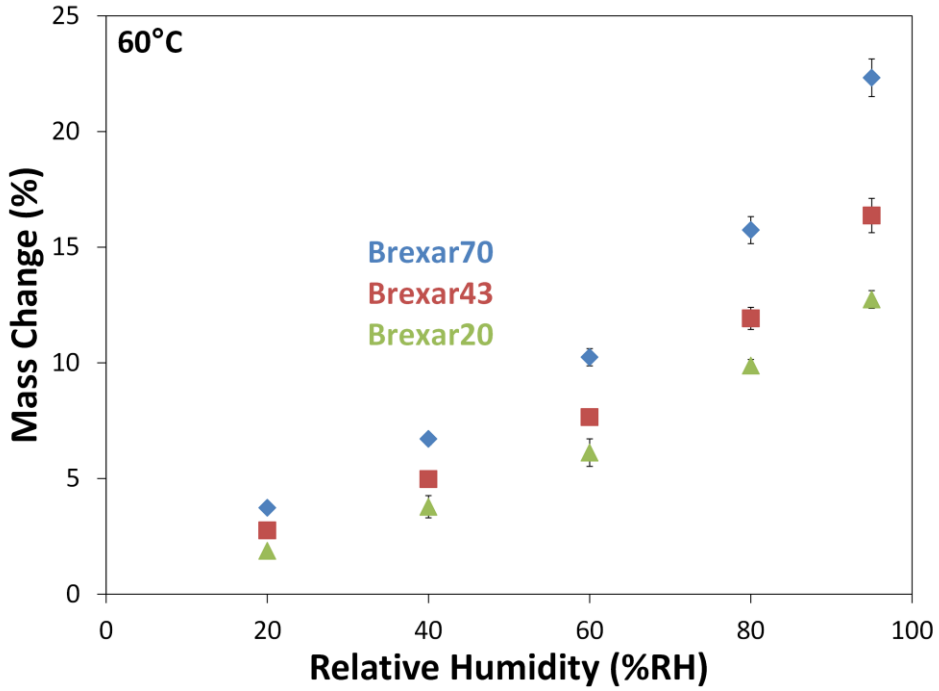

Figure 4.9 Water uptake of the Brexar material as measured by dynamic vapor sorption at 60°C

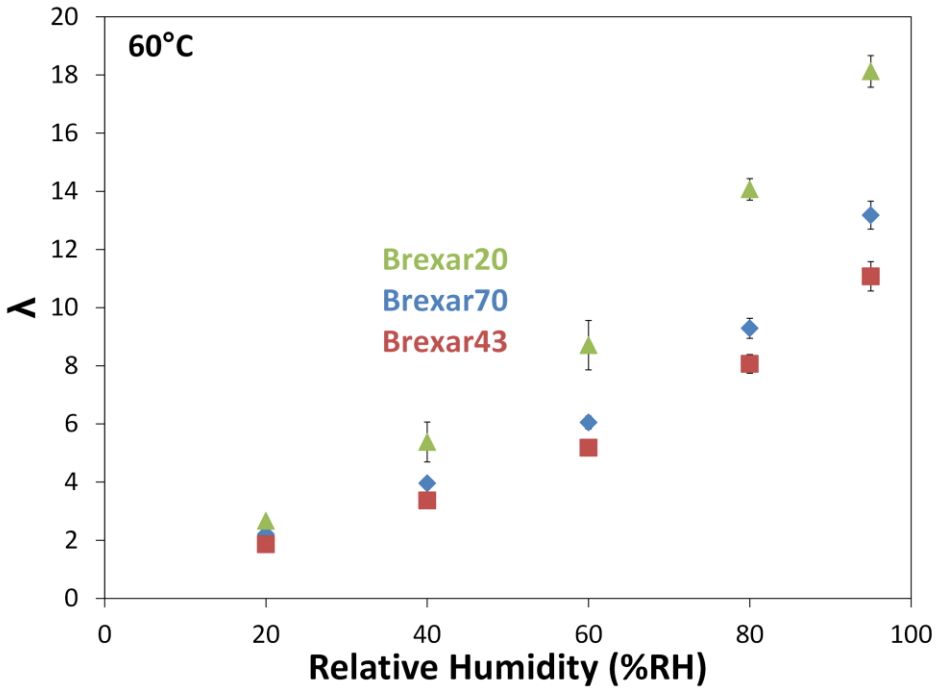

Figure 4.10 Water uptake as a function of hydration value (λ) for the Brexar material

4.4.3 Conductivity

The highest conductivity recorded was 57 mS/cm with the Brexar70 material at 90°C and 95%RH. In many ion exchange membrane systems, conductivity plateaus with increasing IEC [45,47]. In the Brexar material conductivity increased with increasing IEC primarily due to the large hydrophobic weight fraction and lower IEC values compared to other AEMs. The Brexar70 was the highest degree of bromination achieved so it is possible this polymer platform cannot support IEC values high enough to observe a plateau in conductivity. The conductivity values are comparable with other AEMs in literature [18,45,47,115,116].

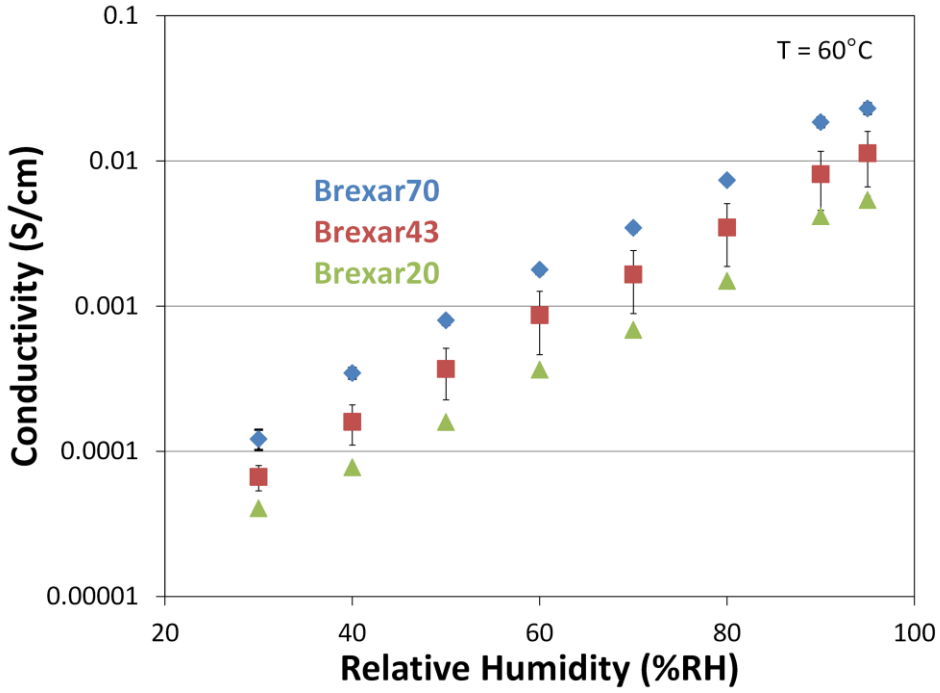

Figure 4.11 Bromide conductivity of varying bromination levels of Brexar at 60°C and varying relative humidity conditions.

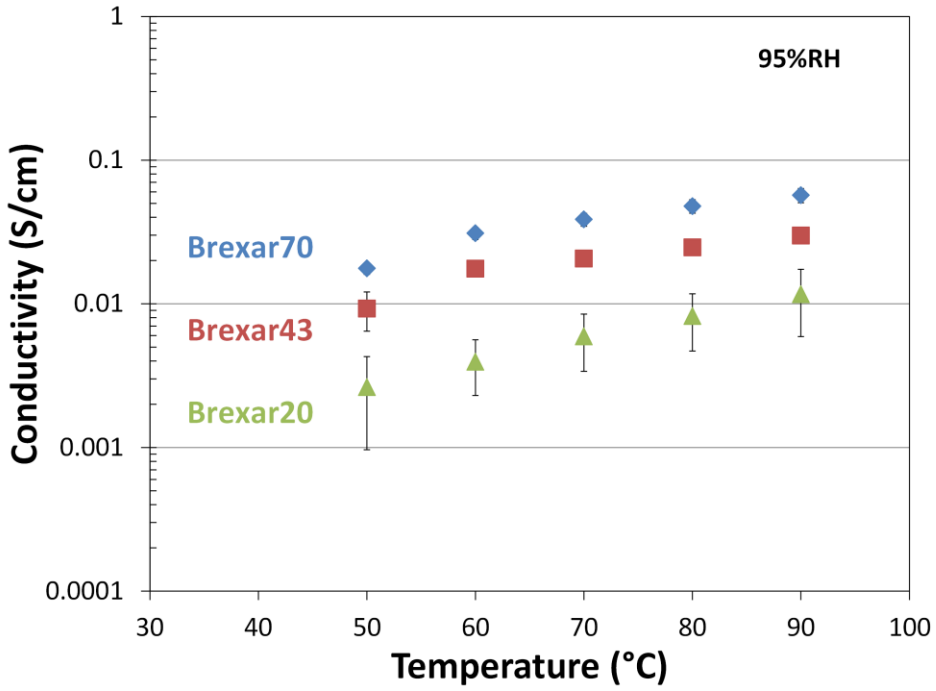

Figure 4.12 Bromide conductivity of varying bromination level of Brexar at saturated relative humidity conditions.

Brexar43 and Brexar70 have similar activation energy (27 kJ/mol), while Brexar20 was 36 kJ/mol (Figure 4.13). The values are in the range of other AEMs [11,48]. Brexar43 and Brexar70 deviate from the linear fit at the lowest temperature reported here (50°C), which could mean the conductivity mechanism is not simply vehicular, but has contributions from the polymer backbone flexibility [117]. Further study is warranted across a wider range of temperatures.

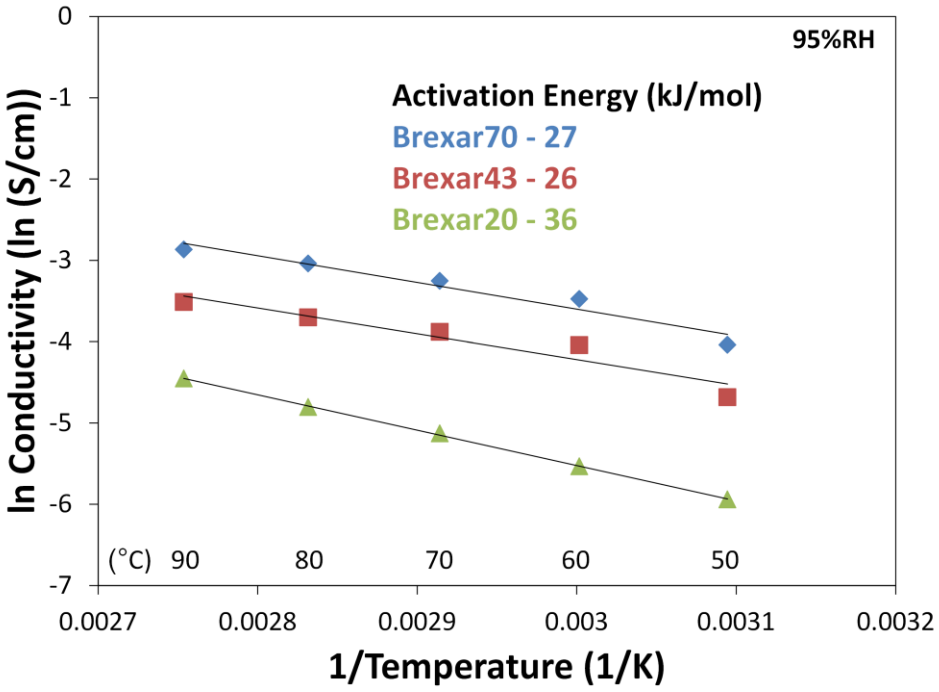

Figure 4.13 Arrhenius plot of bromide conductivity of the Brexar material at 95%RH

4.4.4 Mechanical Characterization

The different block chemistries of the pentablock were designed to provide strength, flexibility, and conductivity in a single polymer. The Brexar0 sample is the unfunctionalized pentablock, which serves as a control. Given the hydrophobicity of the different block chemistries, Brexar0 should display minimal response with changing relative humidity conditions. Kraton published mechanical properties of Nexar MD9150 (IEC = 1.5 meq/g), but

the temperature was not stated. Membranes in electrochemical devices will need to be mechanically strong, handle dimensional swelling from water uptake, and be flexible enough to withstand nonlinear deformation stresses. Tensile testing at 60°C in both dry and wet conditions establishes mechanical performance.

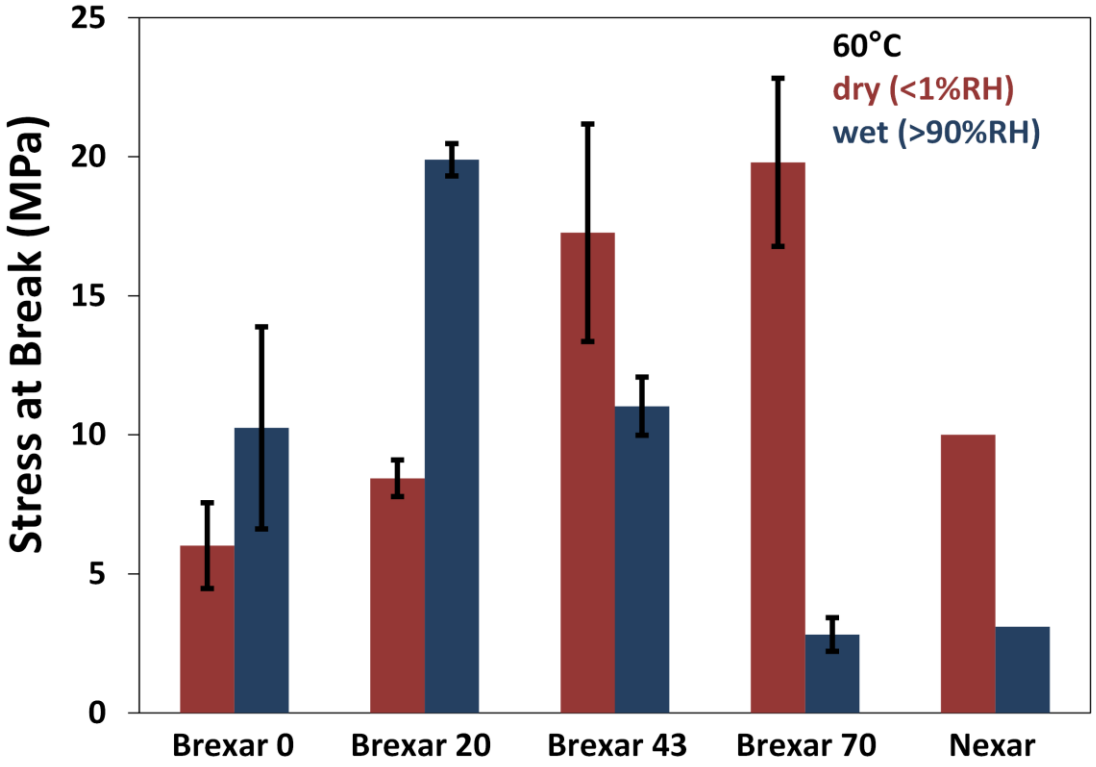

Figure 4.14 Stress at break for Brexar membranes at dry and saturated relative humidity conditions at 60°C. Nexar MD9150 (IEC = 1.5 meq/g) data from Kraton at presumed 25°C conditions is shown for comparison.

The stress at break increases with IEC for dry conditions (red bars in Figure 4.14) and decreases with IEC for saturated RH conditions (blue bars in Figure 4.14) indicating the dramatic effect water can have on the mechanical strength on membranes. The stress at break is ~40 MPa lower than benchmark AEMS in the dry condition and ~15 MPa lower in the wet condition [76]. However, since AEMs are not subject to extensional load during use, only a minimum stress of ~10 MPa is needed to maintain integrity.

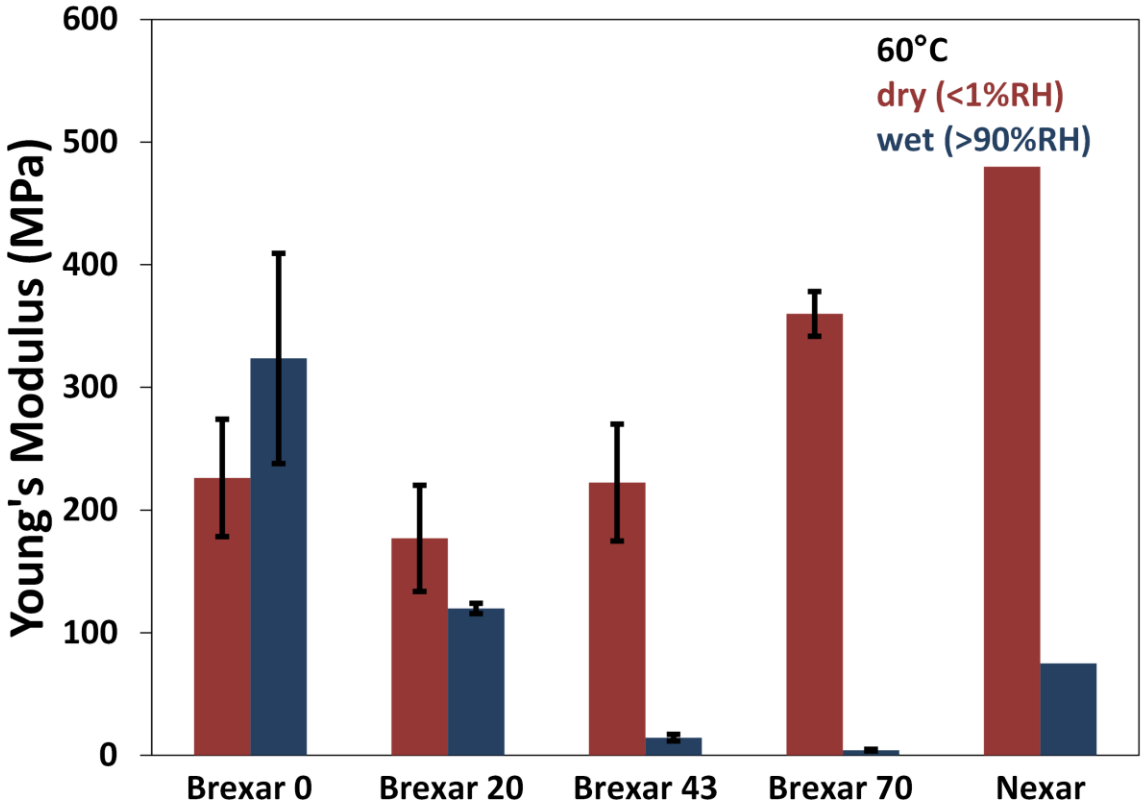

Figure 4.15 Young's modulus of the Brexar membranes under dry and saturated relative humidity conditions at 60°C. Nexar MD9150 (IEC = 1.5 meq/g) data from Kraton at presumed 25°C conditions is shown for comparison.

The same trend is seen with the Young's modulus as with the stress at break. At dry conditions, the film becomes more stiff with increasing IEC due to the stiff nature of the poly(vinyl benzyl trimethylammonium) group which has been observed in other AEM systems.[48] The values of the Young's modulus at dry conditions (150-350 MPa) indicate the membranes can be handled without breaking. Hydration drastically increases the elasticity, thus reducing the Young's modulus by as much as two orders of magnitude in the highest IEC material (360 to 4 MPa for Brexar 70). Despite the low Young's modulus, the Brexar70 material elongates over 100% and maintains 3 MPa of strength.

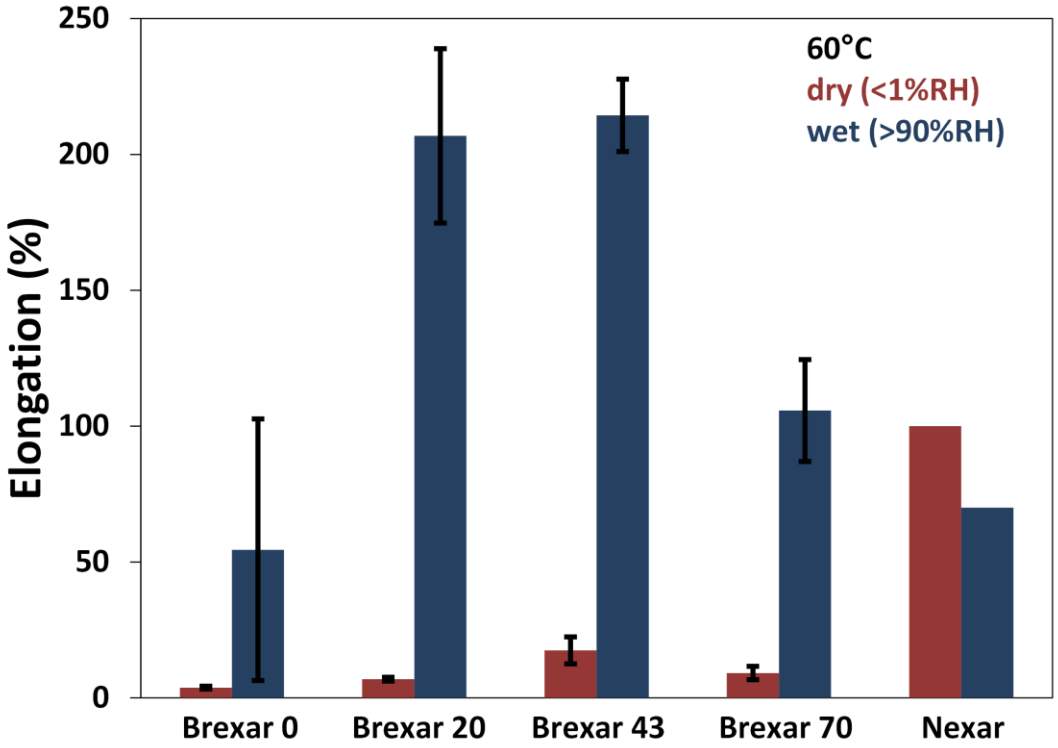

Figure 4.16 Elongation to break of the Brexar membranes at dry and saturated relative humidity conditions at 60°C. Nexar MD9150 (IEC = 1.5 meq/g) data from Kraton at presumed 25°C conditions is shown for comparison.

The elongation values at dry conditions (<1%RH) are low due to the film breaking near the securing pin at the onset of extension. Once the membranes absorbed water, the elongation increased by an order of magnitude.

The tradeoff between conductivity and mechanical performance is clearing seen with the Brexar membranes. Brexar20 has the lowest conductivity, but it is the only one to maintain a modest level of stiffness (120 MPa Young's Modulus) at the high hydration condition. The Brexar70 material has high conductivity, but is very elastic (4 MPa Young's modulus) at the high hydration condition. However, Brexar70 maintained mechanical integrity at 90°C and 95%RH in the conductivity testing so it is still a viable option for practical devices.

4.4.5 Morphology change with extension strain

The morphology of Brexar43 was investigated as function of extensional strain. At rest, the material showed an isotropic pattern with two distinct peaks at about 0.026 and 0.051 $Å^{-1}$, 24 nm and 12 nm in real space, respectively (Figure 4.17). As the film was stretched, two changes occurred. First, the d-spacing along the 180° direction increased and the d-spacing along the 90° direction decreased (Figure 4.18). The changes in d-spacing occurred for both the high and low q-range peaks. Secondly, the ratio between the two peaks remain nearly constant at ~1.9 (±0.07) in both 90° and 180° directions as strain increased all the way to membrane failure (Figure 4.18). Since a peak ratio of 2 is typical for a lamellar structure [118], the scattering suggests the lamellar structure stays intact even as the microdomains get larger.

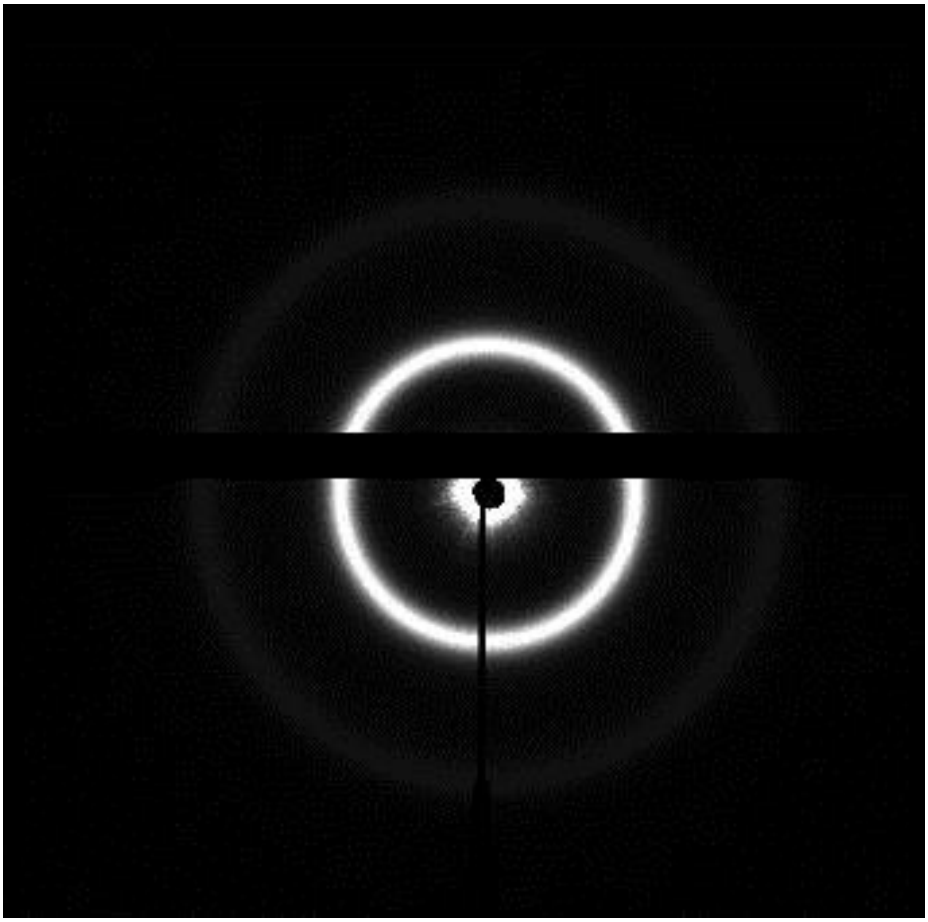

Figure 4.17 2D SAXS pattern of the Brexar43 material at rest before extension

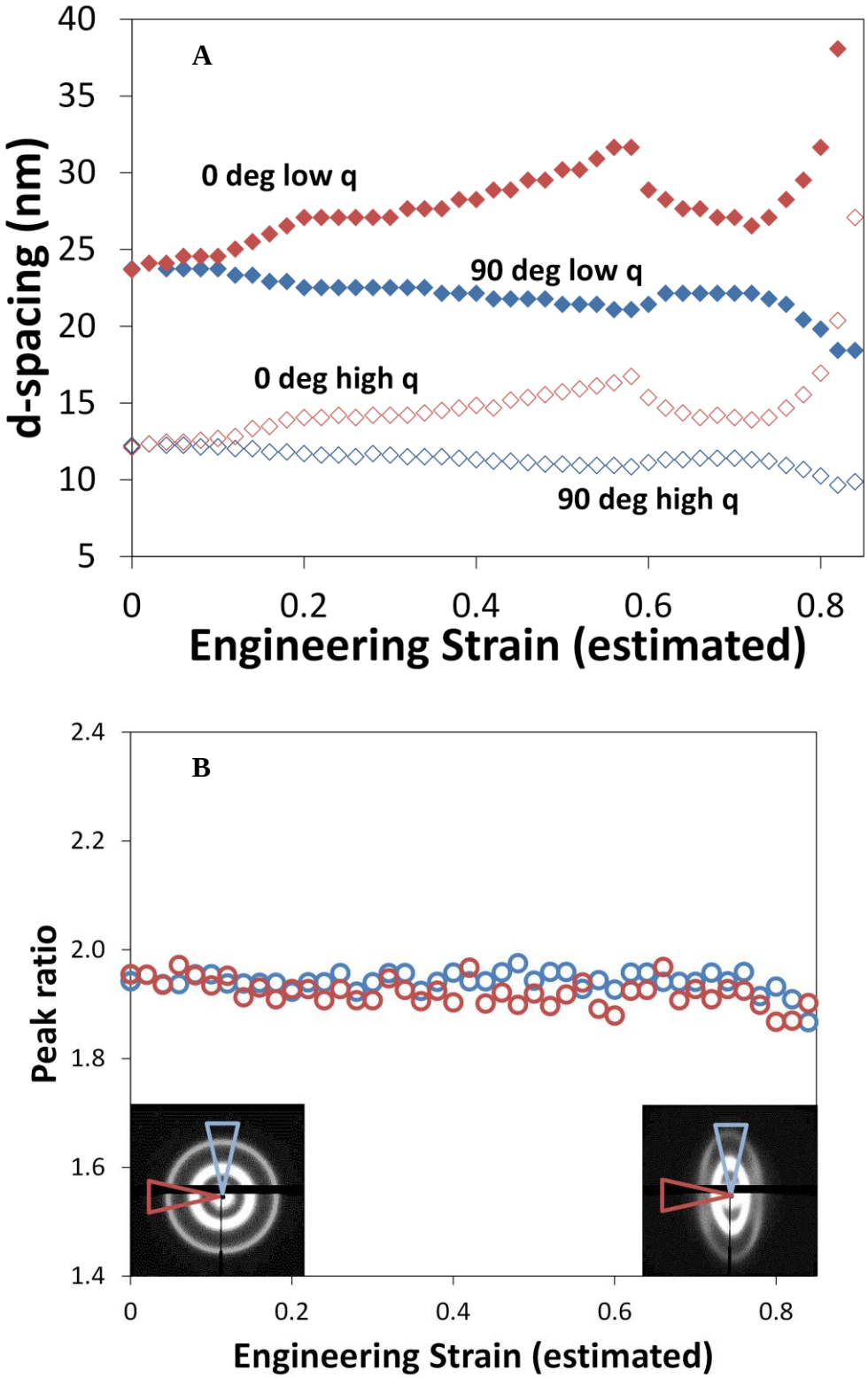

Figure 4.18 (A) The d-space shift of the main peaks in defined wedges at 0 and 90 degrees of the Brexar43 material at 30°C under an extensional strain rate of 0.01 s^{-1} (B) The ratio between the two peaks inside the defined wedges as a function of engineering strain

4.4.6 Structure with changing hydration

Morphology of the Brexar membranes were also investigated as a function of hydration level using small angle x-ray scattering (SAXS) in a humidity controlled oven. The Brexar20 and Brexar43 membranes both have a main peak at a d-spacing of about 34 nm and the peak is the same in both dry and wet conditions. The ratio of the first two peaks for Brexar20 and Brexar43 suggests a lamellar morphology (Figure 4.19). The main peak in the Brexar70 membrane shifts d-spacing from 35 to 39 nm from dry to wet conditions (Figure 4.19). The higher IEC of this material leads to a greater water uptake and the lamellar spacing in the polymer expands to absorb the water. An expansion of the existing structure with water uptake has been observed in other PEMs [119] and AEMs [47] and gives insight to the width of the ion transport channel [50]. In Brexar70 material at 95%RH, higher order peaks were observed, which indicates the lamellar structure is better defined.

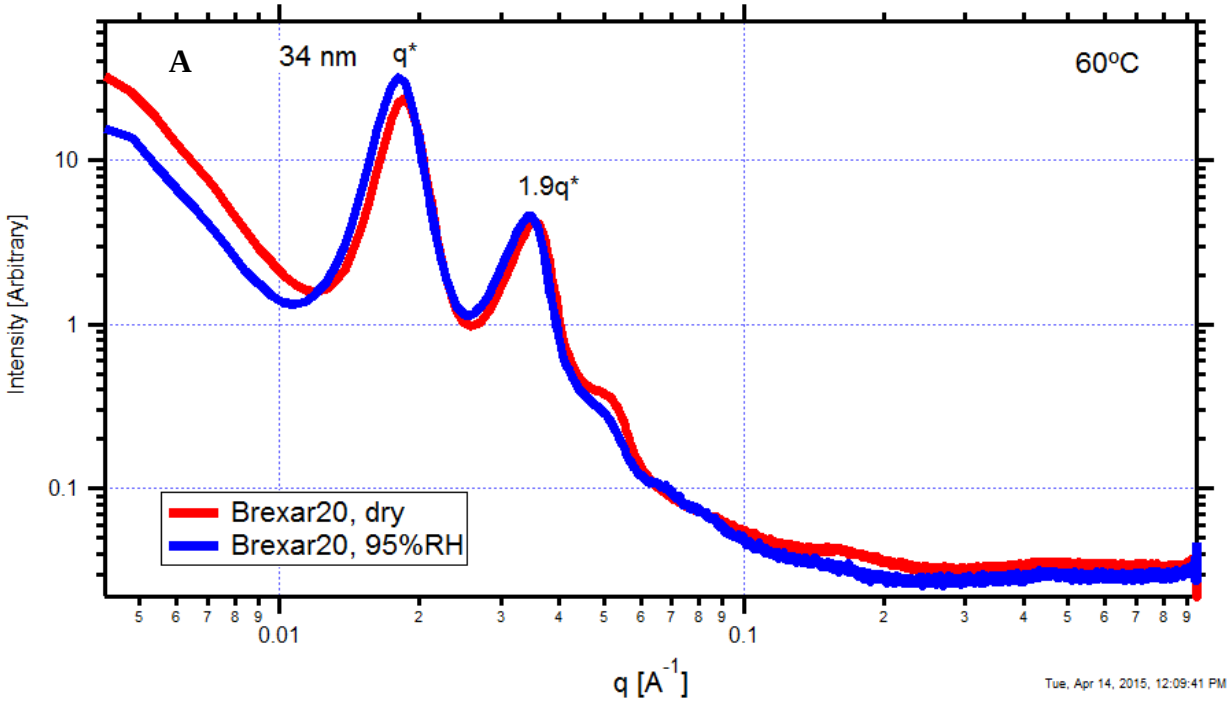

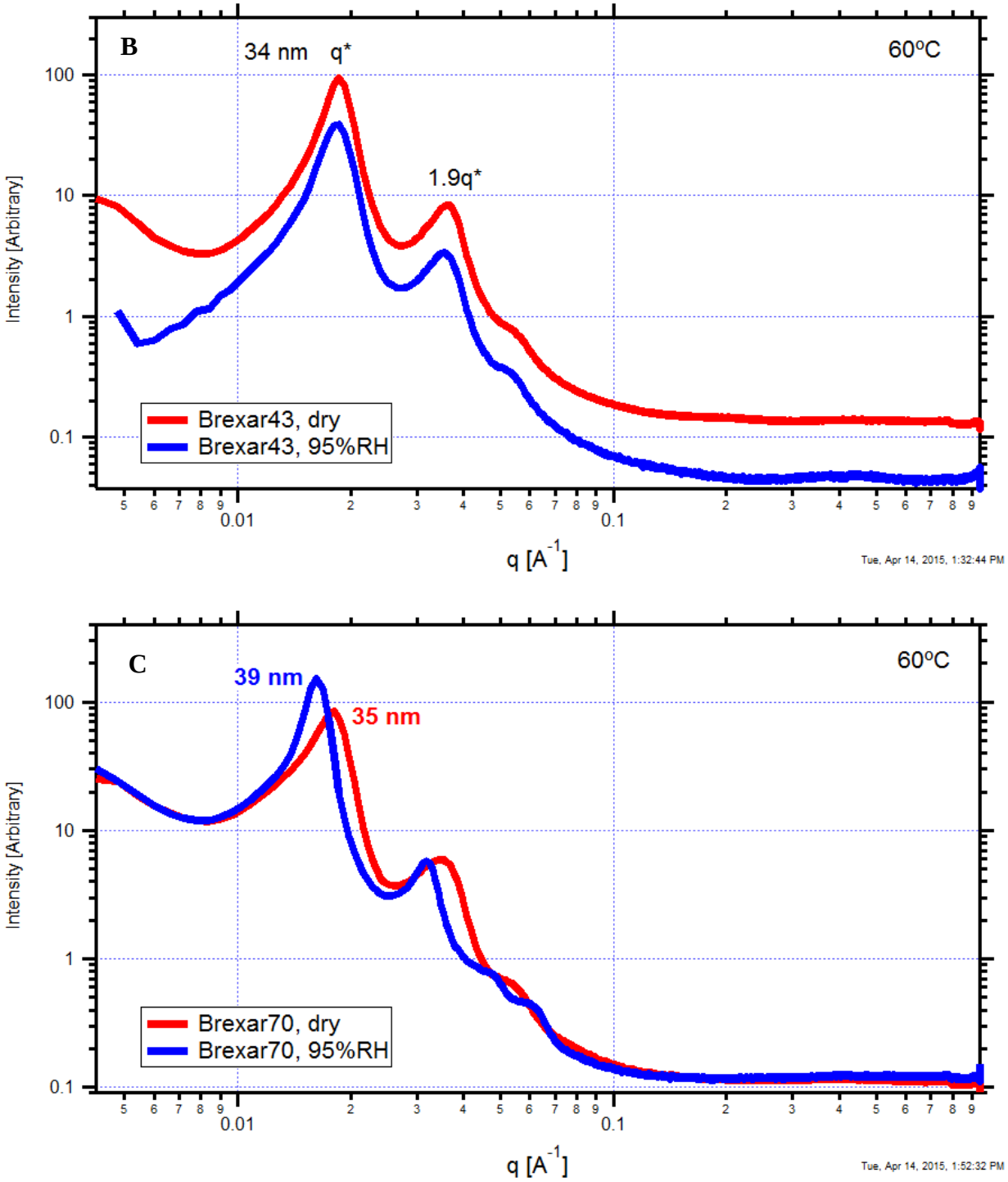

Figure 4.19 SAXS at dry and saturated relative humidity conditions for (A) Brexar20, (B) Brexar43, and (C) Brexar70 at 60°C

4.5 Conclusions

We have demonstrated the modification of a pentablock commercial copolymer system to an anion exchange membrane via bromination chemistry. The polymer is solution processable in THF at a wide range of concentrations. The polymer is highly conductive (up to 60 mS/cm) with a small amount of water absorption (<25%) while maintaining adequate mechanical properties in both dry and hydrated conditions at 60°C. The polymer forms a lamellar structure with a d-spacing of about 35 nm and the structure is maintained under hydration and extensional strain. The Brexar polymer delivers good conductivity with low water uptake and maintains mechanical integrity at high hydration conditions. We have demonstrated how a commercialized pentablock proton exchange membrane can be modified to produce an anion exchange membrane with similar morphology. The AEM can be tuned to a range of ionic conductivity and mechanical integrity to suit applications in fuel cells, barrier layers, or other electrochemical separators. There is also potential to modify the ratio of the blocks to make the polymer more elastic, which may be better for AEM applications. The highest IEC level is a promising material for a separating membrane in an AEM fuel cell, while the lower IEC values are appropriate for applications where mechanical integrity is valued higher than conductivity.

4.6 Acknowledgements

The authors thank the U.S. Army Research Office (MURI Grant #W911NF-10-1-0520 and DURIP Grant #W911NF-11-1-0306) for its support of this work. We also thank S. Piril Ertem in E. Bryan Coughlin's group at the University of Massachusetts-Amherst for the synthesis of Brexar and collaborative work with the solutions and small films at the Advanced Photon Source. We thank Sönke Seifert of the X-Ray Sciences Division at the Advance Photon

Source for his help performing the x-ray experiments and advice on interpretation of the data. We thank M. Zafar Iqbal, Derek Strasser, Melissa A. Vandiver, and Tara P. Pandey for their assistance running experiments at the Advanced Photon Source. We thank Erica McCready and Wesley Burghardt for use of their custom built SER oven for SAXS experiments. We thank NSF sponsored Polymer REU student Joseph Montion for the Brexar0 solution rheology testing.

CHAPTER 5

ACCELERATED MECHANICAL DEGRADATION OF ION EXCHANGE MEMBRANES

5.1 Abstract

Ion exchange membranes are a promising class of materials for use in fuel cells, barrier layers, and water splitting devices. While the focus of the majority of research is on improving the chemical stability and increasing ionic conductivity, the mechanical performance under operating conditions is vital to device lifetime. We report here the mechanical performance of Nafion® 115, polyethylene-b-polyvinyl benzyl trimethylammonium diblock copolymer (PE-b-PVBTMA), poly[t-butyl styrene-b-hydrogenated isoprene-b-vinyl benzyl trimethylammonium-b-hydrogenated isoprene-b-t-butyl styrene] (Brexar43), and aminated tetramethyl polyphenylene (ATMPP) using both tensile testing and humidity cycling. Nafion® 115 was used as a benchmarking material to compare with the developmental anion exchange membranes. A home built environmental chamber attached to a rheometer was utilized to perform all measurements under elevated temperature and relative humidity conditions. The elasticity of the polymer was the leading indicator for mechanical performance under cyclic hyrgal stress.

5.2 Introduction

While chemical degradation remains a significant issue for membrane stability in AEMs, mechanical stability is also an integral factor in fuel cell lifetime [27]. The polymer needs to be processed into thin, durable membranes and withstand the stresses inside a fuel cell at operating conditions. Microcracks formed from continued hydration and dehydration cycles in a fuel cell are the most common form of mechanical failure. Several attempts have been made to correlate mechanical failure with a more common property such as elongation at break [29,31] or Young's

modulus and yield strength [28]. Cycling the humidity correlated well with a reduction in the strain at failure even though the yield stress and yield strain remained largely unchanged [31].

Most of the available literature on mechanical properties of ion conducting polymer membranes is limited to stress-strain curves in various states of hydration [32–35]. Tensile strength and Young's modulus decrease as the polymer gains water. The elongation at break increases due to plasticizing effect of the absorbed water [33]. Also noted by Marestin, et. al [32] is that "Despite the fact that mechanical properties are now often determined for new ionomers, a complete study of the mechanical properties is still necessary including the combined effect of water content and temperature." Custom environmental chambers built around a mechanical tester are common for detailed exploration of properties at intermediate humidities [39,84], and the testing is usually performed at a static temperature and relative humidity condition and time dependence is not considered.

Mechanical properties of films relate to conductivity. In an alkaline exchange quaternary ammonia polysulfone membrane, a sharp increase in water uptake with increasing ion exchange capacity (IEC) correlated exactly with a sharp decrease in Young's modulus [36]. In poly(vinyl alcohol) (PVA) and poly(acrylic acid) (PAA) blends, a 10:5 PVA:PAA ratio "offers a good balance between enhanced ionic conductivity and acceptable mechanical strength for solid polymer electrolyte applications" [37]. In an effort to improve mechanical properties reinforcement with ePFTE has been shown to increase the fuel cell lifetime by an order of magnitude [30].

The membrane undergoes many cycles of small stresses in a fuel cell, which can lead to mechanical failure. The stresses can be mechanical, thermal, chemical, or hygral and a single cycle is not enough to do damage, but the cumulative effect of many cycles leads to microcracks

and membrane failure [120]. The rheological characterization of materials exhibiting non-linear deformation is an example of these kinds of stresses [121,122]. Hygral stress relates to the stress on a material caused by the absorption and desorption of water. Nafion NR111 was put under a cyclic mechanical stress, and a stress of only 1/10 of the tensile strength of the uncycled membrane was needed to break the membrane [38]. It was also concluded "the shrinkage stress generated by the water-uptake is responsible for the mechanical decay of the Nafion PEMs" [38]. The stress change from either cooling or drying Nafion NR111 was shown to be on the order of 0.2 to 2 MPa [38]. General Motors tests for mechanical durability of the membrane electrode assembly (MEA) by exposing the membrane to an alternating two minute cycle of 0%RH and 90°C dewpoint gas at 80°C. Gas crossover (hydrogen) is measured and the membrane must survive at least 20,000 cycles without gas crossover to pass [123].

We build off of the demonstration of a single wet to dry stress measurement [124] and the industrial cyclical tests [123] to introduce a water stress metric based on cycling the membrane between high saturation and dry air conditions at elevated temperature, and compare this new metric with traditional mechanical testing metrics. Our goal with this work is to accurately measure the stress water puts on the membrane as it absorbs and desorbs into and out of the membrane and how this stress changes over many cycles.

5.3 Experimental Methods

The materials and methods used in this work are discussed in the following sections of this chapter.

5.3.1 Materials

Four ion exchange membranes are compared. Nafion® 115 is a commercial proton exchange membrane produced by DuPont that is widely studied in the fuel cell literature [27,125]. Nafion® 115 was obtained from Ion Power, Inc. The film was prepared via the standard method [77] of boiling in 0.5M sulfuric acid for an hour, deionized water for an hour, 3 wt% hydrogen peroxide for an hour, and finally deionized water again for an hour. The membrane was then placed in an oven at 80°C for over 12 hours to dry. PE-b-PVBTMA is a polyethylene-b-polyvinyl benzyl trimethylammonium diblock copolymer with a 70:30 PE:PVBTMA block ratio and molecular weight of 64,800 g/mol [99]. The polymer was cast from xylene at 80°C with a film coater into 300 cm2 films 12 ± 3 μm thick. These films were very flexible and exhibited low dimensional swelling [126]. Brexar43 is based on a commercial pentablock copolymer platform from Kraton Polymers Inc. (Houston, TX). It is comprised of poly[t-butyl styrene-b-hydrogenated isoprene-b-vinyl benzyl trimethylammonium-b-hydrogenated isoprene-b-t-butyl styrene] that has 43% of the mid-block functionalized with benzyl trimethylammonium. The molecular weight of the base pentablock is approximately 15-10-28-10-15 kg/mol [105]. The polymer was produced by S. Piril Ertem of the Coughlin group at the University of Massachusetts-Amherst. The brominated polymer in powder form was cast from tetrahydrofuran (THF) using a film coater. The brominated film was then placed in a 25wt% trimethylamine solution for at least 48 hrs to achieve quaternization of the brominated end group. The final film had a thickness of about 60 μm. ATMPP is an aminated tetramethyl polyphenylene produced by Michael Hibbs of Sandia National Labs [115]. It is well studied and shows promise as a platform for an anion exchange membrane in a working fuel cell.

A

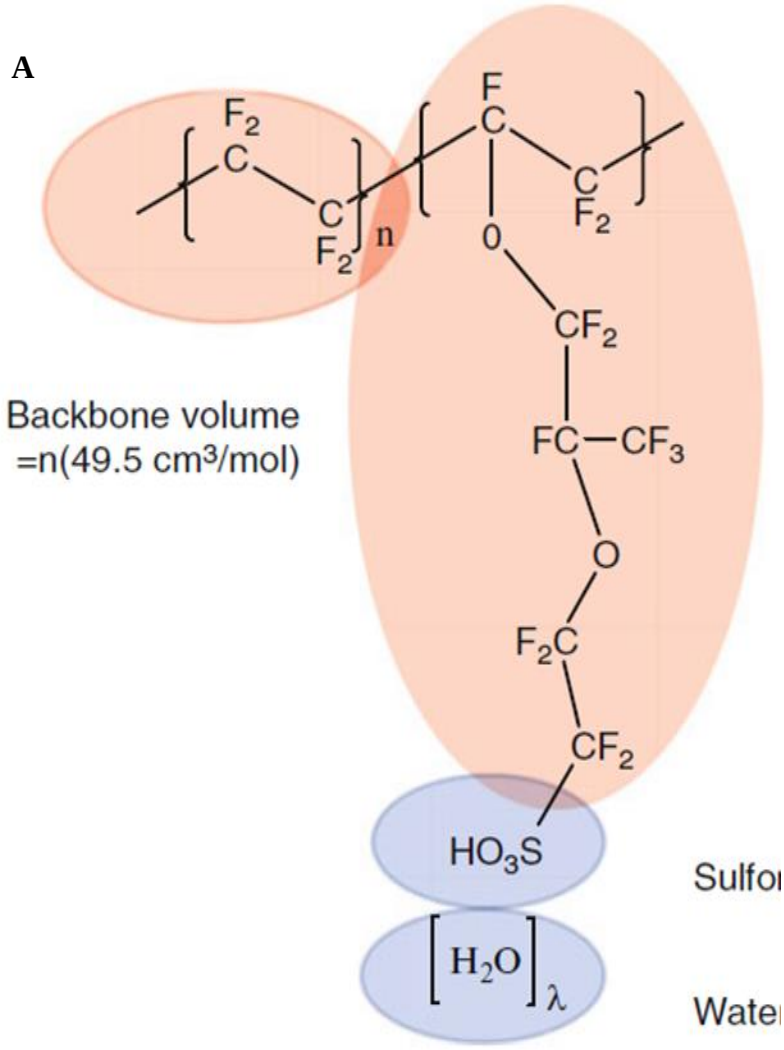

B

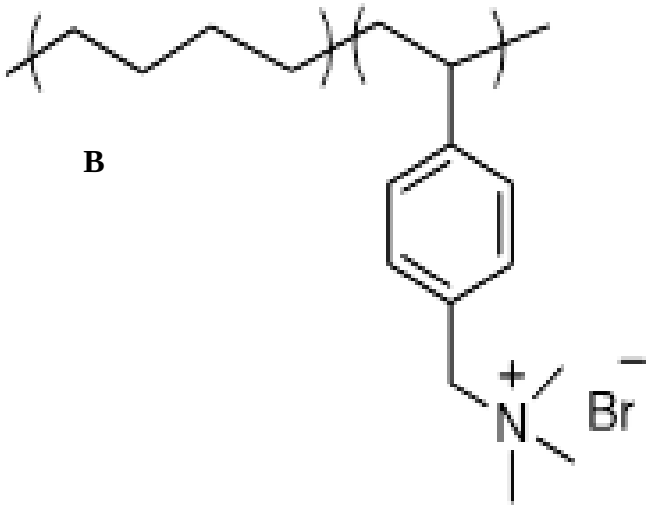

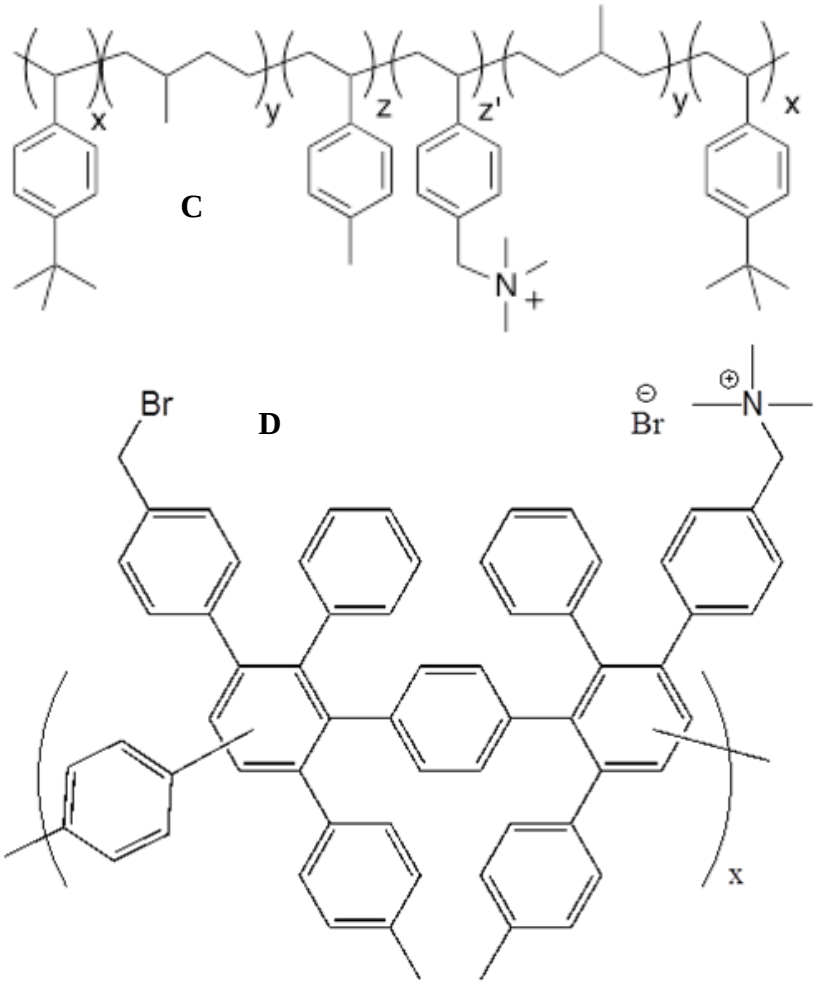

Figure 5.1 Chemical structures of (A) Nafion 115, (B) PE-b-PVBTMA, (C) Brexar43, and (D) ATMPP

5.3.2 Rheometry

Rheological measurements were done on an ARES-G2 rheometer (TA Instruments) using a modified Sentmanat Extensional Rheometer (SER) [40]. Details on the SER fixture are available elsewhere [20]. Samples were cut into rectangles measuring between 2-4 mm and about 20 mm long. Thicknesses ranged from 30-100 microns. Tests were run at various temperature and relative humidity conditions using the custom oven described in Chapter 3. Extensional rates were based on testing conditions modified from ASTM D882, Tensile Properties of Thin Plastic Sheeting [60]. According to the standard, the speed of the testing and the grip separation are dependent on the percent elongation at break. The speed of the testing is calculated from the

initial strain rate multiplied by the initial grip separation. With the SER drums, the speed of the drum rotation can be altered, but the separation distance between the drums is fixed. Using the same formula as the ASTM standard and a fixed grip separation of 12.7 mm (distance between the center point of the two SER drums), a rate of grip separation can be calculated. This grip separation rate is then converted to an engineering strain rate using the geometry of the drums, yielding an engineering strain rate of 0.33 s^{-1} for materials whose elongation to break was greater than 100%. For elongation between 20% and 100%, the rate of 0.0167 s^{-1} was used, and for elongation less than 20% the rate used was 0.0033 s^{-1}. At least five replicates were averaged for the final data. Error bars are one standard deviation.

Extensional tests on the SER measure stress as a function of engineering strain (Figure 5.2). To compare SER data with typical tensile measurements, an Engineering Stress was calculated using the fixed starting area of the sample. Extensional Stress is the property that factors in the exponential decrease in sample area. The stress at break and Young's modulus were calculated from the Engineering Stress. Young's modulus was taken as the slope at low strains in the linear, elastic region. The stress at break was taken as the stress at the break point. Elongation is calculated by multiplying the final engineering strain by 100. A yield stress could be determined from the stress-strain curves, but it is not investigated in this work. At least five tests were run for each sample.

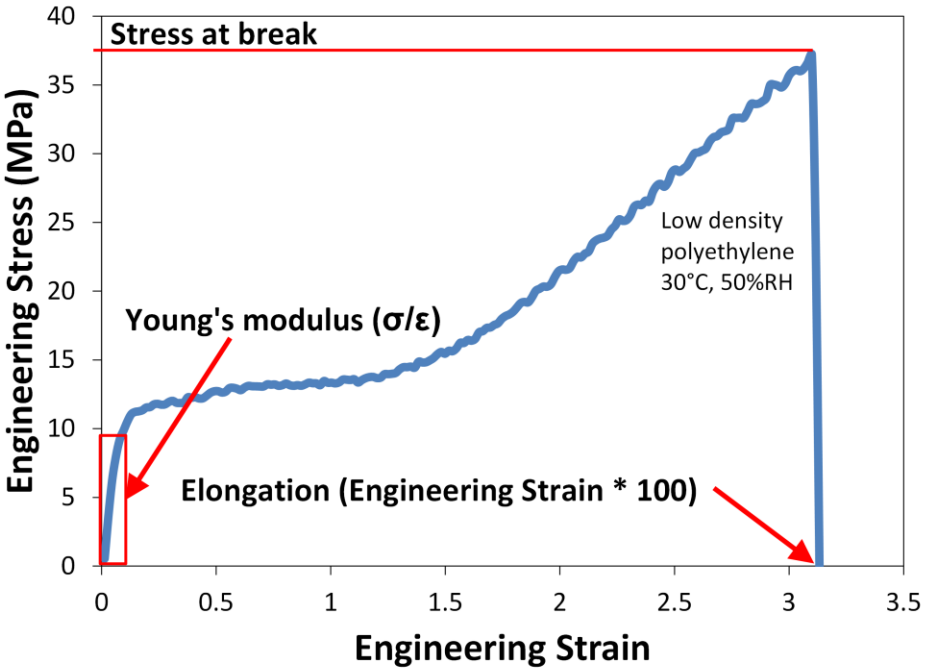

Figure 5.2 Example of a typical stress-strain curve from the modified SER tool. The three main properties (Stress at break, Young's modulus, and Elongation) are depicted.

5.3.3 Conductivity

Ionic conductivity was measured by electrochemical impedance spectroscopy using a four-electrode in-plane conductivity cell. Impedance spectra were obtained over a frequency range of 0.3 to 10^6 Hz using a multi-channel potentiostat (BioLogic VMP3). A TestEquity sample chamber controlled temperature and humidity during data acquisition. Membrane resistance was defined as the low frequency intercept of the Nyquist impedance plot and conductivity, σ, was calculated using the film dimensions where R is the membrane resistance, l is the length between electrodes, and t and w are the thickness and width of the membrane sample, respectively (5.1).

$$\sigma = \frac{l}{R \cdot t \cdot w} \tag{5.1}$$

Reported conductivity data are the average of at least three separate membrane samples and multiple impedance spectra at each steady-state temperature; error bars are one standard deviation.

5.3.4 Water uptake

Water uptake (*WU*) was characterized using a dynamic vapor sorption apparatus (SMS DVS Advantage 1, Allentown, PA). A membrane sample, about 4 mm^2, was placed on a glass weigh plate and the change in mass was measured gravimetrically under different humidity conditions. The *WU* of the membrane was calculated based on equation (5.2).

$$WU = \frac{m_{\%RH} - m_{dry}}{m_{dry}} \times 100 \tag{5.2}$$

where $m_{\%RH}$ is the mass of the sample at the given relative humidity and m_{dry} is the mass of the dry sample. The mass of the dry membrane was taken as the measured mass at the end of the initial 4-h drying period. Given the WU at saturated conditions and the known ion exchange capacity (*IEC*) of the membrane, the hydration level, λ, which is the number of waters per cation functional group, can be calculated using equation (5.3). The molecular weight of water ($m(H_2O)$) is needed to complete the equation.

$$\lambda = \frac{WU}{m(H_2O) \cdot IEC} \tag{5.3}$$

5.3.5 Water stress

The water stress measurement is a method of characterizing the mechanical response of ion exchange membranes under cyclic hydration conditions. The membrane was loaded on the film/fiber tool on the TA Instruments ARES-G2 rheometer. The membrane was loaded and rested an hour at 80°C and 90%RH in order to reach a steady-state mass uptake. The membrane

was then stretched to put a small tension while keeping the film in the elastic region without going to plastic deformation. This region was defined from tensile tests at 60°C, 90%RH. Using the environmentally controlled oven, the membrane was subjected to alternating cycles of 95%RH and 0%RH at 80°C. Short cycle times of 10 minutes were used to accelerate degradation, while 60 minute cycles allowed the membrane to reach steady-state water absorption and desorption for each cycle. Samples were about 3 mm wide and the initial gap was set to 10 mm. Three replicates were done for each reported measurement. The water stress was calculated by subtracting the difference in measured stress from the wet cycle to the dry cycle (Figure 5.3). As the membrane dried, the film contracted and this contraction forced was measured by the rheometer's axial force transducer. Once the humid atmosphere was reintroduced, the film absorbed water and relaxed, thus decreasing the axial force.

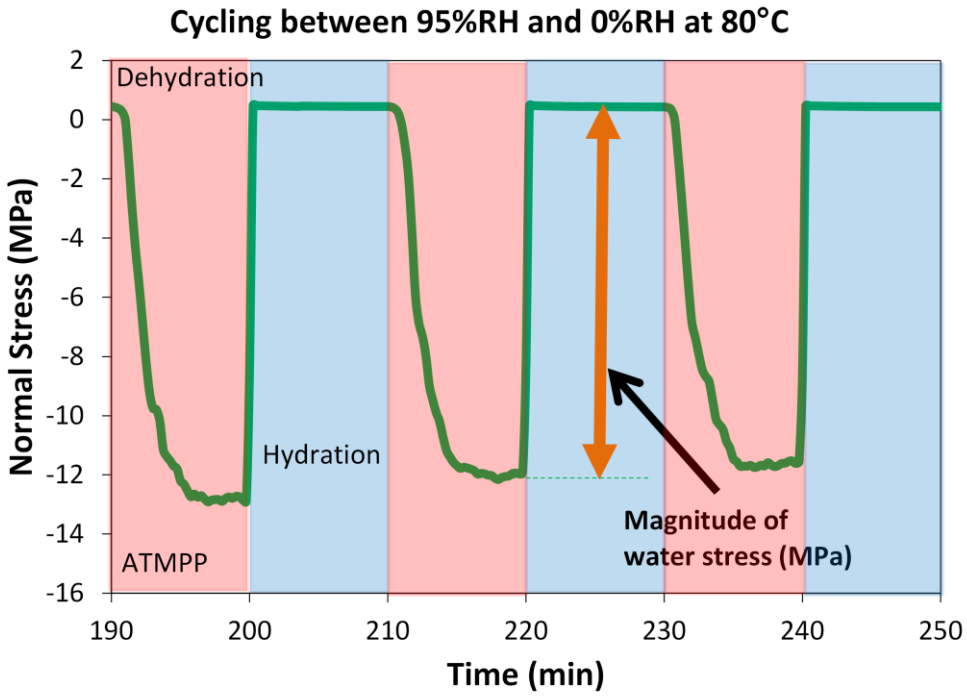

Figure 5.3 Example of data from a water stress experiment

5.4 Results and Discussion

Conductivity, water uptake, and tensile testing data are reported elsewhere for some of these membranes [40,76] and is reproduced here for comparison with the water stress measurements.

5.4.1 Conductivity and water uptake

At 60°C and 95%RH the Brexar43 and ATMPP membranes have an order of magnitude greater conductivity than the PE-b-PVBTMA with about half the water uptake (Table 5-1). All the AEMs still trail Nafion® 115 in conductivity, although in general PEMs will always conduct better than AEMs due to the size difference in mobile species (H^+ vs Br^-). Brexar43 has equivalent conductivity with ATMPP despite having a third of the ion exchange capacity.

Table 5-1 Water uptake and ionic conductivity from current text and literature for Nafion® 115, PE-b-PVBTMA, Brexar43, and ATMPP

	Ion Exchange Capacity (meq/g)	Water uptake (%) 60°C, 95%RH	Dimensional swelling (vol%)	Conductivity (mS/cm) 60°C, 95%RH	Reference
Nafion® 115	0.9	17.1 ± 0.1	21 ± 1	137 ± 17 (H^+)	
PE-b-PVBTMA	1.2	32.3 ± 0.2	14 ± 4	2 ± 0.5 (Br^-)	[126]
Brexar43	0.8	16.4 ± 0.7	34 ± 3	18 ± 2 (Br^-)	
ATMPP	2.5	13.7 ± 0.3	43 ± 3	20 ± 2 (Br^-)	[76]

5.4.2 Tensile testing

The three main mechanical properties taken from a stress-strain curve vary in relevancy to an ion exchange membrane operating in an electrochemical device. The membrane needs to be strong enough to handle when dry or wet and withstand stresses associated with being loaded in a membrane electrode assembly. All four membranes exhibit a stress at break greater than 10 MPa with the exception of the Brexar43 in the high hydration condition (Figure 5.4).

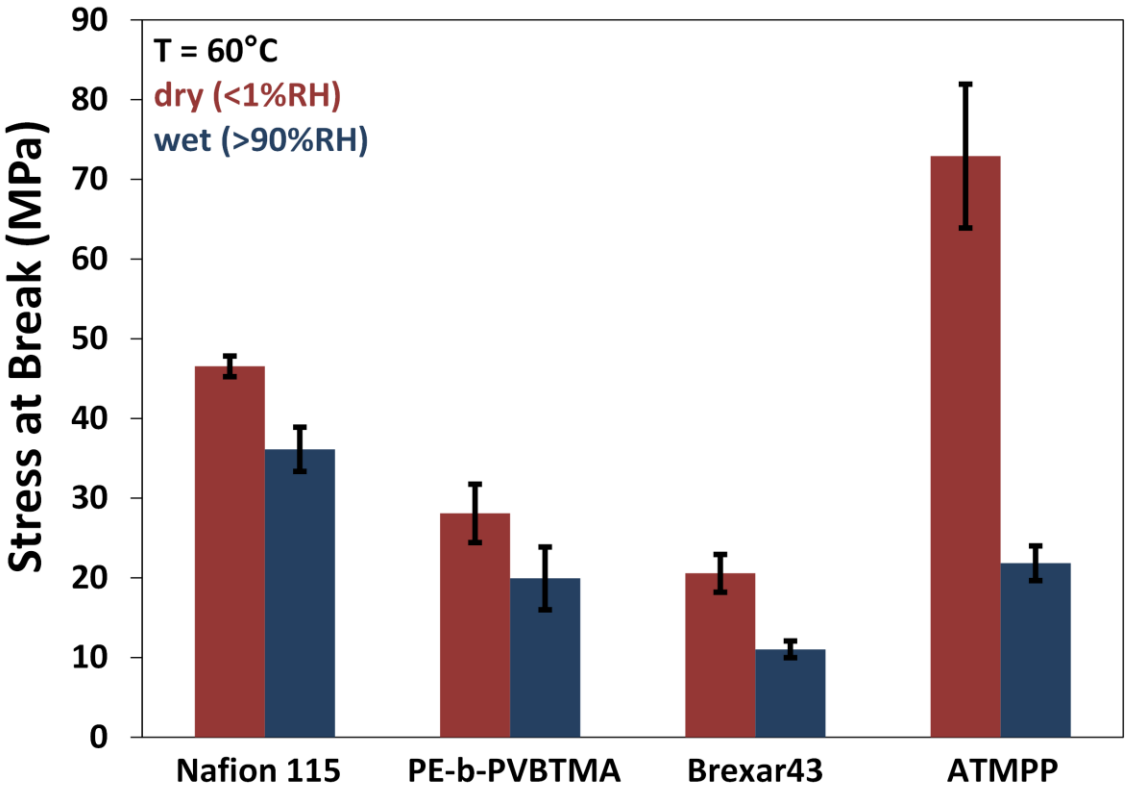

Figure 5.4 Stress at break for Nafion 115 (benchmark), PE-b-PVBTMA, Brexar43, and ATMPP at 60C for both dry and saturated relative humidity conditions

The membrane should be able to handle mechanical dimension strain greater than the dimensional change due to water uptake. A dry elongation greater than 100% is a conservative metric for a minimum elongation needed. The minimum elongation value is membrane specific, and the dimensional change ratio as mechanical elongation over swelling due to hydration should be greater than 10 for a stable membrane (Table 5-2). Nafion® 115 and the PE diblock are both comfortably over this threshold (~20), but ATMPP and Brexar43 are both near 1.

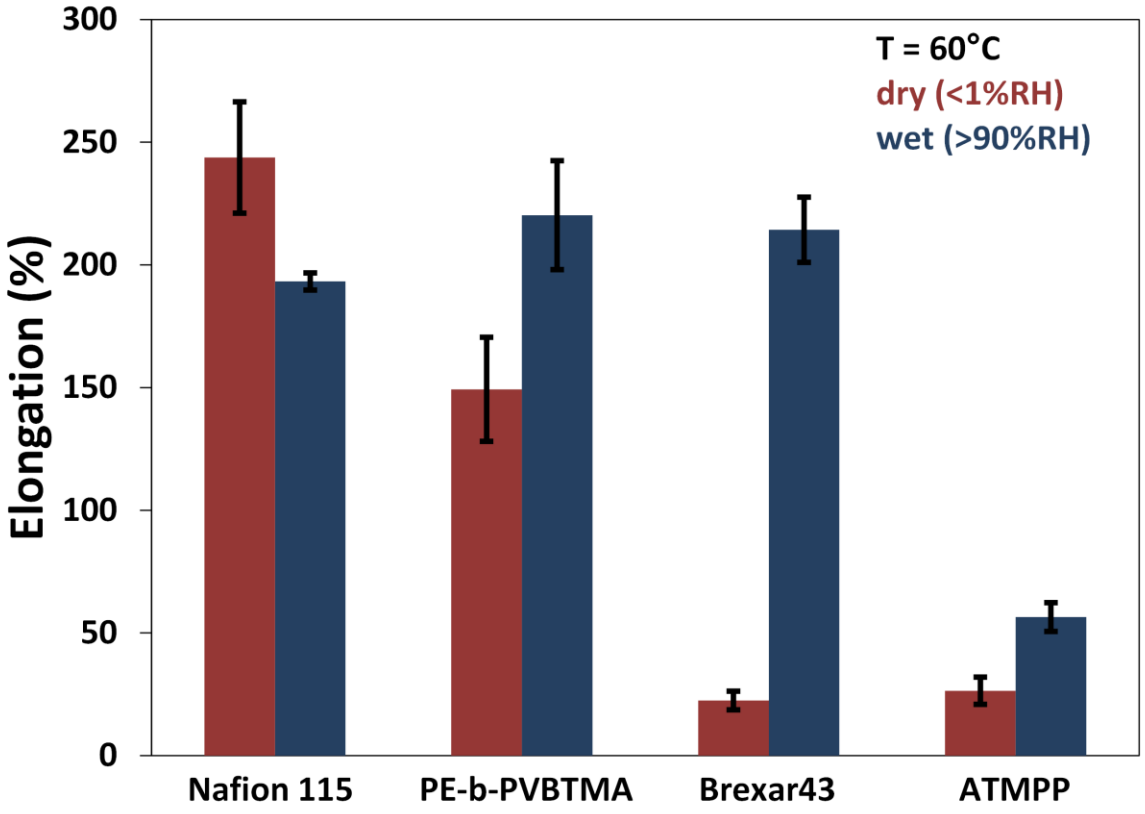

Figure 5.5 Elongation to break for Nafion 115 (benchmark), PE-b-PVBTMA, Brexar43, and ATMPP at 60C for both dry and saturated relative humidity conditions

Table 5-2 Mechanical vs in-plane swelling for Nafion 115, PE-b-PVBTMA, Brexar43, and ATMPP

	Elongation (%) at 60°C, dry	In-plane swelling at 25°C (%)	Mechanical / in-plane swelling ratio	Reference
Nafion® 115	244	12	21	[40]
PE-b-PVBTMA	149	8	18	[126]
Brexar43	17	27	0.6	
ATMPP	26	26	1	[76]

In an electrochemical device from the mechanical viewpoint, a membrane will mainly be subject to oscillations in force, temperature, and relative humidity. Since these osciallations are individually not strong enough to destroy the membrane, an important mechanical characteristic of the membrane is its ability to withstand these small forces and revert back to its original state.

The Young's modulus is the best metric to define the elasticity of the membrane and ideally the value should be ~75-450 MPa. Below 75 MPa, the membrane can behave more like a fluid and above 450 MPa, the membrane is too stiff. The difference between modulus values at dry and hydrated conditions should also be kept to a minimum. Nafion® 115 meets these requirements, but the anion exchange membranes do not. The PE diblock and Brexar43 membranes both become very soft under hydrated conditions at 60°C (<15 MPa). The ATMPP membrane shows less variation, but is too stiff dry and softens considerably when hydrated.

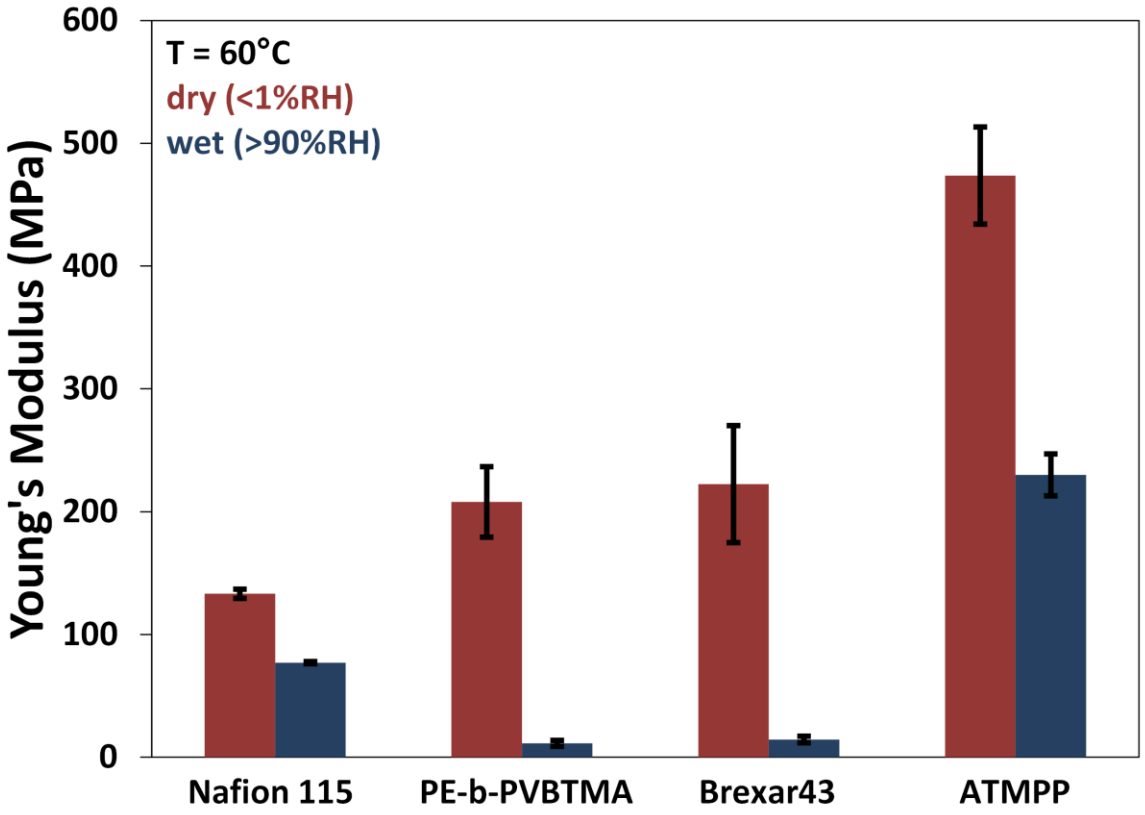

Figure 5.6 Young's modulus for Nafion 115 (benchmark), PE-b-PVBTMA, Brexar43, and ATMPP at 60°C for both dry and saturated relative humidity conditions

5.4.3 Water stress

The tensile testing at static temperature and relative humidity conditions are useful to provide a framework and comparison point for membranes, but it does not represent the smaller,

cyclical stresses imposed on a membrane in a working device. The water stress test attempts to quantify the hyrgal stresses a membrane encounters in a working device.

The water stress tests were run at an accelerated degradation temperature of 80°C. ATMPP exhibits a significantly higher water stress than either the PE diblock, Brexar43, or Nafion® 115, correlating with the higher Young's modulus from the tensile testing (Figure 5.7). ATMPP and Brexar43 lose ~40% of the peak water stress over 20 cycles while the PE diblock and Nafion® 115 lose less than 10%. Nafion® 115 and PE-b-PVBTMA show an initial increase in water stress over the first several cycles before leveling off or trending lower. An ideal membrane would have a low water stress and it would maintain its ability to absorb and desorb water completely reversibly over a large number of cycles, thus losing 0% of its maximum water stress.

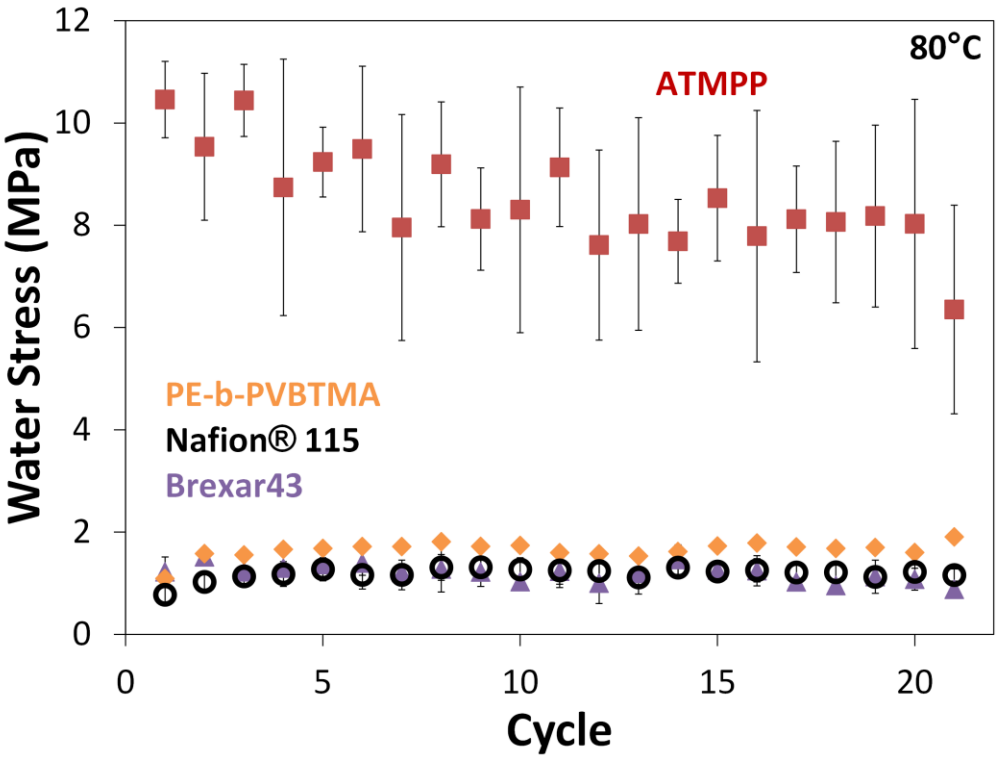

Figure 5.7 Water stress in 10 min hydration/dehydration cycles over 7 hours for ATMPP, PE-b-PVBTMA, Nafion® 115, and Brexar43

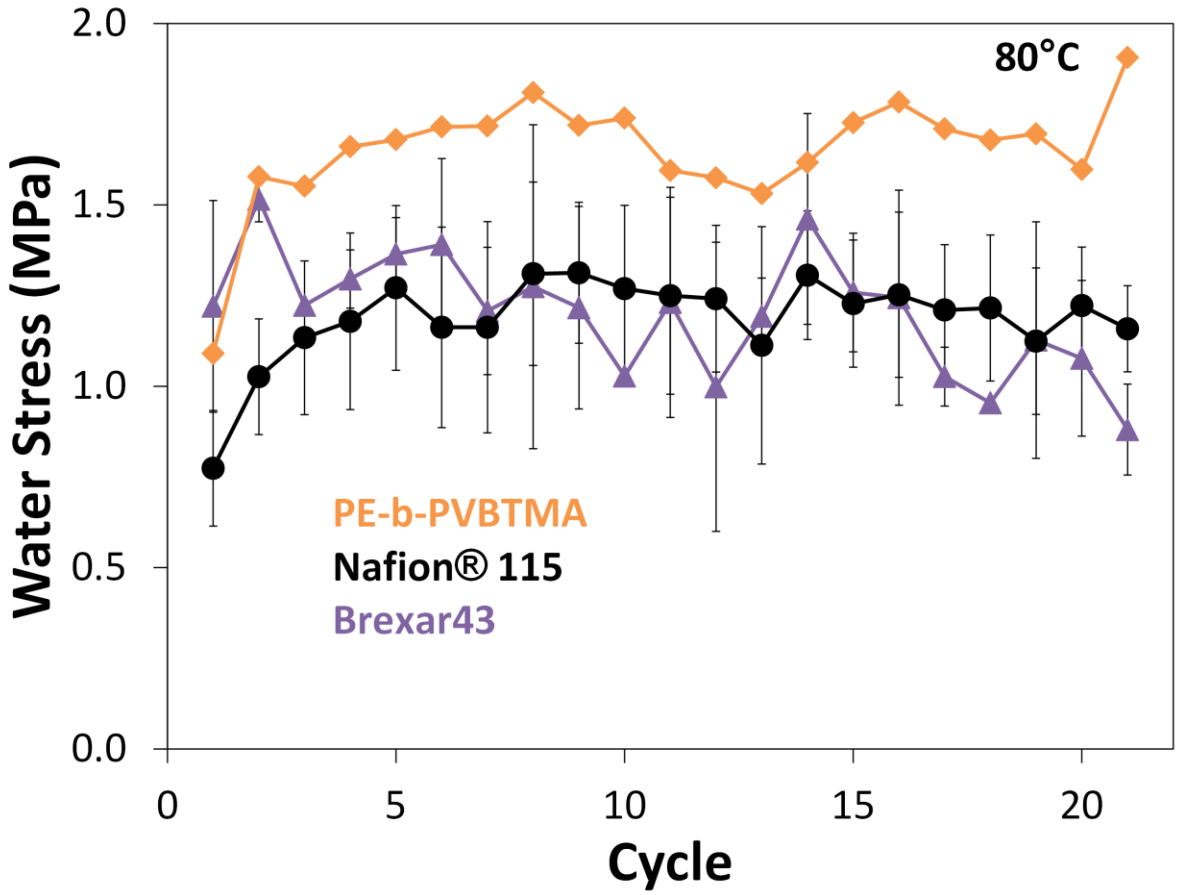

Figure 5.8 Water stress in 10 min hydration/dehydration cycles over 7 hours for PE-b-PVBTMA, Nafion® 115, and Brexar43.

The test was extended out to 100 cycles covering over 33 hours to better gauge long term membrane performance (Figure 5.9). While Nafion® 115 maintained its low water stress and lost less than 5% of its maximum stress, the ATMPP exhibited a higher water stress and loss ~65% of its maximum water stress. Brexar43 also lost ~60% of its maximum water stress, but maintained a lower overall water stress in the range of Nafion® 115. Large error bars on the ATMPP data are most likely due to slow water absorption kinetics. The membrane can not fully absorb and desorb water in the course of a single hydration or dehydration cycle.

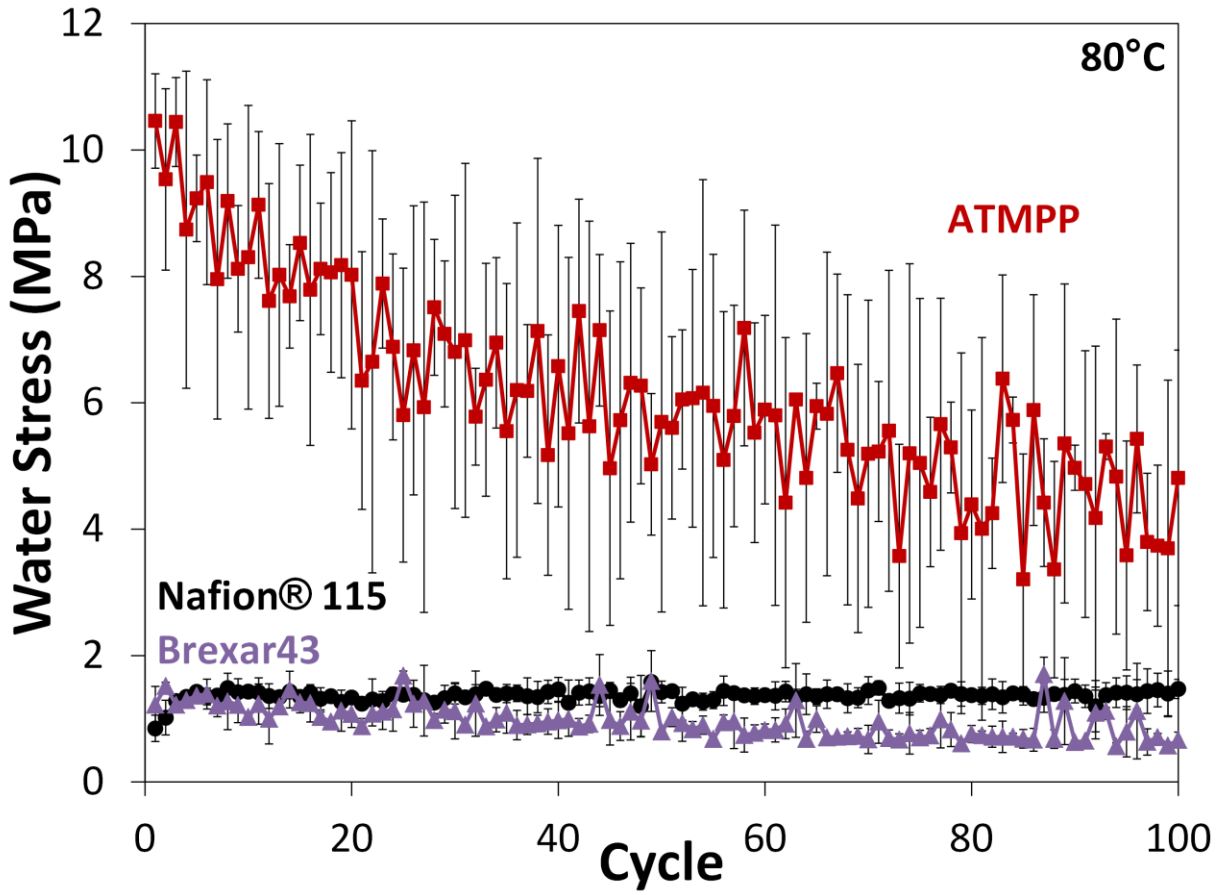

Figure 5.9 Water stress in 10 min hydration/dehydration cycles over 33 hours at 80°C for ATMPP, Nafion® 115, and Brexar43. ATMPP

Due to the longer times needed to reach steady-state mass change for hydration and dehydration, the cycle times were extended to 60 minutes to allow for full water absorption and desortpion. The total test time of 33 hours was maintained. Both membranes still lose nearly 40% from their peak water stress, but the Brexar43 remains in a much lower water stress range (1-2 MPa) (Figure 5.10).

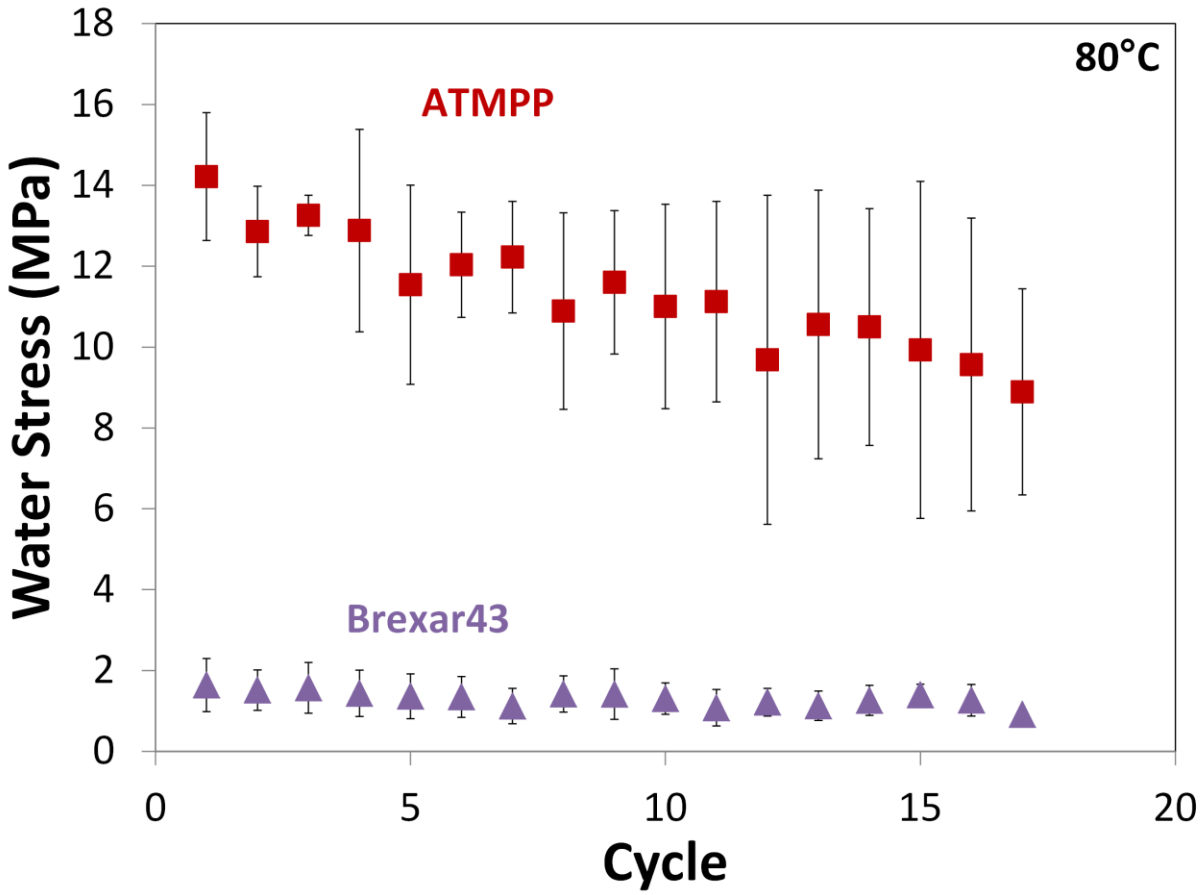

Figure 5.10 Water stress for 17, 60 minute cycles at 80°C for ATMPP and Brexar43

Both of the 33 hour tests were compared to investigate how the cycle time affected the water stress. The 60 min cycle water stress averaged ~50% higher in Brexar43 and ~80% higher in ATMPP than the 10 min cycle water stress at any given time in the test (Figure 5.11, Figure 5.12). Cycling more often over the same period of time resulted in lower water stress values and led to higher degradation in both membranes (Figure 5.13). Cycling more frequently may lead to temperature and relative humidity instabilities in the environmental oven, however, the total testing time could be extended until membrane failure. For quicker screening of membranes, the 10 minute cycling over just 20 cycles (7 hours) differeniated between the four chemistries.

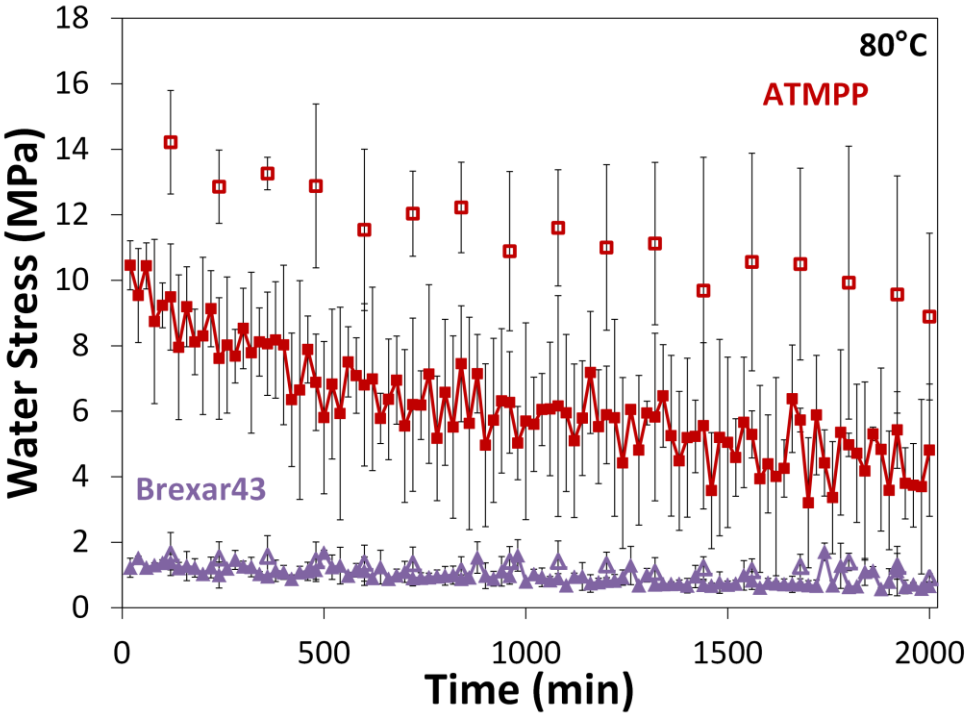

Figure 5.11 Water stress for ATMPP and Brexar43 over 33 hours. The closed symbols are 10 min cycles and the open symbols are 60 minute cycles.

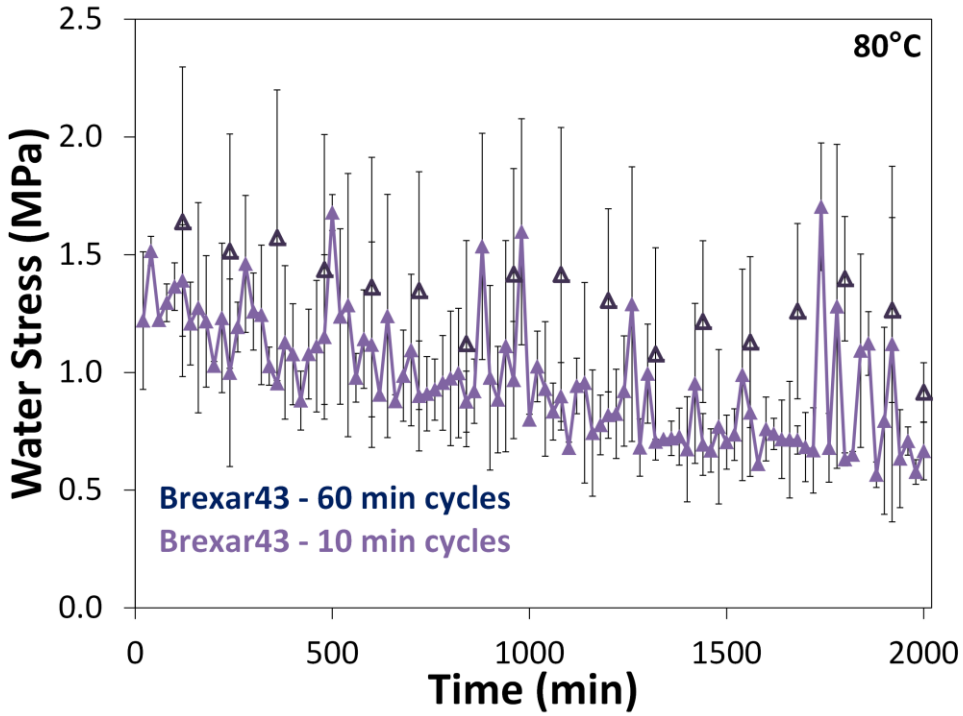

Figure 5.12 Zoomed in water stress for Brexar43 over 33 hours. Darker symbols are 60 min cycles and lighter symbols are 10 min cycles

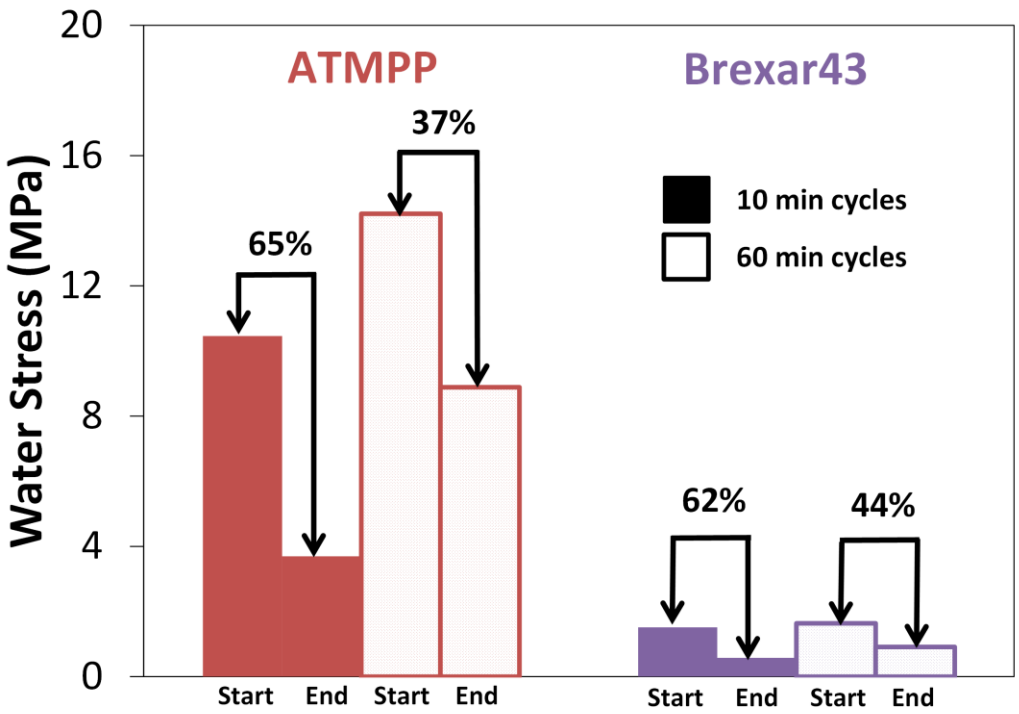

Figure 5.13 Change in water stress from beginning to end of 33 hour test with either 10 minute or 60 minute hydration cycles at 80°C for ATMPP and Brexar43

5.5 Conclusions

We have demonstrated mechanical characterization of chemically different ionomers. Traditional tensile testing was performed under controlled environmental conditions and benchmarks of >10 MPa stress at break, >100% elongation at break, and Young's modulus between 75-400 MPa are proposed. A minimum strength is needed to withstand processing and handling, but the membrane is not under extensional tension in a working device so a higher strength is not needed. The membrane should be able to elongate mechanically at least 10 times more than it swells with water so an elongation at break greater than 100% is proposed. A membrane must have elasticity to withstand many small hygral and mechanical cycles. A low Young's modulus (<75 MPa) indicates the polymer may flow when hydrated, while a Young's modulus above 400 MPa indicates the polymer may be too stiff to accommodate the mechanical

cycling as the polymer absorbs and desorbs water. Nafion® 115 meets all of these criteria as expected, but the AEMs studied all far short in at least one metric. The PE-b-PVBTMA membrane is too elastic when hydrated. The Brexar43 membrane is too weak and elastic when hydrated and has low elongation when dry. The ATMPP membrane is too stiff when dry. The Brexar43 membrane is more mechanically similar to the PE-b-PVBTMA membrane, but has conductivity (20 mS/cm) and water uptake values (~15%) similar to the ATMPP, a much more stiff membrane.

The new water stress metric was able to differentiate between the various chemistries. The stiff ATMPP and the more elastic Brexar43 membranes softened during the course of the short and long term humidity cycling which could mean they will perform poorly over time in a working fuel cell subject to similar humidity cycles. Nafion® 115 performed very well, justifying its wide spread study and use. The PE-b-PVBTMA membrane showed promise in its ability to absorb and desorb water reversibly as its performance most closely resembles that of Nafion® 115. More long term testing is warranted. ATMPP has a Young's modulus greater than 400 MPa at 60°C and dry conditions, while the other three have a Young's modulus less than 250 MPa at the same conditions. While Brexar43 and PE-b-PVBTMA have similar elasticity profiles in the dry and wet conditions, they perform differently in the water stress cycling tests. Young's modulus was not able to differentiate these polymers so another metric may be more useful in predicting membrane performance through hygral cycling.

The ratio of the mechanical elongation at dry conditions over the in-place dimensional swelling was also indicative of water stress performance. Nafion® 115 and PE-b-PVBTMA have ratios ~20, while ATMPP and Brexar43 have ratios near 1. The high T_g components in Brexar43 and ATMPP contribute to a low elongation at dry conditions, suggesting that polymers

containing more low T_g components be used in AEM development. The block ratios in the Brexar43 pentablock could be altered to include a higher fraction of the hydrogenated isoprene and a lesser fraction of the t-butyl styrene for optimal mechanical properties without sacrificing ionic conductivity.

The combination of the static tensile tests and the water stress accelerated testing protocol provide insight on the performance of membranes under mechanical and hygral stresses. A simple metric comparing the mechanical elongation in a dry condition with the in-plane swelling percentage in liquid water can be used to predict how membranes will perform under hygral cycling. In designing anion exchange membranes, we show that elastic components are more favorable than stiff for mechanical robustness under hydration cycling. While improving chemical stability and ionic conductivity will continue to be important issues to address, mechanical performance under device operating conditions is critical to development of robust ion exchange membranes.

5.6 Acknowledgements

The authors thank the U.S. Army Research Office (MURI Grant #W911NF-10-1-0520 and DURIP Grant #W911NF-11-1-0306) for its support of this work. I thank Yifan Li, S. Piril Ertem, and Michael Hibbs for synthesizing the polymers. I also thank Bryan Pivovar at NREL for pointing me in the direction of past work done on mechanical characterization techniques of fuel cell membranes.

CHAPTER 6

CONCLUSIONS AND RECOMMENDATIONS

6.1 Summary and Conclusions

Anion exchange membranes are a promising material with applications in alkaline fuel cells, barrier layers, and water splitters. The research community has introduced many polymer systems attempting to overcome the main challenges of low ionic conductivity and chemical stability in a high pH environment, while maintaining mechanical integrity [18]. Fully mechanical characterization of experimental polymers is a fundamental issue that is needed to develop a practical AEM.

This thesis reports a new platform for mechanical characterization of thin film polymer ion exchange membranes. A home-built humidity controlled oven attached to a TA Instruments ARES-G2 rheometer was designed, constructed, and proven. A Sentmanat Extensional Rheometer was modified to test solid films less than 100 microns in thickness using a tensile geometry. Less than 5% of material needed for traditional tensile testing is used in these tests. The modified SER tool was benchmarked using the humidity controlled oven at conditions relevant to fuel cell operation with the common proton exchange membrane Nafion® 115 and the hydrophobic polymer polyethylene. The new platform characterized over 20 polymers to date, and contributed to this thesis as well as the thesis of Melissa A. Vandiver. Results are summarized in four publications with three additional manuscripts in preparation. The temperature and relative humidity control on the oven were robust enough to handle not only steady-state conditions, but also ramps of temperature at constant relative humidity and ramps of relative humidity at constant temperature. Ramping was used in Vandiver's thesis to explore

mechanical transitions using dynamic mechanical analysis under saturated conditions. The environmental chamber was also used to study alginate hydrogels made by the Krebs group, and preliminary rheology tests were performed on ceramic pastes from Dow Chemical which dry out quickly in ambient conditions. The lifetime of the environmental chamber is expected to be ten years or more.

This thesis contributed to the understanding of a pentablock anion exchange membrane which was one of the first membranes which met minimum metrics in conductivity, water uptake, and mechanical integrity. The combination of high T_g blocks (t-butyl styrene) and low T_g blocks (hydrogenated isoprene) led to adequate mechanical performance and formed a lamellar structure, which was maintained under high hydration conditions and under extensional strain. The extensional strain tests were performed with a novel *in situ* SAXS technique using the modified SER tool.

Chapter 5 introduced a new quantifiable method of mechanically testing fuel cell membranes that more accurately reflects the mechanical forces it undergoes in a working fuel cell as it absorbs and desorbs water. The water stress tests were able to differentiate between stiff, brittle polymers and more elastic polymers, showing a relationship between mechanically straining a polymer and hydration cycling. A low water stress which remains steady through many cycles is desirable and PE-b-PVBTMA met this criteria for short term testing. The combination of the static tensile tests and the water stress accelerated testing protocol take advantage of the home built environmentally controlled oven and the sensitive axial transducer on the ARES G-2 rheometer to give a power tool for characterizing materials sensitive to temperature and water.

My hypothesis that a tensile tester under controlled temperature and relative humidity conditions could be built to provide a better frame of reference for comparison between polymer chemistries has been proven true. The environmentally controlled oven and modified SER tool used to perform tensile testing on 10-100 micron films using milligrams of material contributes to the field by generating quantifiable mechanical metrics for a wide array of experimental polymers. I believed that a relationship between the Young's modulus, elongation, and water uptake could be used to predict membrane durability in a working electrochemical device. I believe the ratio between the dry elongation to break and in-plane water swelling in liquid water captures the interplay between the mechanical and hygral forces in a single metric. The mechanical elongation needs to be 10 times greater than the in-plane water swelling to handle the hydration cycling seen in a working fuel cell.

In total, this thesis developed novel instrumentation for the mechanical characterization of environmentally sensitive materials. Anion exchange membranes were characterized with tensile testing and hydration cycling leading to quantifiable metrics for membrane performance. A pentablock AEM with a balance of stiff and elastic blocks was shown to have adequate conductivity, low water uptake, and good mechanical integrity, even under strain or high hydration conditions. The work presented here was used in support of multiple thesis efforts and has the potential to be used for applications such ion exchange membranes, hydrogels, chewing gum, or pastes in the future.

6.2 Recommendations for future work

The development and characterization of anion exchange membranes is still a growing field and there are many opportunities to pursue in the future. The mechanical testing system

developed in this thesis is a versatile platform which can be used in the characterization of many other environmentally sensitive materials outside of anion exchange membranes.

At the extreme dry condition (<1%RH) used in these tests, many membranes failed to bend around the SER drums, causing them to crack at the securing pin instead of breaking in the open space between the drums. There are few instances where a membrane would see relative humidity conditions that dry so it is recommended to change dry condition testing to 25%RH instead of 0% since 25%RH is closer to ambient conditions in most of the world. This change could prevent artificially low elongation values less than 10%.

The accelerated water stress test should be able to bring a membrane to failure. Hygral stresses form microcracks in membranes and it would be good to match the mechanical cycling data with testing methods that rely on permeation through the membrane to determine failure. A stress at microcrack propagation may be identified which can add value to both testing protocols. The water stress test may also be extended from a hundred cycles to a thousand cycles to push the hygral fatigue even further. Testing the conductivity of membranes after cyclical mechanical, thermal, or hygral stresses should also be investigated. The non-linear stresses may cause significant mechanical and structural changes in membranes affecting their transport properties. Nafion® 115 had a small increase in water stress before plateauing suggesting there may be a "break-in" water absorption mechanism which could affect conductive pathways. The significant decrease in water stress in Brexar43 over time may affect the as-cast morphology and conductivity. Conditioning membranes with humidity cycling made lead to a more defined water channel for ion conduction or it may destabilize the backbone and collapse the water channel needed for ion conduction.

It was recently reported that removing electron withdrawing substituents, such as sulfone or bromine groups, from the polymer backbone helps to mitigate cation trigger backbone degradation [127]. It is recommended to synthesize a "Clexar" polymer to compare with the Brexar material to investigate this phenomenon further as stability in alkaline environments is critical for anion exchange membranes.

An ideal anion exchange membrane must be mechanically stable, highly conductive, and chemically stable in high pH environments. From the mechanical viewpoint, I believe the most important property is reversibility under cyclical mechanical and hygral stresses. A Young's modulus of 200-250 MPa at 60°C, dry conditions and a 60°C, dry elongation greater than 10 times the in-plane water swelling work well in the cyclical water stress tests performed. The Brexar pentablock or the PE-b-PVBTMA are the membranes I worked with that came closest to these metrics. The PE-b-PVBTMA is a good membrane to study, but it is limited for practical applications since the conductivity is so low (2 mS/cm at 60°C, 95%RH). The higher IEC versions of the polymer (with higher block ratios of PVBTMA) had higher conductivity, but became mechanically unstable with hydration. The Brexar family of polymer performed poorly in the elongation metric, most likely due to the high weight fraction of the high T_g components t-butyl styrene and poly (vinyl benzyltrimethylammonium).

The Brexar platform has some potential with a few changes. As mentioned earlier, synthesizing the polymer with chlorinated chemicals may help with hydroxide stability. Since the membrane becomes stiffer with higher functionalization, I would counteract this effect by adjusting the block ratios. The current pentablock has a molecular weight of 15-10-28-10-15 kg/mol. The outer blocks of t-butyl styrene should be reduced and the inner blocks of hydrogenated isoprene should be increased, which should make the polymer more elastic and

increase the mechanical elongation. I would suggest trying to make a 5-20-28-20-5 kg/mol pentablock and then performing the functionalization to make an AEM. Since the IEC should remain nearly the same, the new polymer would have better mechanical integrity and remain highly conductive.

Another area that was not explored was the cation's effect on the mechanical properties. The only cation studied in-depth was benzyl trimethylammonium. Although the MURI team has created phosphonium and cobaltocenium cations, it has been a challenge to attach them to polymers. A mechanical study attaching multiple cations to the same polymer backbone would be interesting. Trimethylammonium cations are moderately stable in hydroxide, but the phosphonium and cobaltocenium cations have shown promise of improved stability in hydroxide. A mechanical study would investigate if improving the chemical stability effected the mechanical stability.

REFERENCES

[1] A.M. Herring, G.A. Voth, T.A. Witten, E.B. Coughlin, Y. Yan, D.M. Knauss, et al., MURI Proposal for “Ion Transport in Complex Heterogeneous Organic Materials,” (2010).

[2] H.A. Gasteiger, S.S. Kocha, B. Sompalli, F.T. Wagner, Activity benchmarks and requirements for Pt, Pt-alloy, and non-Pt oxygen reduction catalysts for PEMFCs, Appl. Catal. B Environ. 56 (2005) 9–35. doi:10.1016/j.apcatb.2004.06.021.

[3] Y. Bing, H. Liu, L. Zhang, D. Ghosh, J. Zhang, Nanostructured Pt-alloy electrocatalysts for PEM fuel cell oxygen reduction reaction., Chem. Soc. Rev. 39 (2010) 2184–202. doi:10.1039/b912552c.

[4] J.R. Varcoe, R.C.T. Slade, Prospects for Alkaline Anion-Exchange Membranes in Low Temperature Fuel﷒Cells, Fuel Cells. 5 (2005) 187–200. doi:10.1002/fuce.200400045.

[5] S. Gamburzev, K. Petrov, A.J. Appleby, Silver – carbon electrocatalyst for air cathodes in alkaline fuel cells, J. Appl. Electrochem. (2002) 805–809.

[6] M. Schulze, E. Gülzow, Degradation of nickel anodes in alkaline fuel cells, J. Power Sources. 127 (2004) 252–263. doi:10.1016/j.jpowsour.2003.09.021.

[7] N. Wagner, M. Schulze, E. Gülzow, Long term investigations of silver cathodes for alkaline fuel cells, J. Power Sources. 127 (2004) 264–272. doi:10.1016/j.jpowsour.2003.09.022.

[8] G.F. McLean, T. Niet, S. Prince-Richard, N. Djilai, An assessment of alkaline fuel cell technology, Int. J. Hydrogen Energy. 27 (2002) 507–526. doi:10.1016/S0360-3199(01)00181-1.

[9] H. Long, K. Kim, B.S. Pivovar, Hydroxide Degradation Pathways for Substituted Trimethylammonium Cations: A DFT Study, J. Phys. Chem. C. (2012) 120423124503008. doi:10.1021/jp3014964.

[10] G.K.S. Prakash, F.C. Krause, F. a. Viva, S.R. Narayanan, G. a. Olah, Study of operating conditions and cell design on the performance of alkaline anion exchange membrane based direct methanol fuel cells, J. Power Sources. 196 (2011) 7967–7972. doi:10.1016/j.jpowsour.2011.05.056.

[11] R. Janarthanan, J.L. Horan, B.R. Caire, Z.C. Ziegler, Y. Yang, X. Zuo, et al., Understanding anion transport in an aminated trimethyl polyphenylene with high anionic conductivity, J. Polym. Sci. Part B Polym. Phys. (2012) n/a–n/a. doi:10.1002/polb.23164.

[12] R. O'Hayre, S.-W. Cha, W. Colella, R.B. Prinz, Fuel Cell Fundamentals (2nd ed.), John Wiley and Sons, Inc., Hoboken, NJ, 2009.

[13] M. Faraj, E. Elia, M. Boccia, A. Filpi, A. Pucci, F. Ciardelli, New anion conducting membranes based on functionalized styrene-butadiene- styrene triblock copolymer for fuel cells applications, J. Polym. Sci. Part A Polym. Chem. 49 (2011) 3437–3447. doi:10.1002/pola.24781.

[14] L. Wang, V. Bambagioni, M. Bevilacqua, C. Bianchini, J. Filippi, A. Lavacchi, et al., Sodium borohydride as an additive to enhance the performance of direct ethanol fuel cells, J. Power Sources. 195 (2010) 8036–8043. doi:10.1016/j.jpowsour.2010.06.101.

[15] I. Kruusenberg, L. Matisen, Q. Shah, a. M. Kannan, K. Tammeveski, Non-platinum cathode catalysts for alkaline membrane fuel cells, Int. J. Hydrogen Energy. 37 (2012) 4406–4412. doi:10.1016/j.ijhydene.2011.11.143.

[16] G. Couture, A. Alaaeddine, F. Boschet, B. Ameduri, Polymeric materials as anion-exchange membranes for alkaline fuel cells, Prog. Polym. Sci. 36 (2011) 1521–1557. doi:10.1016/j.progpolymsci.2011.04.004.

[17] G. Merle, M. Wessling, K. Nijmeijer, Anion Exchange Membranes for Alkaline Fuel Cells: A Review, J. Memb. Sci. (2011). doi:10.1016/j.memsci.2011.04.043.

[18] M.A. Hickner, A.M. Herring, E.B. Coughlin, Anion exchange membranes: Current status and moving forward, J. Polym. Sci. Part B Polym. Phys. 51 (2013) 1727–1735. doi:10.1002/polb.23395.

[19] R. Farber, J. Dealy, Strain History of the Melt in Film Blowing, Polym. Eng. Sci. (1974).

[20] M.L. Sentmanat, Miniature universal testing platform : from extensional melt rheology to solid-state deformation behavior, Rheol. Acta. (2004) 657–669. doi:10.1007/s00397-004-0405-4.

[21] M.L. Sentmanat, B.N. Wang, G.H. McKinley, Measuring the transient extensional rheology of polyethylene melts using the SER universal testing platform, J. Rheol. (N. Y. N. Y). 49 (2005) 585–606. doi:10.1122/1.1896956.

[22] F.J. Stadler, a. Nishioka, J. Stange, K. Koyama, H. Münstedt, Comparison of the elongational behavior of various polyolefins in uniaxial and equibiaxial flows, Rheol. Acta. 46 (2007) 1003–1012. doi:10.1007/s00397-007-0190-y.

[23] F. Baldi, A. Franceschini, T. Riccò, Determination of the elongational viscosity of polymer melts by melt spinning experiments. A comparison with different experimental techniques, Rheol. Acta. 46 (2007) 965–978. doi:10.1007/s00397-007-0181-z.

[24] C. Hadinata, D. Boos, C. Gabriel, E. Wassner, M. Rüllmann, N. Kao, et al., Elongation-induced crystallization of a high molecular weight isotactic polybutene-1 melt compared to shear-induced crystallization, J. Rheol. (N. Y. N. Y). 51 (2007) 195–215. doi:10.1122/1.2426977.

[25] Y. Wang, S.-Q. Wang, From elastic deformation to terminal flow of a monodisperse entangled melt in uniaxial extension, J. Rheol. (N. Y. N. Y). 52 (2008) 1275–1290. doi:10.1122/1.2995858.

[26] W. Sambaer, M. Zatloukal, D. Kimmer, The use of novel digital image analysis technique and rheological tools to characterize nanofiber nonwovens, Polym. Test. 29 (2010) 82–94. doi:10.1016/j.polymertesting.2009.09.008.

[27] R. Borup, J. Meyers, B. Pivovar, Y.S. Kim, R. Mukundan, N. Garland, et al., Scientific aspects of polymer electrolyte fuel cell durability and degradation., Chem. Rev. 107 (2007) 3904–51. doi:10.1021/cr050182l.

[28] S. Kundu, L.C. Simon, M. Fowler, S. Grot, Mechanical properties of Nafion^{TM} electrolyte membranes under hydrated conditions, Polymer (Guildf). 46 (2005) 11707–11715. doi:10.1016/j.polymer.2005.09.059.

[29] S.J. Hamrock, M.A. Yandrasits, Proton Exchange Membranes for Fuel Cell Applications, J. Macromol. Sci. Part C Polym. Rev. 46 (2006) 219–244.

[30] W. Liu, K. Ruth, G. Rusch, Membrane Durability in PEM Fuel Cells, J. New Mater. Mater. Electrochem. Syst. 4. 4 (2001) 227–231.

[31] X. Huang, R. Solasi, Y. Zou, Mechanical endurance of polymer electrolyte membrane and PEM fuel cell durability, J. Polym. Sci. Part B Polym. Phys. 44 (2006) 2346–2357. doi:10.1002/polb.

[32] C. Marestin, G. Gebel, D. Régis, Sulfonated Polyimides, Adv. Polym. Sci. 216 (2008) 185–258. doi:10.1007/12_2008_155.

[33] N. Li, Z. Cui, S. Zhang, W. Xing, Synthesis and characterization of rigid-rod sulfonated polyimides bearing sulfobenzoyl side groups as proton exchange membranes, J. Memb. Sci. 295 (2007) 148–158. doi:10.1016/j.memsci.2007.03.006.

[34] K. Miyatake, H. Zhou, T. Matsuo, H. Uchida, M. Watanabe, Proton Conductive Polyimide Electrolytes Containing Trifluoromethyl Groups : Synthesis , Properties , and DMFC Performance, Macromolecules. 37 (2004) 4961–4966.

[35] G. Meyer, C. Perrot, G. Gebel, L. Gonon, S. Morlat, J.-L. Gardette, Ex situ hydrolytic degradation of sulfonated polyimide membranes for fuel cells, Polymer (Guildf). 47 (2006) 5003–5011. doi:10.1016/j.polymer.2006.04.007.

[36] J. Pan, S. Lu, Y. Li, A. Huang, L. Zhuang, J. Lu, High-Performance Alkaline Polymer Electrolyte for Fuel Cell Applications, Adv. Funct. Mater. 20 (2010) 312–319. doi:10.1002/adfm.200901314.

[37] G.M. Wu, S.J. Lin, C.C. Yang, Preparation and characterization of PVA/PAA membranes for solid polymer electrolytes, J. Memb. Sci. 275 (2006) 127–133. doi:10.1016/j.memsci.2005.09.012.

[38] H. Tang, S. Peikang, S.P. Jiang, F. Wang, M. Pan, A degradation study of Nafion proton exchange membrane of PEM fuel cells, J. Power Sources. 170 (2007) 85–92. doi:10.1016/j.jpowsour.2007.03.061.

[39] P.W. Majsztrik, A.B. Bocarsly, J.B. Benziger, An instrument for environmental control of vapor pressure and temperature for tensile creep and other mechanical property measurements., Rev. Sci. Instrum. 78 (2007) 103904. doi:10.1063/1.2794736.

[40] B.R. Caire, M.A. Vandiver, M.W. Liberatore, Mechanical testing of small, thin samples in a humidity-controlled oven, Rheol. Acta. 54 (2015) 253–261. doi:10.1007/s00397-014-0834-7.

[41] O. Glatter, O. Kratky, Small Angle X-ray Scattering, 1982.

[42] C.G. Vonk, G. Kortleve, X-Ray Small-Angle Scattering of Bulk Polyethylene, Kolloid-Zeitschrift Und Zeitschrift Für Polym. 220 (1967) 19–24.

[43] Y. Liu, J. Horan, G. Schlichting, B.R. Caire, M.W. Liberatore, S.J. Hamrock, et al., A Small-Angle X-ray Scattering Study of the Development of Morphology in Films Formed from the 3M Perfluorinated Sulfonic Acid Ionomer, Macromolecules. 45 (2012) 7495–7503. http://pubs.acs.org/doi/abs/10.1021/ma300926e (accessed March 7, 2013).

[44] G.J. Schlichting, J.L. Horan, J.D. Jessop, S.E. Nelson, S. Seifert, Y. Yang, et al., A Hybrid Organic/Inorganic Ionomer from the Copolymerization of Vinylphosphonic Acid and Zirconium Vinylphosphonate, Macromolecules. 45 (2012) 3874–3882. doi:10.1021/ma300196y.

[45] T.-H. Tsai, A.M. Maes, M. a. Vandiver, C. Versek, S. Seifert, M. Tuominen, et al., Synthesis and structure-conductivity relationship of polystyrene- block -poly(vinyl benzyl trimethylammonium) for alkaline anion exchange membrane fuel cells, J. Polym. Sci. Part B Polym. Phys. (2013). doi:10.1002/polb.23170.

[46] M. a. Vandiver, J.L. Horan, Y. Yang, E.T. Tansey, S. Seifert, M.W. Liberatore, et al., Synthesis and characterization of perfluoro quaternary ammonium anion exchange membranes, J. Polym. Sci. Part B Polym. Phys. 51 (2013) 1761–1769. doi:10.1002/polb.23171.

[47] T.-H. Tsai, S.P. Ertem, A.M. Maes, S. Seifert, A.M. Herring, E.B. Coughlin, Thermally Cross-Linked Anion Exchange Membranes from Solvent Processable Isoprene Containing Ionomers, Macromolecules. 48 (2015) 655–662. doi:10.1021/ma502362a.

[48] M.A. Vandiver, B.R. Caire, Z. Poskin, Y. Li, S. Seifert, D.M. Knauss, et al., Durability and performance of polystyrene- b -poly(vinylbenzyl trimethylammonium) diblock copolymer and equivalent blend anion exchange membranes, J. Appl. Polym. Sci. (2015) n/a–n/a. doi:10.1002/app.41596.

[49] H.N. Sarode, G.E. Lindberg, Y. Yang, L.E. Felberg, G.A. Voth, A.M. Herring, Insights into the Transport of Aqueous Quaternary Ammonium Cations: A Combined Experimental and Computational Study., J. Phys. Chem. B. (2014). doi:10.1021/jp4085662.

[50] D.C. Herbst, T.A. Witten, T. Tsai, E.B. Coughlin, A.M. Maes, M. Andrew, Water uptake profile in a model ion-exchange membrane : Conditions for water-rich channels Water uptake profile in a model ion-exchange membrane : Conditions for water-rich channels, 114906 (2015). doi:10.1063/1.4914512.

[51] T.P. Pandey, A.M. Maes, H.N. Sarode, B.D. Peters, S. Lavina, K. Vezzù, et al., Interplay between water uptake, ion interactions, and conductivity in an e-beam grafted poly(ethylene-co-tetrafluoroethylene) anion exchange membrane, Phys. Chem. Chem. Phys. 17 (2015) 4367–4378. doi:10.1039/C4CP05755D.

[52] Y. Liu, J. Wang, Y. Yang, T.M. Brenner, S. Seifert, Y. Yan, et al., Anion transport in a chemically stable, sterically bulky α-C modified imidazolium functionalized anion exchange membrane, J. Phys. Chem. C. 118 (2014) 15136–15145. doi:10.1021/jp5027674.

[53] J.L. Horan, A. Lingutla, H. Ren, M.C. Kuo, S. Sachdeva, Y. Yang, et al., Fast proton conduction facilitated by minimum water in a series of divinylsilyl-11-silicotungstic acid-co-butyl acrylate-co-hexanediol diacrylate polymers, J. Phys. Chem. C. 118 (2014) 135–144. doi:10.1021/jp4089657.

[54] A.M. Maes, T.P. Pandey, M. a. Vandiver, L.K. Lundquist, Y. Yang, J.L. Horan, et al., Preparation and characterization of an alkaline anion exchange membrane from chlorinated poly(propylene) aminated with branched poly(ethyleneimine), Electrochim. Acta. 110 (2013) 260–266. doi:10.1016/j.electacta.2013.04.033.

[55] Y. Liu, K. Cui, N. Tian, W. Zhou, L. Meng, L. Li, et al., Stretch-Induced Crystal−Crystal Transition of Polybutene-1: An in Situ Synchrotron Radiation Wide-Angle X-ray Scattering Study, Macromolecules. 45 (2012) 2764–2772.

[56] N. Tian, W. Zhou, K. Cui, Y. Liu, Y. Fang, X. Wang, et al., Extension Flow Induced Crystallization of Poly (ethylene oxide), Macromolecules. 44 (2011) 7704–7712.

[57] Y. Mao, C. Burger, X. Li, B.S. Hsiao, A.K. (ExxonMobil) Mehta, A.H. Tsou, Time-Resolved Synchrotron X-ray Scattering Study on Propylene− 1-Butylene Random Copolymer Subjected to Uniaxial Stretching at High Temperatures, Macromolecules. 45 (2012) 951–961.

[58] T. Kamal, T.J. Shin, S.-Y. Park, Uniaxial Tensile Deformation of Poly(ε-caprolactone) Studied with SAXS and WAXS Techniques Using Synchrotron Radiation, Macromolecules. 45 (2012) 8752–8759. doi:10.1021/ma301714f.

[59] S. Polizzi, P. Btsecke, N. Stribeck, H.G. Zachmann, Small-angle X-ray scattering investigations of styrenc butadienc styrene block copolymers during stretching, Polymer (Guildf). 31 (1990) 638–645.

[60] ASTM, Standard Test Method for Tensile Properties of Thin Plastic Sheeting, ASTM Int. D882-12 (2012) 1–12. doi:10.1520/D0882-12.

[61] R. Mao, E.M. McCready, W.R. Burghardt, Soft Matter Structural response of an ordered block copolymer melt to uniaxial extensional fl ow, Soft Matter. 10 (2014) 6198–6207. doi:10.1039/C4SM00613E.

[62] E.M. McCready, W.R. Burghardt, In Situ SAXS Studies of Structural Relaxation of an Ordered Block Copolymer Melt Following Cessation of Uniaxial Extensional Flow, Macromolecules. 48 (2015) 264–271. doi:dx.doi.org/10.1021/ma501633f.

[63] J. Ilavsky, Nika : software for two-dimensional data reduction, J. Appl. Crystallogr. 45 (2012) 324–328. doi:10.1107/S0021889812004037.

[64] J. Ilavsky, P.R. Jemian, Irena : tool suite for modeling and analysis of small-angle scattering, J. Appl. Crystallogr. 42 (2009) 347–353. doi:10.1107/S0021889809002222.

[65] G.A. Bell, D.M. Bielinski, B.D. Beake, Influence of Water on the Nanoindentation Creep Response of Nylon 6, J. Appl. Polym. Sci. 107 (2008) 577–582. doi:10.1002/app.

[66] G.J. Kettle, Variation of the glass transition temperature of nylon-6 with changing water content, Polymer (Guildf). 18 (1977) 742–743.

[67] I. Merdas, F. Thominette, a Tcharkhtchi, J. Verdu, Factors governing water absorption by composite matrices, Compos. Sci. Technol. 62 (2002) 487–492. doi:10.1016/S0266-3538(01)00138-5.

[68] V. Miri, O. Persyn, J.-M. Lefebvre, R. Seguela, Effect of water absorption on the plastic deformation behavior of nylon 6, Eur. Polym. J. 45 (2009) 757–762. doi:10.1016/j.eurpolymj.2008.12.008.

[69] C.M.O. Müller, J.B. Laurindo, F. Yamashita, Effect of cellulose fibers addition on the mechanical properties and water vapor barrier of starch-based films, Food Hydrocoll. 23 (2009) 1328–1333. doi:10.1016/j.foodhyd.2008.09.002.

[70] G.I. Olivas, G. V. Barbosa-Cánovas, Alginate–calcium films: Water vapor permeability and mechanical properties as affected by plasticizer and relative humidity, LWT - Food Sci. Technol. 41 (2008) 359–366. doi:10.1016/j.lwt.2007.02.015.

[71] A. Jiménez, M.J. Fabra, P. Talens, A. Chiralt, Edible and Biodegradable Starch Films: A Review, Food Bioprocess Technol. 5 (2012) 2058–2076. doi:10.1007/s11947-012-0835-4.

[72] D.G. Thompson, J.C. Osborn, E.M. Kober, J.R. Schoonover, Effects of hydrolysis-induced molecular weight changes on the phase separation of a polyester polyurethane, Polym. Degrad. Stab. 91 (2006) 3360–3370. doi:10.1016/j.polymdegradstab.2006.05.019.

[73] C.C. White, D.L. Hunston, K.T. Tan, J. Hettenhouser, J.D. Garver, An accelerated exposure and testing apparatus for building joint sealants., Rev. Sci. Instrum. 84 (2013) 095113. doi:10.1063/1.4821880.

[74] L. Martinetti, A.M. Mannion, W.E. Voje, R. Xie, R.H. Ewoldt, L.D. Morgret, et al., A critical gel fluid with high extensibility: The rheology of chewing gum, J. Rheol. (N. Y. N. Y). 58 (2014) 821–838. doi:10.1122/1.4874322.

[75] W.D. Callister, Materials Science and Engineering: An Introduction, 7th ed., John Wiley & Sons, Inc., New York, NY, 2007.

[76] M.A. Vandiver, B.R. Caire, J.R. Carver, K. Waldrop, M.R. Hibbs, J.R. Varcoe, et al., Mechanical Characterization of Anion Exchange Membranes by Extensional Rheology under Controlled Hydration, J. Electrochem. Soc. 161 (2014) H677–H683. doi:10.1149/2.0971410jes.

[77] T.A. Zawodzinski, T.E. Springer, J. Davey, R. Jestel, C. Lopez, J. Valeria, et al., A Comparative Study of Water Uptake By and Transport Through Ionomeric Fuel Cell Membranes, J. Electrochem. Soc. 140 (1993) 1981–1985.

[78] K.A. Patankar, D.A. Dillard, S.W. Case, M.W. Ellis, Y.-H. Lai, C.S. Gittleman, Linear Hygrothermal Viscoelastic Characterization of Nafion NRE 211 Proton Exchange Membrane, Fuel Cells. 12 (2012) 787–799. doi:10.1002/fuce.201100134.

[79] F. Bauer, S. Denneler, M. Willert-Porada, Influence of temperature and humidity on the mechanical properties of Nafion 117 polymer electrolyte membrane, J. Polym. Sci. Part B Polym. Phys. 43 (2005) 786–795. doi:10.1002/polb.20367.

[80] Y. Li, D.A. Dillard, Y.-H. Lai, S.W. Case, M.W. Ellis, M.K. Budinski, et al., Experimental Measurement of Stress and Strain in Nafion Membrane during Hydration Cycles, J. Electrochem. Soc. 159 (2012) B173–B184. doi:10.1149/2.065202jes.

[81] DuPont, DuPont Nafion PFSA Membranes, (2009) Nafion PFSA Membranes.

[82] A. Kusoglu, M. a. Modestino, A. Hexemer, R. a. Segalman, A.Z. Weber, Subsecond Morphological Changes in Nafion during Water Uptake Detected by Small-Angle X-ray Scattering, ACS Macro Lett. 1 (2012) 33–36. doi:10.1021/mz200015c.

[83] A.Z. Weber, J. Newman, Transport in Polymer-Electrolyte Membranes, J. Electrochem. Soc. 150 (2003) A1008. doi:10.1149/1.1580822.

[84] Y. Tang, A.M. Karlsson, M.H. Santare, M. Gilbert, S. Cleghorn, W.B. Johnson, An experimental investigation of humidity and temperature effects on the mechanical properties of perfluorosulfonic acid membrane, Mater. Sci. Eng. A. 425 (2006) 297–304. doi:10.1016/j.msea.2006.03.055.

[85] N. Jalani, P. Choi, R. Datta, TEOM: A novel technique for investigating sorption in proton-exchange membranes, J. Memb. Sci. 254 (2005) 31–38. doi:10.1016/j.memsci.2004.12.020.

[86] M.B. Satterfield, P.W. Majsztrik, H. Ota, J.A.Y.B. Benziger, A.B. Bocarsly, Mechanical Properties of Nafion and Titania / Nafion Composite Membranes for Polymer Electrolyte Membrane Fuel Cells, J. Polym. Sci. Part B Polym. Phys. 44 (2006) 2327–2345. doi:10.1002/polb.

[87] M.B. Satterfield, Mechanical and water sorption properties of Nafion and composite Nafion/titanium dioxide membranes for polymer electrolyte membrane fuel cells, Dissertation, Princeton University, 2007.

[88] S.-Y. Ahn, Y.-C. Lee, H.Y. Ha, S.-A. Hong, I.-H. Oh, Properties of the reinforced composite membranes formed by melt soluble ion conducting polymer resins for PEMFCs, Electrochim. Acta. 50 (2004) 571–575. doi:10.1016/j.electacta.2004.01.133.

[89] S. Bhadra, N.H. Kim, J.S. Choi, K.Y. Rhee, J.H. Lee, Hyperbranched poly(benzimidazole-co-benzene) with honeycomb structure as a membrane for high-temperature proton-exchange membrane fuel cells, J. Power Sources. 195 (2010) 2470–2477. doi:10.1016/j.jpowsour.2009.11.083.

[90] J. Park, T.-H. Kim, H.J. Kim, J.-H. Choi, Y.T. Hong, Crosslinked sulfonated poly(arylene ether sulfone) membranes for fuel cell application, Int. J. Hydrogen Energy. 37 (2012) 2603–2613. doi:10.1016/j.ijhydene.2011.10.122.

[91] P. Choi, N.H. Jalani, T.M. Thampan, R. Datta, Consideration of Thermodynamic , Transport , and Mechanical Properties in the Design of Polymer Electrolyte Membranes for Higher Temperature Fuel Cell Operation, J. Polym. Sci. Part B Polym. Phys. 44 (2006) 2183–2200. doi:10.1002/polb.20858.

[92] E. Roberti, G. Carlotti, S. Cinelli, G. Onori, a. Donnadio, R. Narducci, et al., Measurement of the Young's modulus of Nafion membranes by Brillouin light scattering, J. Power Sources. 195 (2010) 7761–7764. doi:10.1016/j.jpowsour.2009.11.033.

[93] J. Benziger, A. Bocarsly, M.J. Cheah, P.W. Majsztrik, M.B. Satterfield, Q. Zhao, Mechanical and Transport Properties of Nafion: Effects of Temperature and Water Activity, Struct. Bond. 141 (2011) 85–113. doi:10.1007/430.

[94] S. Shi, D. Liu, D. Liu, P. Tae, C.Y. Gao, L. Yan, et al., Mechanical properties and microstructure changes of proton exchange membrane under immersed conditions, Polym. Eng. Sci. 54 (2014) 2215–2221. doi:10.1002/pen.23770.

[95] A. Kusoglu, S. Savagatrup, K.T. Clark, A.Z. Weber, Role of Mechanical Factors in Controlling the Structure–Function Relationship of PFSA Ionomers, Macromolecules. 45 (2012) 7467–7476. doi:10.1021/ma301419s.

[96] A. Berger, R. a. Segalman, J. Newman, Material requirements for membrane separators in a water-splitting photoelectrochemical cell, Energy Environ. Sci. 7 (2014) 1468. doi:10.1039/c3ee43807d.

[97] F.S. Bates, G.H. Fredrickson, Block Copolymers—Designer Soft Materials, Phys. Today. 52 (1999) 32. doi:10.1063/1.882522.

[98] Z. Gadjourova, Y.G. Andreev, D.P. Tunstall, P.G. Bruce, Ionic conductivity in crystalline polymer electrolytes., Nature. 412 (2001) 520–523. doi:10.1038/35087538.

[99] Y. Li, Block Copolymers for Alkaline Fuel Cell Membrane Materials, Colorado School of Mines, 2014.

[100] J.-H. Choi, A. Kota, K.I. Winey, Micellar Morphology in Sulfonated Pentablock Copolymer Solutions, Ind. Eng. Chem. Res. 49 (2010) 12093–12097. doi:10.1021/ie1002476.

[101] J.-H. Choi, C.L. Willis, K.I. Winey, Structure–property relationship in sulfonated pentablock copolymers, J. Memb. Sci. 394-395 (2012) 169–174. doi:10.1016/j.memsci.2011.12.036.

[102] J.-H. Choi, C.L. Willis, K.I. Winey, Effects of neutralization with Et3Al on structure and properties in sulfonated styrenic pentablock copolymers, J. Memb. Sci. 428 (2013) 516–522. doi:10.1016/j.memsci.2012.10.051.

[103] E.J. Laprade, C.-Y. Liaw, Z. Jiang, K.R. Shull, Mechanical and microstructural characterization of sulfonated pentablock copolymer membranes, J. Polym. Sci. Part B Polym. Phys. (2014) n/a–n/a. doi:10.1002/polb.23623.

[104] K.P. Mineart, X. Jiang, H. Jinnai, A. Takahara, R.J. Spontak, Morphological Investigation of Midblock-Sulfonated Block Ionomers Prepared from Solvents Differing in Polarity., Macromol. Rapid Commun. (2014) 1–7. doi:10.1002/marc.201400627.

[105] C.L. Willis, Amine neutralized sulfonated block copolymers and method for making same, EP 2488562 A1, 2012.

[106] A.V. Dobrynin, R.H. Colby, M. Rubinstein, Scaling Theory of Polyelectrolyte Solutions, Macromolecules. 28 (1995) 1859–1871. doi:10.1021/ma00110a021.

[107] R.H. Colby, Structure and linear viscoelasticity of flexible polymer solutions: Comparison of polyelectrolyte and neutral polymer solutions, Rheol. Acta. 49 (2010) 425–442. doi:10.1007/s00397-009-0413-5.

[108] Y. Takahashi, Y. Isono, I. Noda, Zero-Shear Viscosity of Linear Polymer Solutions over a Wide Range of Concentration, Macromolecules. 1008 (1985) 1002–1008. doi:10.1021/ma00147a033.

[109] M.G. McKee, M.T. Hunley, J.M. Layman, T.E. Long, Solution rheological behavior and electrospinning of cationic polyelectrolytes, Macromolecules. 39 (2006) 575–583. doi:10.1021/ma051786u.

[110] D.J. Burnett, A.R. Garcia, F. Thielmann, Measuring moisture sorption and diffusion kinetics on proton exchange membranes using a gravimetric vapor sorption apparatus, J. Power Sources. 160 (2006) 426–430. doi:10.1016/j.jpowsour.2005.12.096.

[111] M.J. Park, K.H. Downing, A. Jackson, E.D. Gomez, A.M. Minor, D. Cookson, et al., Increased Water Retention in Polymer Electrolyte Membranes at Elevated Temperatures Assisted by Capillary Condensation, Nano Lett. 7 (2007) 3547–3552. doi:10.1021/nl072617l.

[112] Y.S. Li, T.S. Zhao, W.W. Yang, Measurements of water uptake and transport properties in anion-exchange membranes, Int. J. Hydrogen Energy. 35 (2010) 5656–5665. doi:10.1016/j.ijhydene.2010.03.026.

[113] X. Lin, L. Wu, Y. Liu, A.L. Ong, S.D. Poynton, J.R. Varcoe, et al., Alkali resistant and conductive guanidinium-based anion-exchange membranes for alkaline polymer electrolyte fuel cells, J. Power Sources. 217 (2012) 373–380. doi:10.1016/j.jpowsour.2012.05.062.

[114] C. Fujimoto, D.-S. Kim, M. Hibbs, D. Wrobleski, Y.S. Kim, Backbone stability of quaternized polyaromatics for alkaline membrane fuel cells, J. Memb. Sci. 423-424 (2012) 438–449. doi:10.1016/j.memsci.2012.08.045.

[115] M.R. Hibbs, C.H. Fujimoto, C.J. Cornelius, Synthesis and Characterization of Poly(phenylene)-Based Anion Exchange Membranes for Alkaline Fuel Cells, Macromolecules. 42 (2009) 8316–8321. doi:10.1021/ma901538c.

[116] A.D. Mohanty, Y. Lee, L. Zhu, M.A. Hickner, C. Bae, Anion Exchange Fuel Cell Membranes Prepared from C–H Borylation and Suzuki Coupling Reactions, Macromolecules. (2014). doi:10.1021/ma500125t.

[117] G. a Giffin, G.M. Haugen, S.J. Hamrock, V. Di Noto, Interplay between structure and relaxations in perfluorosulfonic acid proton conducting membranes., J. Am. Chem. Soc. 135 (2013) 822–34. doi:10.1021/ja3099799.

[118] N. Hadjichristidis, S. Pispas, G. Floudas, Block Copolymer Morphology, in: Block Copolym. Synth. Strateg. Phys. Prop. Appl., John Wiley & Sons, Inc., 2003: pp. 346–361.

[119] Y. Liu, J.L. Horan, G.J. Schlichting, B.R. Caire, M.W. Liberatore, S.J. Hamrock, et al., A Small-Angle X-ray Scattering Study of the Development of Morphology in Films Formed from the 3M Perfluorinated Sulfonic Acid Ionomer, Macromolecules. 45 (2012) 7495–7503.

[120] C.S. Gittleman, F.D. Coms, Y.H. Lai, Membrane Durability: Physical and Chemical Degradation, in: M.M. Mench, E.C. Kumbur, T.N. Veziroglu (Eds.), Polym. Electrolyte Fuel Cell Degrad., 2011: pp. 15–88. doi:10.1016/B978-0-12-386936-4.10002-8.

[121] R.H. Ewoldt, A.E. Hosoi, G.H. McKinley, New measures for characterizing nonlinear viscoelasticity in large amplitude oscillatory shear, J. Rheol. (N. Y. N. Y). 52 (2007) 1427–1458. doi:10.1122/1.2970095.

[122] K. Hyun, M. Wilhelm, C.O. Klein, K.S. Cho, J.G. Nam, K.H. Ahn, et al., A review of nonlinear oscillatory shear tests: Analysis and application of large amplitude oscillatory shear (LAOS), Prog. Polym. Sci. 36 (2011) 1697–1753. doi:10.1016/j.progpolymsci.2011.02.002.

[123] Y.-H. Lai, C.K. Mittelsteadt, C.S. Gittleman, D.A. Dillard, Viscoelastic Stress Analysis of Constrained Proton Exchange Membranes Under Humidity Cycling, J. Fuel Cell Sci. Technol. 6 (2009) 021002. doi:10.1115/1.2971045.

[124] H. Tang, S. Peikang, S.P. Jiang, F. Wang, M. Pan, A degradation study of Nafion proton exchange membrane of PEM fuel cells, J. Power Sources. 170 (2007) 85–92. doi:10.1016/j.jpowsour.2007.03.061.

[125] K. a Mauritz, R.B. Moore, State of understanding of nafion., Chem. Rev. 104 (2004) 4535–85.

[126] M.A. Vandiver, Effect of hydration on the mechanical properties of anion exchange membranes, Colorado School of Mines, 2015.

[127] C.G. Arges, L. Wang, M. -s. Jung, V. Ramani, Mechanically Stable Poly(arylene ether) Anion Exchange Membranes Prepared from Commercially Available Polymers for Alkaline Electrochemical Devices, J. Electrochem. Soc. 162 (2015) F686–F693. doi:10.1149/2.0361507jes.

CONTRIBUTIONS TO THE WORK OF OTHERS

Attached are publications in which the thesis author was listed as a co-author. A brief description of the contributions is listed before each publication.

Melissa A. Vandiver, Benjamin R. Caire, Yifan Li, Sönke Seifert, Daniel M. Knauss, Andrew M. Herring, Matthew W. Liberatore. Effect of hydration on the mechanical properties and ion conduction in a polyethylene-b-poly(vinylbenzyl trimethylammonium) anion exchange membrane, in preparation (2015)

The platform for mechanical testing and relative humidity control as well the tensile testing protocol described in this thesis was used for the mechanical characterization done in this work.

Melissa A. Vandiver, Benjamin R. Caire, S. Piril Ertem, Tsung-Han Tsai, E. Bryan Coughlin, Andrew M. Herring, and Matthew W. Liberatore. Mechanical performance of polyisoprene copolymer anion exchange membranes by varying crosslinking method, J. Electrochem. Soc. 162 (2015) H206-H212.

The platform for mechanical testing and relative humidity control as well the tensile testing protocol described in this thesis was used for the mechanical characterization done in this work.

Melissa A. Vandiver, Benjamin R. Caire, Zach Poskin, Yifan Li, Sönke Seifert, Daniel M. Knauss, Andrew M. Herring, Matthew W. Liberatore. Durability and performance of polystyrene-b-poly(vinylbenzyl trimethylammonium) diblock copolymer and equivalent blend anion exchange membranes, J. Applied Polymer Sci. 132 (2015) 41596

The platform for mechanical testing and relative humidity control as well the tensile testing protocol described in this thesis was used for the mechanical characterization done in this work.

Melissa A. Vandiver, Benjamin R. Caire, Jordan R. Carver, KrystaWaldrop, Michael R. Hibbs, John R. Varcoe, Andrew M. Herring, and Matthew W. Liberatore. Mechanical Characterization of Anion Exchange Membranes by Extensional Rheology under Controlled Hydration, 161 (2014) H677-H683

The platform for mechanical testing and relative humidity control as well the tensile testing protocol described in this thesis was used for the mechanical characterization done in this work.

Rajeswari Janarthanan, James L. Horan, Benjamin R. Caire, Zachary C. Ziegler, Yuan Yang, Xiaobing Zuo, Matthew W. Liberatore, Michael R. Hibbs, Andrew M. Herring. Understanding anion transport in an aminated trimethylpolyphenylene with high anionic conductivity, 51 J. Poly. Sci. B. (2013) 1743-1750

The testing apparatus and protocol for the measurement of hydroxide conductivity while rigorously excluding carbon dioxide was done by the author of this thesis. The BekkTech platform was modified to include a second mass flow controller to enable control of relative humidity via a wet gas/ dry gas mix instead of the previous method which controlled relative humidity by setting the saturator to the dewpoint associated with the relative humidity condition desired in the test cell. The old method was proven to be unreliable once a dewpoint sensor was placed inside the BekkTech cell for more accurate measurement of relative humidity. The new system was also coded into the existing LabView platform. The reported hydroxide conductivity under water vapor conditions was one of the first reported tests of this nature.

Yuan Liu, James L. Horan, Gregory J. Schlichting, Benjamin R. Caire, Matthew W. Liberatore, Steven J. Hamrock, Gregory M. Haugen, Michael A. Yandrasits, Sönke Seifert, and Andrew M. Herring. A Small-Angle X-ray Scattering Study of the Development of Morphology in Films Formed from the 3M Perfluorinated Sulfonic Acid Ionomer, 45 Macromolecules (2012) 7495-7503

The thesis author helped the primary author on the paper set up and run the kinetic experiments performed at the Advanced Photon Source. The thesis author also modified Figure 2 in the paper to more accurately reflect the environmental control system

COPYRIGHT PERMISSIONS

This Appendix includes expressed, written permission from the copyright holders granting permission for republication of the material contained in Chapter 3. Written consent for republication from all Co-authors is also included.

SPRINGER LICENSE
TERMS AND CONDITIONS

May 04, 2015

This is a License Agreement between Benjamin R Caire ("You") and Springer ("Springer") provided by Copyright Clearance Center ("CCC"). The license consists of your order details, the terms and conditions provided by Springer, and the payment terms and conditions.

All payments must be made in full to CCC. For payment instructions, please see information listed at the bottom of this form.

License Number	3622131333076
License date	May 04, 2015
Licensed content publisher	Springer
Licensed content publication	Rheologica Acta
Licensed content title	Mechanical testing of small, thin samples in a humidity-controlled oven
Licensed content author	Benjamin R. Caire
Licensed content date	Jan 1, 2015
Volume number	54
Issue number	4
Type of Use	Thesis/Dissertation
Portion	Full text
Number of copies	1
Author of this Springer article	Yes and you are the sole author of the new work
Order reference number	None
Title of your thesis / dissertation	MECHANICAL CHARACTERIZATION OF ANION EXCHANGE MEMBRANES UNDER CONTROLLED ENVIRONMENTAL CONDITIONS
Expected completion date	May 2015
Estimated size(pages)	130
Total	0.00 USD
Terms and Conditions	

Introduction

The publisher for this copyrighted material is Springer Science + Business Media. By clicking "accept" in connection with completing this licensing transaction, you agree that the following terms and conditions apply to this transaction (along with the Billing and Payment terms and conditions established by Copyright Clearance Center, Inc. ("CCC"), at the time that you opened your Rightslink account and that are available at any time at http://myaccount.copyright.com).

Limited License

With reference to your request to reprint in your thesis material on which Springer Science

established by CCC on its behalf in its Billing and Payment terms and conditions for this licensing transaction.

Indemnity
You hereby indemnify and agree to hold harmless Springer Science + Business Media and CCC, and their respective officers, directors, employees and agents, from and against any and all claims arising out of your use of the licensed material other than as specifically authorized pursuant to this license.

No Transfer of License
This license is personal to you and may not be sublicensed, assigned, or transferred by you to any other person without Springer Science + Business Media's written permission.

No Amendment Except in Writing
This license may not be amended except in a writing signed by both parties (or, in the case of Springer Science + Business Media, by CCC on Springer Science + Business Media's behalf).

Objection to Contrary Terms
Springer Science + Business Media hereby objects to any terms contained in any purchase order, acknowledgment, check endorsement or other writing prepared by you, which terms are inconsistent with these terms and conditions or CCC's Billing and Payment terms and conditions. These terms and conditions, together with CCC's Billing and Payment terms and conditions (which are incorporated herein), comprise the entire agreement between you and Springer Science + Business Media (and CCC) concerning this licensing transaction. In the event of any conflict between your obligations established by these terms and conditions and those established by CCC's Billing and Payment terms and conditions, these terms and conditions shall control.

Jurisdiction
All disputes that may arise in connection with this present License, or the breach thereof, shall be settled exclusively by arbitration, to be held in The Netherlands, in accordance with Dutch law, and to be conducted under the Rules of the 'Netherlands Arbitrage Instituut' (Netherlands Institute of Arbitration).***OR:***

All disputes that may arise in connection with this present License, or the breach thereof, shall be settled exclusively by arbitration, to be held in the Federal Republic of Germany, in accordance with German law.

Other terms and conditions:

v1.3

Benjamin Caire <bcaire@mymail.mines.edu>

Thesis - permission to reproduce

Melissa Vandiver <melissa.vandiver10@gmail.com> Thu, Apr 30, 2015 at 7:43 PM
To: Benjamin Caire <bcaire@mymail.mines.edu>

I hereby permit Benjamin R. Caire to reproduce the work entitled, "Mechanical testing of small, thin samples in a humidity controlled oven" published in *Rheologica Acta* (2015) **54**, 253-261, DOI 10.1007/s00397-014-0834-7 as part of his thesis.

Melissa Vandiver
melissa.vandiver10@gmail.com

On Apr 30, 2015, at 2:33 PM, Benjamin Caire wrote:

Melissa,

You know the drill...

I hereby permit Benjamin R. Caire to reproduce the work entitled, "Mechanical testing of small, thin samples in a humidity controlled oven" published in *Rheologica Acta* (2015) **54**, 253-261, DOI 10.1007/s00397-014-0834-7 as part of his thesis.

Thanks!

Ben